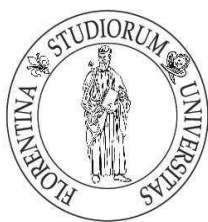# POLYMER SUPPORTED METAL NANOPARTICLES FOR THE GREEN SYNTHESIS OF FINE CHEMICALS

CARMEN MORENO MARRODAN

Università degli Studi di Firenze

DOTTORATO DI RICERCA IN
SCIENZE CHIMICHE
CICLO XXV

COORDINATORE Prof. Andrea Goti

POLYMER SUPPORTED METAL NANOPARTICLES
FOR THE GREEN SYNTHESIS OF FINE CHEMICALS

Settore Scientifico Disciplinare CHIM/03

Submitted by   **Tutor**

M. Carmen Moreno Marrodán   Prof. Pierluigi Barbaro

Anni 2010 / 2013

A mi hermana

por su apoyo incondicional

Abstract

The development of greener and more economical routes for chemicals production is one of the major current concerns at industrial level. This is particularly true in the fine chemicals sector, where the large amount of waste produced contribute to the characteristic high *E*-factor (Kg waste/Kg product). Catalysis may be the key to solve the problem provided that active and selective catalysts are elaborated. These are the distinctive features of homogeneous phase catalysts, which indeed dominate the sector. However, they show severe drawbacks in terms of recovery and reuse of the precious catalysts. The immobilization of chemical catalysts onto solid insoluble supports offers significant benefits to this regard.

The present Thesis reports a simple one-pot strategy for the synthesis of solid-supported metal catalysts based on ion-exchange resins, and *in-situ* formed metal nanoparticles under mild catalytic hydrogenation conditions (room temperature, 1 bar H_2). The so-formed heterogeneous palladium system was carefully characterized and tested in hydrogenations processes for the synthesis of high added value chemicals. The catalyst showed high activity and selectivity and could be readily reused several times with neither detectable metal leaching in solution nor significant efficiency decay under batch conditions. Application to the synthesis of the leaf alcohol *cis*-3-hexen-1-ol was explored both under batch and continuous mode showing significant advantages compared to established industrial process.

Keywords: metal supported nanoparticles, hydrogenations, fine chemicals

Contents

Chapter 3. Polymer Supported Metal Nanoparticles. Synthesis and Characterization 53

1

Introduction

1.1 OVERVIEW

This chapter outlines the principles of green chemistry and explains the connection between green chemistry, sustainable technology and catalysis. It covers the concepts of atom economy and E factor and focuses in the synthesis of fine chemicals, pointing out the drawbacks and the role that catalysis can play to improve the processes. Next, a general outlook of the different types of catalysis is given paying special attention to heterogeneous systems and, in particular, to supported metal nanoparticles in its catalytic role. Among the vast variety of supported catalytic systems (organic, inorganic supports), the special case of ion exchange resins is explained in detail, summarizing the state of art in the field. In the last section, a brief introduction of continuous flow processes is given. The reader will arrive at the end of this chapter with all the required information to understand the aim of this work and evaluate the relevance of the goal itself.

1.2. SUSTAINABLE CHEMISTRY

The increasingly severe environmental legislation has generated an urgent need for cleaner methods of chemical production.[1] The trend towards what is known as "Green Chemistry" or "Sustainable Technology"[2] necessitates a paradigm shift from traditional concepts of process efficiency, that focus largely in chemical yield, to one that assigns economic value to eliminating waste at source and avoiding the use of toxic and/or hazardous reagents and solvents.[3]

The Organization for Economic Cooperation and Development (OECD) defines sustainable chemistry as the design, manufacture and use of efficient, effective, safe and more environmentally benign chemical products and processes.[4] Within the broad framework of sustainable development, government, academia and industry should strive to maximize resource efficiency through activities such as energy and non-renewable resource conservation, risk minimization, pollution prevention, minimization of waste at all stages of a product life-cycle, and the development of products that are durable and can be reused and recycled. Essentially, sustainable chemistry is about doing more and better with less.[5]

Sustainable Chemistry is a concept sometimes opposed and sometimes confused with Green Chemistry. However, there is a key difference between these two concepts, as shown in Fig. 1.1.

Sustainability...

Meeting the needs of the present generation without compromising the needs of future generations

... is the goal

Green Chemistry...

Technologies that are energy efficient,minimise or preferably eliminate the formation of waste,avoid the use of toxic and/or hazardous solvents and reagents and, where possible,utilise renewable raw materials.

... is the means

Fig. 1.1. Difference between Sustainability and Green Chemistry.

As Anastas and Warner[2a] have pointed out, the guiding principle of Green Chemistry is the design of environmentally benign products and processes. In order to illustrate what this definition means in practice, the *12 Principles of Green Chemistry* were formulated. The principles provide the guidelines to lower the ecological footprint of the chemicals produced and the processes by which such chemicals are made:

1. **Prevention:** It is better to prevent waste than to treat or clean up waste after it has been created.

2. **Atom economy:** Synthetic methods should be designed to maximize the incorporation of all materials used in the process into the final product.

3. **Less hazardous chemical synthesis:** Wherever practicable, synthetic methods should be designed to use and generate substances that possess little or no toxicity to human health and the environment.

4. **Designing safer chemicals:** Chemical products should be designed to effect their desired function while minimizing their toxicity.

5. **Safer solvents and auxiliaries:** The use of auxiliary substances (e.g., solvents, separation agents, etc.) should be made unnecessary wherever possible and innocuous when used.

6. **Design for energy efficiency:** Energy requirements of chemical processes should be recognized for their environmental and economic impacts and should be minimized. If possible, synthetic methods should be conducted at ambient temperature and pressure.

7. **Use of renewable feedstocks:** A raw material or feedstock should be renewable rather than depleting whenever technically and economically practicable.

8. **Reduced derivatives:** Unnecessary derivatization (use of blocking groups, protection / deprotection, temporary modification of physical / chemical processes) should be minimized or avoided if possible, because such steps require additional reagents and can generate waste.

9. **Catalysis:** Catalytic reagents (as selective as possible) are superior to stoichiometric reagents.

10. **Design for degradation:** Chemical products should be designed so that at the end of their function they break down into innocuous degradation products and do not persist on the environment.

11. **Real-time analysis for pollution prevention:** Analytical methodologies need to be further developed to allow for real-time in-process monitoring and control prior to the formation of hazardous substances.

12. **Inherently safer chemistry for accident prevention:** Substances and the form of a substance used in a chemical process should be chosen to minimize the potential for chemical incidents, including releases, explosions and fires.

However, quantifying the improvement of a chemical process in terms of Green Chemistry is not as easy as calculating yield improvements and/or selectivity increases of a chemical reaction, where simple percentages are suitable. Among the different metrics formulated to this purpose, there are two useful measures[6] that give an idea about the potential environment acceptability of chemical processes:

- *E factor*: It is the actual amount of waste produced in the process, defined as everything but the desired product. It is calculated by dividing the amount of waste generated by the amount of product obtained (kg waste / kg product). It takes the chemical yield into account and includes

reagents, solvents losses, all process aids. There is one exception, water is excluded from the calculation, otherwise this would lead to exceptionally high E factors that can make meaningful processes comparisons.

- *Atom efficiency*: extremely useful tool for rapid evaluation of the amounts of waste that will be generated by alternative processes. It is calculated by dividing the molecular weight of the product by the total amount of the molecular weights of all substances formed in the stoichiometric equation.

The theoretical E factor is readily derived from the atom efficiency. A higher E factor means more waste and, consequently, greater negative environmental impact. The ideal E factor is 0 with no waste generated, but it can reach values up to 100 as it can be seen in the Table 1.1., adapted from Sheldon.[7]

Table 1.1. Estimation of the E factor in various segments of the chemical industry.

Industry segment	Product tonnage per year	Kg waste / Kg product
Oil refining	10^6-10^8	< 0.1
Bulk chemicals	10^4-10^6	1 - 5
Fine chemicals	10^2-10^4	5 - 50
Pharmaceuticals	10-10^3	25 - 100

In addition, to precisely evaluate the environmental impact of a chemical process it must be consider, not only the amount of waste but also, the nature of this waste.

The work developed in this Thesis is placed in a sector with one of the highest E-factor, the Fine Chemicals synthesis. In the next sections an overview about the synthesis of these kind of products is given, as well as some of the potential tools that can decrease the E-factor when synthesizing these chemicals.

1.3. SYNTHESIS OF FINE CHEMICALS

Although there are not universally accepted definitions, chemicals can be classified on the basis of product volume and product value into four categories,[8] as is shown in the diagram of Fig. 1.2.
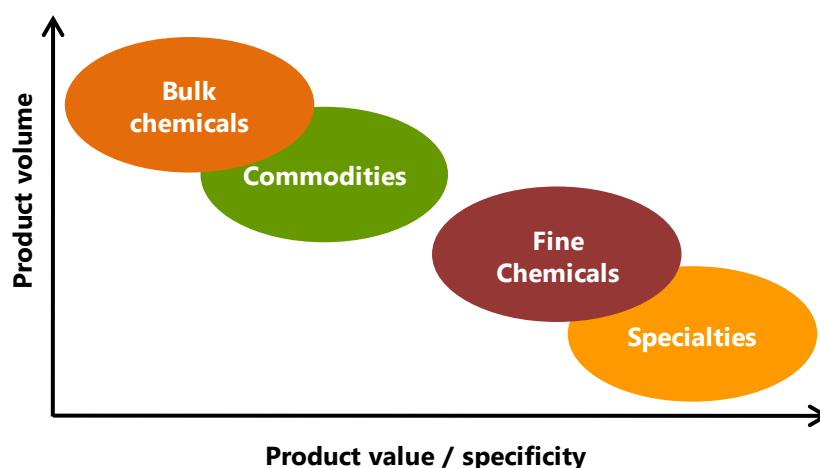
Fig. 1.2. Segmentation within the chemical industry.

Bulk chemicals and *commodities* are large-volume, low-price, and standardized chemicals produced in dedicated plants and used for a large variety of applications. Petrochemicals, basic chemicals, heavy organic and inorganic chemicals (large-volume) monomers, commodity fibers, and plastics, are all part them. While bulk chemicals are sold on the basis of industry specification (e.g. acetone, ethylene, phenol) and there is essentially no difference in the product from different suppliers, commodities are sold on the basis of their performance (e.g. polymers, surfactant, paints), the product is formulated and its properties can differ from one supplier to another.

Fine chemicals are products of high and well-defined purity, which are manufactured in relatively small amounts and sold at relatively high price.[9] They can be divided in two basic groups; those that are used as *intermediates* for other products and those that, by their nature, have a specific activity and are

used based on their performance characteristics. The latter are called *specialty chemicals*.

Fine chemicals and *specialties* are complex, multifunctional molecules, single, pure chemical substances produced in limited quantities. The former are produced in multipurpose plants by multistep batch chemical or biotech processes. They are sold on the basis of exact specifications (what they are), for further processing within the chemical industry, e.g. pharmaceutical and agrochemical intermediates. The latter are formulations of chemicals containing one or more fine chemicals as active ingredients. They are identified according to performance properties (what they can do). Pharmaceuticals, pesticides, flavours and fragrances or specialty polymers are some examples. In the life science industry, the active ingredients of drugs are fine chemicals and the formulated drugs are specialties.

Bulk and fine chemicals are identified according to specifications;[10] some of them are summarized in Table 1.2.

Table 1.2. Characteristics of bulk and fine chemicals manufacture.

	Bulk	Fine Chemicals
Volume (t/a)	> 10000	< 10000
Price ($/Kg)	< 10	10-25
Lifecycle	long	relatively short
Added value	low	high
Molecules	simple	complex, several functionalities
Applications	many	limited (often one)
Synthesis	few steps, one or few routes	multi steps, various routes
Catalysis	often	rarely
Processing	continuous, mostly gas phase, fixed bed	batch, multi-step, mostly liquid phase
Plan type	Dedicated	Multipurpose
E-factor	0-5	5 - 50

In general, expensive raw materials are processed to obtain fine chemicals which possess relatively complicated structure, being in general polyfunctional molecules that require multistep, highly selective (chemo-, regio-, diastereo-, and/or enantioselective) synthetic methods. In this regard, the required selectivity has been traditionally provided by highly selective reagents used in stoichiometric, or even over-stoichiometric, amounts. As a consequence, the waste generated per kg of product, the so-called E factor, in the fine chemicals industry is much higher than in the commodities industry, and it makes necessary the adoption of environmentally more friendly catalytic methods to substitute the stoichiometric ones. Catalysis should play a crucial role in the development of cleaner methods for fine chemicals production.

1.4. CATALYSIS ROLE IN THE SYNTHESIS OF FINE CHEMICALS

The term "catalysis" was introduced as early as 1836 by Berzelius.[11] But was Ostwald who gave to the theory of catalysis its modern form, formulating in 1894 a definition that is still valid today: "a catalyst accelerates a chemical reaction without affecting the position of the equilibrium".[12] Apart from accelerating reactions, catalysts have another important property: they can influence the selectivity of chemical reactions. Industrially, this targeted reaction control is often even more important than the catalytic activity.[10]

Nowadays, catalysis is one of the most active research areas in chemistry and the key for the innovation in chemical industrial processes, having a big influence on many aspects of a chemical process (see Fig 1.3.). According to some estimates,[13] catalysts are used in 90% of the world's chemical processes with 60% of all commercially produced chemical products requiring catalysts at some stage of their manufacture.
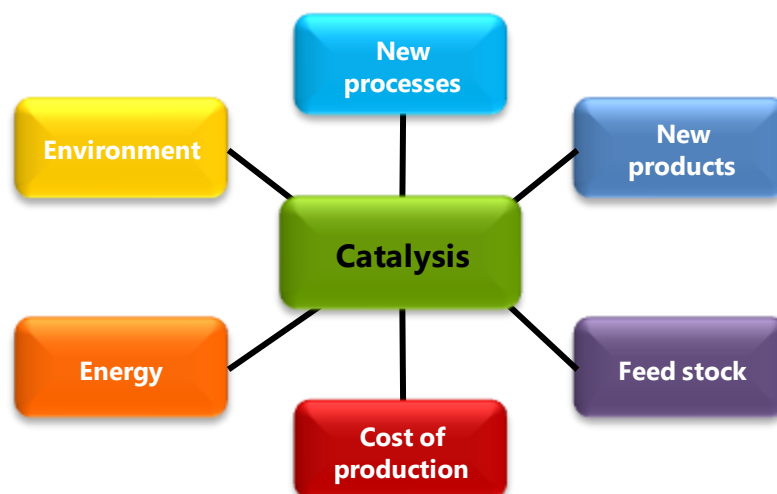
Fig. 1.3. Catalysis behind sustainable energy and chemicals.[14]

As was shown in the previous section, one of the biggest problems in fine chemicals industry is the large amount of waste generated. This waste consists primarily in inorganic salts and it is a direct consequence of the use of stoichiometric inorganic reagents.[15] Many of these reagents are polluting, moreover, they contain many atoms that are not incorporated in the final products and therefore, must be disposed of. This is not only bad for the environment, but also very costly. Examples are stoichiometric reductions with metals (Na, Mg, Zn, Fe) and metal hydride reagents (LiAlH$_4$, NaBH$_4$); oxidations with permanganate, manganese dioxide and chromium (VI) reagents; and a wide variety of reactions such as sulfonations, nitrations, halogenations or Friedel-Crafts acylations that employ stoichiometric amounts of mineral acids (H$_2$SO$_4$, HF, H$_3$PO$_4$) and Lewis acids (AlCl$_3$, ZnCl$_2$, BF$_3$). The solution is evident: replacement of old stoichiometric methodologies with cleaner catalytic alternatives.[16] Indeed, a major challenge in fine chemicals manufacture is to develop processes based on H$_2$, O$_2$, H$_2$O$_2$, CO, CO$_2$ and NH$_3$ as the direct source of H, O, C and N. Catalytic hydrogenation, oxidation and carbonylation are good examples of highly atom efficient, low-salt processes.[17] Catalysis is the key to increase selectivity, it can improve yield and cut down reactions steps in the characteristic multi-step synthesis of fine chemicals.

The suitability of catalysts for an industrial process depends mainly on its activity, selectivity and stability.[10]

- *Activity* is a measure of how fast the reaction proceeds in the presence of the catalyst. It can be evaluated through the turnover frequency (TOF) parameter. It quantifies the ratio of moles of reactant converted per mole of catalyst per unit of time.

$$\text{TOF} \quad = \quad \frac{\text{converted moles of substrate}}{\text{moles of catalyst used x time}} \quad = \quad [\text{time}^{-1}] \qquad \textbf{Eq. 1.1.}$$

For most relevant industrial applications the TOF is in the range $10^{-2}\text{-}10^{2}\ \text{s}^{-1}$.

In the case of flow processes, besides the activity of the catalyst, it is necessary to calculate its productivity which, in general, is given relative to the catalyst mass or volume, so that reactors of different size or construction can be compared with one another. This quantity is known as the space–time yield (STY):[18]

$$\text{STY} \quad = \quad \frac{\text{mass of product obtained}}{V_{\text{reactor}}\ \text{x time}} \qquad \textbf{Eq. 1.2.}$$

- The *selectivity* of a reaction is the fraction of starting material that is converted into the desired product.

$$\text{Selectivity} \quad = \quad \frac{\text{moles of desired product}}{\text{converted moles of substrate}} \qquad \textbf{Eq. 1.3.}$$

Industrially, a high selectivity is essential from both economical and ecological point of views.

- The chemical, thermal and mechanical *stability* of a catalyst determines its lifetime. Catalyst stability is influenced by numerous factors including

sintering, decomposition, modification of the active sites, attrition, coking or poisoning. It can be calculated in terms of turnover number (TON), which specifies the maximum use that can be made of a catalyst.

$$TON = TOF \ [time^{-1}] \ x \ lifetime \ of \ the \ catalyst \ [time] \qquad \textbf{Eq. 1.4.}$$

For industrial applications the TON is in the range 10^6-10^7.

Suitability of a catalyst for a particular process, is usually decided considering the following order of priority: Selectivity > Stability > Activity.

The great variety of catalysts known today can be classified according to different criteria.[19] Usually, they are considered homogeneous or heterogeneous, depending on whether they exist in the same or different phase than reagents and products. Biocatalysts (enzymes) are often seen as a separate group.

- *Homogeneous catalysis* takes place when catalyst, reactants and products are in the same phase (usually liquid). Homogeneous catalysts are generally well-defined chemical compounds which, together with the reactants, are molecularly dispersed in the reaction media. Examples are mineral acids and transition metal complexes.

- *Heterogeneous catalysis* takes place when catalyst, reactants and products are in different phases. Generally, the catalyst is a solid and the reactants are gas or liquids. When a homogeneous catalyst is attached to a solid (supported catalysts) is considered part of this group.

- *Biocatalysis* is a rather special case, somewhere between homogeneous and heterogeneous catalysis. In most cases, the biocatalyst is an enzyme; protein molecules of colloidal size that catalyze the reactions in living cells.

Table 1.3. shows a summary with the main advantages and disadvantages of homogeneous and heterogeneous systems.

Table 1.3. Schematic comparison between homogeneous and heterogeneous catalysts.

	Homogeneous	Heterogeneous
Form	metal complex	solid, often metal or metal oxide
Activity	high	variable
Selectivity	high	variable
Thermal stability	often decomposes <100ºC	high
Reaction conditions	mild	drastic
Lifetime	variable	long
Poisoning	low	high
Diffusion problems	none	possible
Recycling	difficult (expensive)	easy
Recovery	difficult	easy
Variation of steric and electronic properties	possible	difficult
Intelligibily of the mechanism	possible	difficult

Currently, catalytic synthesis of fine chemicals is largely dominated by homogeneous phase systems, which adds environmental issues to the overall procedures.[2b,20] The immobilization of chemical catalysts onto solid, insoluble support materials offers significant benefits in terms of ease of reuse of the precious catalysts, clean catalyst separation as well as integration in existing reactor equipments.[21] Due to this, chemical industry has a great preference for solid catalysts for both economical and environmental reasons, provided that: i) they are easily accessible in the requested amount at competitive costs, ii) show significant operationally advantages over the corresponding homogeneous systems and iii) their scope and limitations are known.[22] However, further efforts are necessary in the design of new heterogeneous catalysts to reach competitive activity and selectivity values compared to homogeneous ones.

1.5. HETEROGENEOUS CATALYSIS

In the last two decades, with the advancement in green chemistry, heterogeneous catalysis has moved into the fine chemicals and pharmaceuticals industry.[23] There has been a considerable amount of research carried out in the development of new catalytic systems featured by high activity and selectivity, characteristic from homogeneous catalysis, and ease of recovering and recycling typical from heterogeneous catalysts, filling like this the gap between these two worlds. One of the strategies adopted has been the heterogenization of homogeneous systems. Therefore, solid catalysts can be divided into bulk/unsupported catalysts and impregnated/supported catalysts.[24]

- *Unsupported catalysts* are typically (mixed) metals or oxides where the entire catalyst is made of active material. Some examples are zeolites (acid) or Raney catalysts.

- *Supported catalysts* are commonly used in the case of precious metals or unstable compounds. They are also known as *heterogenized catalysts*. The active metal precursor (metal salt, organometallic complex, coating powder) is deposited on a porous bulk support. The support can be an oxide (e.g. silica, titania, alumina or ceria), an activated carbon, or even an organic or hybrid polymer resin. Examples include Pd/C hydrogenation catalysts[25] or Pt/Sn/Al$_2$O$_3$ dehydrogenation catalyst.[26] From now on, all the attention will be paid to this kind of catalysts considering that the catalytic system developed in the present thesis belong to the mentioned group.

There are different synthetic protocols for preparing supported catalysts, they are summarized in Scheme 1.1.[22a,27]
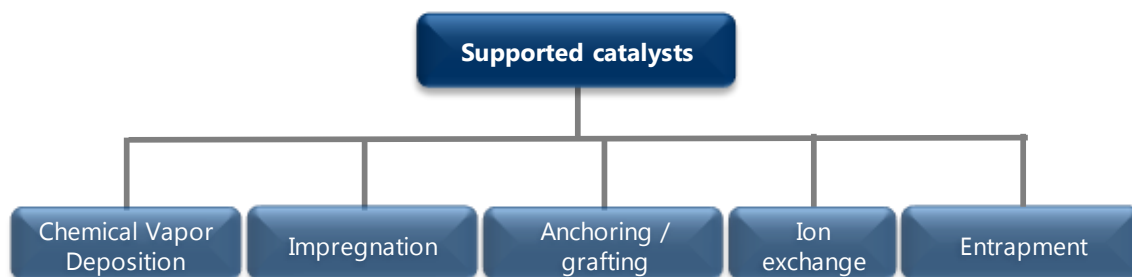
Scheme 1.1. Preparation methods for supported catalysts.

- *Chemical Vapor Deposition (CVD):* Catalyst preparation can be conducted by vaporizing a suitable precursor and adsorbing it on the support material. Subsequently, as a result of a surface reaction with or without a co-reactant, the adsorbate is transformed to the catalytically active specie. The key to controlling metal's dispersion is the understanding of the relationship between the precursor properties and the surface reactivity.

- *Impregnation*: Several impregnation methods may be used:

(i) by immersion (dipping) where the calcined support is immersed in an excess of solution containing the metal compound. The solution fills the pores and is also adsorbed on the support surface. The excess volume is drained off.

(ii) by incipient wetness: a solution containing the metal compound and having a volume equal or slightly less than the pore volume of the support is added to a porous solid. Capillary action draws the solution into the pores, keeping the metallic compound exclusively into them. Then, the impregnated support is dried and calcined.

(iii) difussional: the support is saturated with water or acid solution and then immersed into the aqueous solution containing the metal compound.

- *Anchoring* or *grafting* is a process in which stable, covalent bonds are formed between a homogeneous transition metal complex and an inert polymer or inorganic support. The aim is to combine the potential versatility

and selectivity of homogeneous catalysts with the practical advantages of a solid material. There is a chemical reaction between functional groups (e.g. hydroxyl groups in silica materials) on the surface of the support and an appropriately selected inorganic or organometallic compound of the active element (e.g. terminal triethoxysilane groups).

- *Ion exchange*: The metal ions are deposited by ion exchange onto a support that can be inorganic (zeolites) or organic (functionalized resins), and then reduced. Well-dispersed materials are obtained. The metal loading is restricted by the ion exchange capacity of the support utilized.

- *Entrapment or 'Ship in a bottle'*: In both cases, the catalyst gets occluded within the pores of a solid support and cannot diffuse out. However, the synthetic approach is different; while the *entrapment* strategy consists in synthesizing the inorganic support starting from a solution that contains the homogeneous catalyst, in the *ship in a bottle* method the catalyst is built inside the pores of a pre-existing support.

Many supports can be used as carrier material. They are featured by chemical nature, morphology, surface area, pore volume, pore size distribution, particle size, corrosion resistance, acid-base properties and ability to give rise to metal-support interaction. The support plays an active role in the catalytic reaction, thus in order to make a catalyst feasible and effective for a specific application, attention must be paid to: i) reduction the amount of expensive active metal loading, ii) increase the metal dispersion, iii) stabilization of metal particle size, iv) improvement of mechanical resistance, v) generation of additional active sites leading to bifunctional catalysts.

Catalysts in which the active component is a metal are much used in fine chemical industry, generally to perform hydrogenations[28,29] and oxidations.[29,30] When the metal precursor has been deposited onto a support, the catalyst can

be activated by further reduction obtaining afterwards supported metal nanoparticles (MNPs)

1.5.1. METAL NANOPARTICLES IN HETEROGENEOUS CATALYSIS

Metal nanoparticles, with their unique optical and catalytic properties, have attracted substantial attention over the past few decades.[31] At least one dimension of these nanomaterials is in between 1 and 100nm, being this the reason to exhibit unusual chemical and physical properties different from those of the bulk material or of the atoms.[32] One of the important factors of the nanosize regime is the presence of a large percentage of atoms at the surface (high surface area to volume ratio), what enhances its catalytic activity.[33] In addition, the concentration of low coordinated sites (defect sites) is relatively abundant. These sites usually show low activation barrier,[34] so nanoparticles can easily undergo aggregation, hence the need to be stabilized by ligands, surfactants or by the support where they are immobilized on. On the other hand, when nanoclusters are deposited on surfaces, their physical and chemical properties are strongly dependent not only on their particle size and chemical composition, but also on the structure of the surface and that of the metal/substrate interface.

In fine chemicals industry, when Raney type catalysts do not have the required activity and selectivity, the employment of precious metals is needed.[35] Because of the high price of precious metals, the use of nanoparticles represents a clear advantage, since larger metallic surfaces than in bulk materials can be obtained.

The acceleration of a chemical reaction by solid catalysts proceeds at the surface of the catalyst. The catalytic activity is generally proportional to the surface area of the nanoparticle per unit volume, however, the species involved

must get *to* and *from* the surface, and thus the diffusion phenomenon must be also considered (see Fig. 1.4.).
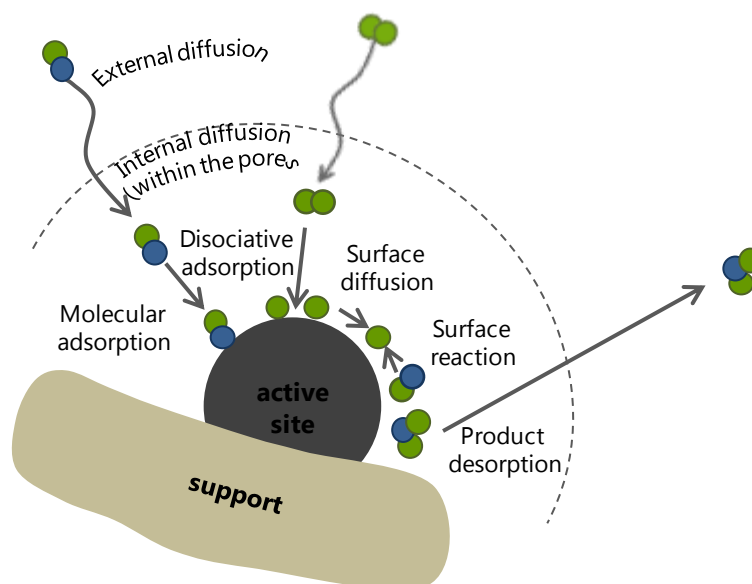
Fig. 1.4. Steps involved in a chemical reaction catalyzed by supported MNPs.

For supported metal nanoparticles, the term *dispersion* refers to the ratio of the number of metal atoms on the surface to the total number of metal atoms within the nanoparticle.[36] As shown in Fig 1.5., in an 8-atom cluster all the atoms are on the surface, nevertheless, the dispersion declines rapidly with increasing cluster size and so the surface area on which the reaction is carried out.
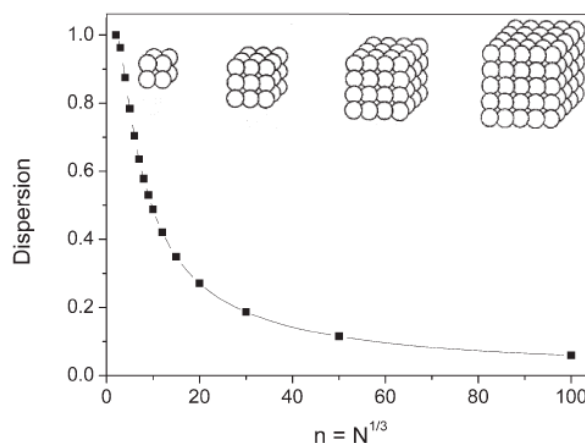
Fig. 1.5. Evolution of the *dispersion* as a function of *n* for cubic clusters up to n=100 (N=10^6). The structure of the first four clusters is displayed.[37]

Precious metals need to be employed as very small particles with most of the metal atoms in the surface, which calls for metal dimension of ca 2 to 5nm and metal loading usually less than ca 3 wt%.

Solid MNPs-based catalysts are largely employed in everyday life processes, including pollutants abatement, processing of raw materials, synthesis of base organic chemicals and energy production.[38] Some examples are the synthesis of ammonia with iron nanoparticles supported on inorganic oxides like Al_2O_3, MgO, CaO, K_2O;[39] platinum nanoparticles supported onto alumina/silica for hydrocarbon cracking;[40] or palladium nanoparticles onto organic polymers for the synthesis methyl isobutyl ketone and methyl-*tert*-butyl ether.[41] However, MNPs for application in regio-, chemo-, stereo- or enantioselective catalysis on large scale are far less developed.[42] Indeed, despite the aforementioned favorable opportunities, MNP catalysts have not yet found broad opportunities in complex molecule synthesis, with few applications thus far limited to cross-couplings and oxidations/reductions. Processes are in place with the hydrogenation of alkynes by the Pd Lindlar-type catalysts,[43] and for the production of the herbicide Prosulfuron[TM] and the sunscreen agent 2-ethylhexyl-*p*-methoxy-cinnamate by the Pd Heck reaction.[44]

Nevertheless, all preparation methods for supported MNPs suffer from one or more drawbacks, including lack of reproducibility and/or complex synthetic procedure. Moreover, the routes described in the literature normally use organic solvents, hazardous reagents ($NaBH_4$, hydrazine), stabilizing agents or harsh conditions. In order to make their industrial application acceptable, more sustainable methods for MNPs synthesis than those currently used are thus required. The need of routes involving minimal reagents and mild conditions has been already mentioned (see Section 1.3.).

1.5.2. ION EXCHANGE RESINS AS SUPPORTS FOR MNPs

Ion exchange resins are polymers that are capable of exchanging particular ions within the polymer with ions in a solution that is passed through them. These exchanges take place without any physical alteration to the ion exchange material. The basic chemical structure of ion exchangers is the same for most of them. They are quite often formed by polystyrene-divinylbenzene (PS-DVB) cross-linked frameworks, with different kind and degree of functionalization, cross-linking degree, specific surface area and porosity.[45] Some examples of different functionalized ion exchange resins are shown in Scheme 1.2.
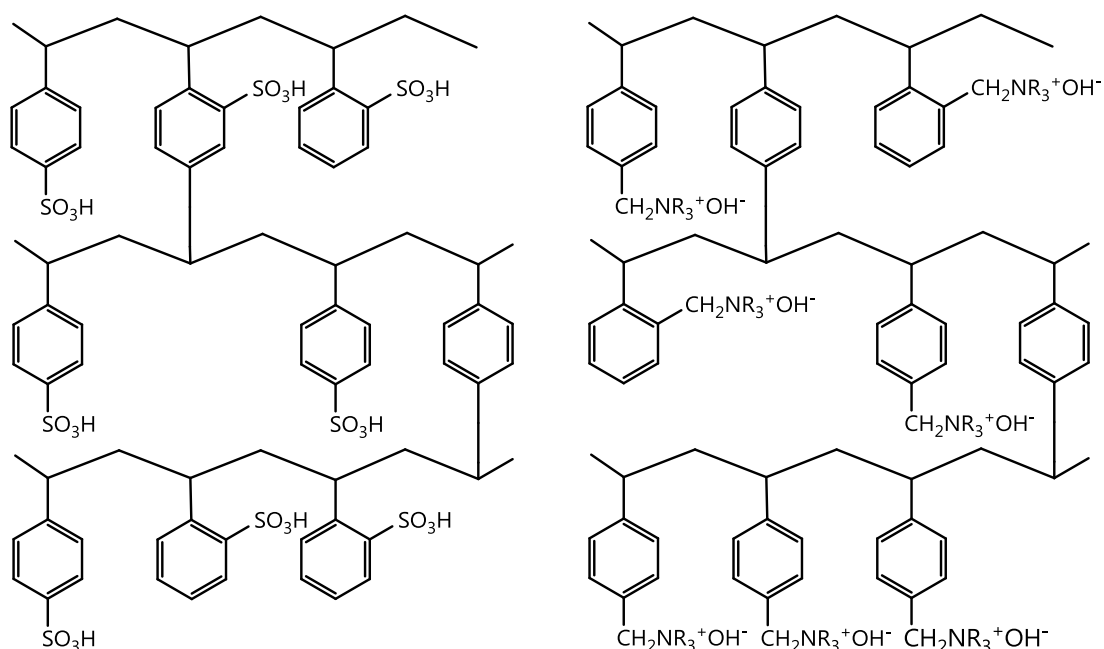
Scheme 1.2. Examples of ion exchange resins with different functionalization, a strongly acidic sulphonated polystyrene cation exchange resin (left) and a strongly basic quaternary ammonion anion exchange resin.

The resins are commercially prepared as spherical beads with a solid appearance.[46] The beads have either a dense internal structure with no discrete pores (gel resins, also called microporous resins) or a porous, multichannelled structure (macroporous or macroreticular resins). A simplified comparison between the gel-type and macroreticular resins at different scales, from micro-

to nanometric scale, is depicted in Fig. 1.6. As shown in the figure, level 1 represents the dry materials. Level 2 is a representation of the microporous swollen materials at the same linear scale; swelling involves the whole polymeric mass in the gel-type resin and the macropore walls in the macroreticular resin. The morphology of the swollen polymer mass is similar in both gel-type and macroreticular resins (level 3). In the smallest scale, level 4, nanopores are formed by the void space surrounding the polymeric chains.[47]

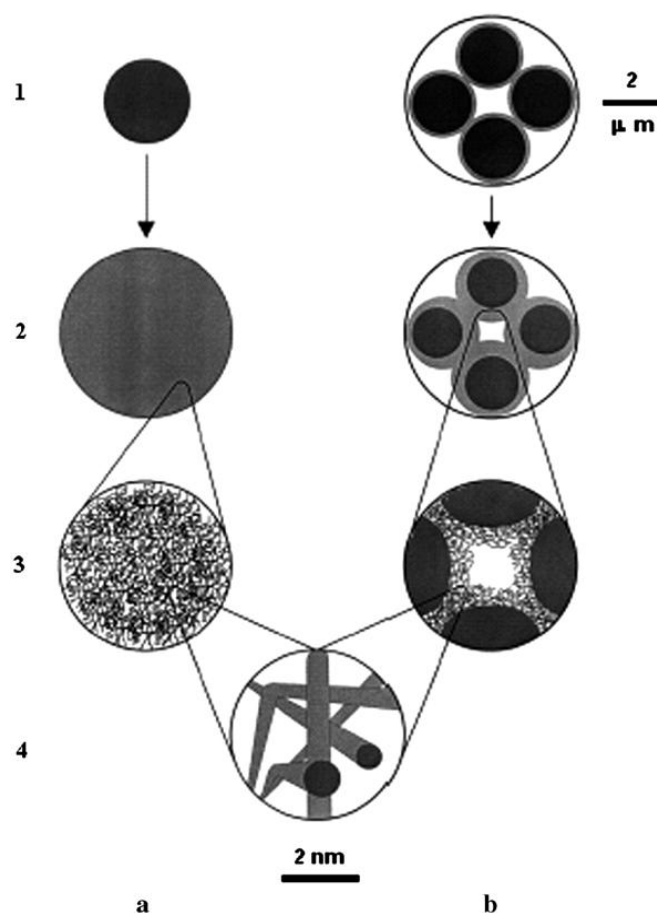**Fig. 1.6.** Schematic representation of the micro- and nanoscale morphology of gel-type **(a)** and macroreticular **(b)** resins. (Reprinted from reference [48])

The crucial feature of cross-linked functional polymers (CFP) is that they swell, to variable extent, when put in contact with some liquids. For this reason, their ability to accomplish a chemical task is limited only to their swollen state.[49]

These synthetic resins were initially used for purifying water and other applications including separating out some elements. The affinity of the functionalized resins for ions varies with the ionic size and charge of the ion, as example, for sulphonic acid resins the affinity is greatest for large ions with high valence (for dilute solutions, the order of affinity for some common cations is: $Hg^{2+}<Li^{+}<Na^{+}<<<Al^{3+}<Fe^{3+}$). However, the ready availability of these materials attracted the attention of chemists interested into chemical synthesis and processing, from both the academia and the industry. By the mid seventies, the catalytic potential of CFPs based on PS-DVB skeleton was demonstrated in heterogeneous acid catalysis,[50] and nowadays a few industrial processes catalyzed by CFP-based catalysts are in operation (see Table 1.4.), from them by far the most important one is the synthesis of MTBE (total capacity plant about 20×10^6 tons per year).[51,52]

Table 1.4. Selection of industrial acid-catalyzed reactions promoted by CFPs.

Product	Reagents	Catalyst
Alifatic esters	Carboxylic acids + olefins	N.A. [a]
Acrylic esters	Acrylic acid + olefins	N.A.
Isopropanol	Propene + water	Macroreticular, 8–10% DVB[b]
Bisphenol A[c]	Phenol + acetone	Gel-type, modified with cysteamine[d]
o-Phenylphenol[e]	Cyclohexanone	Macroreticular
Phenol alkylates	Phenol + olefins	Macroreticular
1-Butene oligomers	Isobutene	Powdered, diameter ca. 30 μm
MTBE[f]	Methanol + isobutene	Macroreticular

[a] Not available. [b] Divinylbenzene. [c] 2,2-di(4-hydroxy)phenylpropane. [d] The –SH function serves as the co-catalyst. [e] Via dianone, 2-(1-cyclohexenyl)-cyclohexanone. [f] Methyl *t*-butyl ether.

But in spite of the scientific novelty and of potential further technological breakthroughs shown for these polymeric supports, the concept of CFPs-supported heterogeneous metal catalysts has not been very successful. Besides a few patents issued to Bergbau Chemie[53] and to Mobil Oil[54] describing the use of

CFPs as supports for metal nanoclusters and as carriers for heterogenized metal complexes respectively, not many papers have been published on this subject.

Nevertheless, in the last ten years, research in this field has clearly accelerated with main contributions from Corain and associates[55] and from Ley's group in Cambridge.[56] Development of Ley's work has even led to the commercialization of the micro-encapsulated Pd^{II} and Pd^{0}-EnCat catalysts.[57]

One of the possible reasons why CFPs have not been much explored as catalysts supports can be the higher price with respect to conventional inorganic supports. This is clearly a disadvantage where the catalyst's price is a major processing cost, due to low added value of the product and/or to the huge catalyst's loads typical of large-scale production. However, fine chemicals are usually organic substances of relatively low thermal stability and are synthesized under mild to moderate conditions, which are compatible with the employment of cross-linked polymers as supports for metal catalysts. In this perspective the use of CFPs as catalytic supports is economically feasible. The (industrial) synthesis of fine chemicals is typically carried out on a relatively small scale and the products have generally a high added value. These circumstances can make the catalyst cost acceptable even for relatively expensive ones.

In conclusion, the scope of polymeric supports in heterogeneous metal catalysis has been steadily expanding in recent years and it is expected that it will be even more so in the close future, with predictable scientific and technological breakthroughs.

1.6. FLOW CATALYSIS

It has been mentioned several times along this *Introduction* chapter the need of developing greener and safer chemical processes for the large scale production of fine chemicals. The first approach would be the use of selective catalysts instead of stoichiometric reagents, which reduces the large amounts of waste generated, characteristic from fine chemicals manufacture (high E factors). In a second step, the substitution of homogeneous catalysts (extensively used in industry) by heterogeneous ones, offers significant benefits in terms of clean separation and reuse of the precious catalyst. An additional value is the use of MNPs catalysts supported onto insoluble materials. So then, the final step in this race would be the use of the cited supported catalysts in continuous flow mode instead of batchwise. Use of continuous-flow reactors allow reactions to be carried out with greater efficiency and much lower energy and space requirements compared to the corresponding batch processes. Basically, in a continuous process, reactants flow through a catalytic "chamber" where they react to form the desired products that subsequently leave that chamber to be collected. The continuous removal of the reaction products also enhances the catalyst's lifetime and minimizes the purification procedures. Of course, this is an easy way to describe the situation, in practice, is not that simple.

Nowadays, flow chemistry, an old process concept for industry, has reached chemical laboratories, being conducted in miniaturized apparatuses in the laboratory.[58] Common miniaturized bench-size flow devices can be classified depending on the inner diameter of the tubes/channels that form the reactor in:

- Micro flow reactors: 10-500 μm i.d.

- Mini (meso) flow reactors: 500 μm to several mm i.d.

A comparative chart explaining the main advantages and disadvantages of these two systems is shown in Table 1.5.

Table 1.5. Micro versus mini (meso) flow reactors.

	Microfluidic		Minifluidic
✓	high heat transfer surface to product volume ratios	X	lower heat transfer surface
✓	good heat transfer capabilities	X	poor heat transfer capabilities
X	micro channels suffer from restricted flow capacity	✓	improved flow capacities
X	high pressure drop	✓	lower pressure drop
X	tendency to block	✓	no blocking of channels
✓	ideally suited for optimizing reactions conditions	✓	preparation of multigram to multikilogram quantities
✓	efficient mixing	✓	possibility to work with packed bed reactors

In both cases, continuous flow reactors show several advantages comparing to batch processes in terms of safety, scale production, and scale-up issues. The excellent heat and mass transfer properties, together with efficient mixing of miniaturized flow devices have made them ideal tools for carrying out i) highly exothermic reactions that if performed in batch mode it could be unsafe or unfeasible due to thermal decomposition of the products, ii) synthesis using hazardous reagents, or iii) creation of highly reactive intermediates.[59] On the other hand, continuous flow reactors are generally smaller than batch reactors but in an ideal setup and under optimized conditions, they are able to produce bigger amount of product in a given time than an analogous batch reactor.[60] Furthermore, reaction parameters such as temperature, concentration, composition of reactants established for a small scale process can directly be transferred to larger flow reactors, without the need for substantial re-optimization.[61]

In addition to simple tube-like hollow reactors, packed bed reactors have lately seen application in the synthesis of drug chemicals. These fix bed reactors are often functionalized with heterogeneous supported catalysts, but one must be aware that when packing is irregular they show uncontrolled fluid dynamics which results in poor efficiency due to hot spot formation, stagnation zones and broad residence time distribution.

Working under flow conditions offers other possibilities such as multi-step synthesis by using linearly link flow reactors, thereby minimizing work-up and isolation protocols, multicomponent reactions or photochemical synthesis.[62] In any case, even if it cannot be assured that it will solve the current problems in the pharmaceutical sector, flow technology is a powerful tool that has to be taken into account and correctly evaluated when new catalytic systems are developed.

1.7. MOTIVATION AND AIM OF THE WORK

The development of sustainable routes for the large scale production of fine chemicals, i.e. cost-effective and environmentally friendly, is one of the major current concerns at the industrial level. Highly active and selective catalysts may significantly contribute to solve the problem, however, their elaboration often ends up being very sophisticated and expensive. Moreover, catalytic synthesis of fine chemicals is still largely dominated by homogeneous phase systems, which adds environmental issues on the overall procedures. Among the strategies proposed to achieve low-impact processes, the immobilization of chemical catalysts onto insoluble support materials offers significant benefits in terms of ease of reuse of the precious catalysts, clean catalyst separation as well as integration in reactor equipments. Due to this, chemical industry has a great preference for solid heterogeneous catalysts. On the other hand, use of

continuous-flow reactors represents a considerable added value in this regard, as they allow reactions to be carried out with greater efficiency and much lower energy and space requirements compared to the corresponding batch processes, in addition, continuous removal of the reaction products enhances the catalyst's lifetime and simplifies the purification procedures.

The present work aims to overcome this challenging task by developing a simple and green method, devoid of harsh conditions or polluting agents and based on commercial products, for the synthesis of solid-supported catalysts easily integrated in both batch and flow reactor equipments. These catalysts will be deeply explored and optimized for the preparation of chemicals whose synthesis requires highly selective processes (pharmaceuticals, agrochemicals, fragrances). The project will contribute to fill the gap between the potential of heterogeneous catalysis and the application to sustainable production of fine chemical compounds.

REFERENCES

1   P. Sands, J. Peel, A. Fabra, R. MacKenzie, *Principles of International Environmental Law*, Cambridge University Press, New York, **2012**.

2   a) P.T. Anastas, J.C. Warner (Eds), *Green Chemistry: Theory and Practice*, Oxford University Press, New York, **1998**. b) F. Cavani, G. Centi, S. Perathoner, F. Trifirò (Eds), *Sustainable Industrial Chemistry*, Wiley-VCH, Weinheim, **2009**. c) P.T. Anastas, T.C. Williamson (Eds), *Green Chemistry: Frontiers in Chemical Synthesis and Processes*, Oxford University Press, New York, **1998.**

3   a) J.A. Dahl, B.L.S. Maddux, J. E. Hutchison, *Chem. Rev.*, 107, **2007**, 2228; b) V.L. Budarin, J.H. Clark, R. Luque, D.J. Macquarrie, J. White, *Green Chem.*, 10, **2008**, 382.

4   Information obtained from the official website of The Organisation for Economic Cooperation and Development, (*http://www.oecd.org*). Retrieved Oct **2012**.

5   Information obtained from the official website of European Technology Platform for Sustainable Chemistry, (*http://www.suschem.org*). Retrieved in Oct **2012**.

6   a) R.A. Sheldon, *Green Chem.*, 9, **2007**, 1273. b) R.A. Sheldon, *Pure Appl. Chem.*, 72, **2000**, 1233.

7   R.A. Sheldon, *Chemtech,* 24, **1994**, 38.

8   M. Kanneigiesser, *Value Chain Management in the Chemical Industry: Global Value Chain Planning of Commodities*, Physica-Verlag, Heidelberg, **2008**.

9   A. Cybulski, M.M. Sharma, R.A. Sheldon, J.A. Moulijn, *Fine Chemicals Manufacture: Technology and Engineering*, Elsevier Science B.V., Amsterdam, **2001**.

10   J. Hagen, *Industrial Catalysis: A Practical Approach*, Wiley-VCH, Weinheim, Germany, **2006**.

11   K.J. Laidler, J.H. Meiser (Eds), *Physical Chemistry: A Solution Manual*, Benjamin-Cummings Publishing, **1982**, 423.

12   F.W. Ostwald, *Ibid.*, 15, **1894**, 706.

13   "Recognizing the Best in Innovation: Breakthrough Catalyst", *R&D Magazine*, September **2005**, 20.

14   http://www.climatetechnology.gov/library/2005/tech-options/tor2005-143.pdf

15   R.A. Sheldon, H. van Bekkum, *Fine Chemicals through Heterogeneous Catalysis*, Wiley-VCH, Weinheim, Germany, **2001**.

16   German Catalysis Society, Roadmap for catalysis research in Germany, March **2010**.

17   R.A. Sheldon , *J. Chem. Tech. Biotechnol.*, 68, **1997**, 381.

18   M. Boudart, *Chem. Rev.*, 95, **1995**, 661.

19   G. Rothenberg, *Catalysis: Concepts and Green Applications*, Wiley-VCH, Weinheim, Germany, **2008**.

20   a) J.H. Clark, D.J. Macquarrie, *Handbook of Green Chemistry and Technology,* Blackwell Science, Oxford, **2002**; c) J.H. Clark, *Green Chem.*, 8, **2006**, 17.

21   a) P. Barbaro, F. Liguori (Eds)*, Heterogenized Homogeneous Catalysts for Fine Chemicals Production*, Springer, London, **2010**; b) D.J. Cole-Hamilton, R.P. Tooze (Eds), *Catalyst Separation, Recovery and Recycling; Chemistry and Process Design*, Springer, Dordrecht, **2006**; c) M. Benaglia (Ed)*, Recoverable and Recyclable Catalysts*, Wiley-VCH, Weinheim, **2009**; d) J.A. Gladysz (Ed), *Recoverable Catalysts and Reagents*, S*pecial issue of Chem. Rev.*, 102, **2002**, 3215.

22   a) B. Pugin, H.U. Blaser, *Top. Catal.*, 53, **2010**, 953. b) N. End, K.U. Schöning in *Immobilized Catalysts: Solid Phases, Immobilization and Applications* (Ed A. Kirschning), Springer, Heidelberg, **2004**, 241.

23   C.H. Peterson, S.D. Rice, J.W. Short, D. Esler, J.L. Bodkin, B.E. Ballachey, D.B. Irons, *Science*, 302, **2003**, 2082.

24 a) C. Perego, P. Villa, *Catal. Today*, 34, **1997**, 281. b) J.A. Schwarz, C. Contescu, A. Contescu, *Chem. Rev.*, 95, **1995**, 477.

25 Multitude of reports about Pd/C catalysts can be found elsewhere, for a review about supported Pd catalysts see: H-U. Blaser, A. Indolese, A. Schnyder, H Steiner, M. Studer, *J. Mol. Catal. A: Chem.*, 173, **2001**, 3.

26 a) F.C. Wilhelm, U.S. Patent 3909451, **1974**; b) T. Imai, C.W. Hung, U.S. Patent 4866211, **1989**.

27 a) B. Delmon, P.A. Jacobs, R. Maggi, J.A. Martens, P. Grange, G. Poncelet (Eds), *Preparation of Catalysts VII*, Vol. 118, Elsevier, Amsterdam, **1998**; b) D.S.J. Jones, P. R: Pujadó (Eds), *Handbook of Petroleum Processing*, Springer, Dordrecht, The Netherlands, **2006**; c) G. Ertl, H. Knözinger, J. Weitkamp (Eds), *Preparation of solid catalysts*, Wiley-VCH, Weinheim, Germany, **1999.**

28 a) H-U. Blaser, C. Malan, B. Pugin, F. Spindler, H. Steiner, M. Studer, *Adv. Synth. Catal.*, 345, **2003**, 103; b) R.M. Machado, K.R. Heier, R.R. Broekhuis, *Curr. Opin. Drug Discov. Devel.*, 4, **2001**, 745.

29 a) S.M. Roberts, G. Poignant (Eds), Catalysts for Fine Chemical Synthesis: Hydrolysis, Oxidation and Reduction, Vol. 1, John Wiley & Sons Ltd., Chichester, UK, **2002**; b) S.M. Roberts, J. Whittall, Catalysts for Fine Chemical Synthesis: Regio- and Stereo-Controlled Oxidations and Reductions, Vol. 5, John Wiley & Sons Ltd., Chichester, UK, **2007**.

30 a) W.F. Hoelderich, F. Kollmer, *Pure Appl. Chem.*, 72, **2000**, 1273; b) T. Mallat, A. Baiker (Eds), *Special issue of Catal. Today*, 57, **2000**.

31 T. Anniyev, H. Ogasawara, M.P. Ljungbrg, K.T. Wikfeldt, J.B. MacNaughton, L.A. Näslund, U. Bergmann, S. Koh, P. Strasser, L.G.M. Pettersson, A. Nilsson, *Phys. Chem. Chem. Phys.*, 12, **2010**, 5694.

32 G. Schmud (Ed), *Nanoparticles: From Theory to Application*, Wiley-VCH, Weinheim, Germany, **2010**.

33 A.S.K. Hashmi, G.J. Hutchings, *Angew. Chem. Int. Ed.*, 45, **2006**, 7896.

34 C.J. Weststrate, A. Resta, R. Westerström, E. Lundgren, A. Mikkelsen, J.N. Andersen, *J. Phys. Chem. C*, 112, **2008**, 6900.

35 a) H-U. Blaser, M. Studer, *Appl. Catal. A: Gen.*, 189, **1999**, 191; b) W. Mägerlein, C. Dreisbach, H. Hugl, M.K. Tse, M. Klawonn, S. Bhor, M. Beller, *Catal. Today*, 121, **2007**, 140.

36 J.E. Benson, M. Boudart, *J. Catal.*, 4, **1965**, 704.

37 E. Roduner, *Chem. Soc. Rev.*, 35, **2006**, 583.

38 a) D. Astruc (Ed), *Nanoparticle and Catalysis*, Wiely-VCH, Weinheim, **2007**; b) B.F.G. Johnson, *Top. Catal.*, 24, **2003**, 147; c) R.J. White, R. Luque, V.L. Budarin, J.H. Clark, D.J. Macquarrie, *Chem. Soc. Rev.*, 38, **2009**, 481; d) B. Zhou, S. Hermans, G. A. Somorjai (Eds), *Nanotechnology in Catalysis*, Springer, Berlin, **2004**, Vol. 1; e) S. Wang, Z. Wang, Z. Zha, *Dalton Trans.*, **2009**, 9363; f) L. Durán Pachón, G. Rothenberg, *Appl. Organomet. Chem.*, 22, **2008**, 288.

39 a) N.D. Spencer, R.C. Schoonmaker, G.A. Somorjai, *J. Catal.*, 74, **1982**, 129; b) D.R. Strongin, J. Carrazza, S.R. Bare, G.A. Somorjai, *J. Catal.*, 103, **1987**, 213.

40 a) T.L.M. Maesen, M.J.P. Botman, T.M. Slaghek, L-Q. She, J.Y. Zhang, V. Ponec, *Appl. Catal.*, 25, **1986**, 35; b) T. Kusakari, K. Tomishige, K. Fujimoto, *Appl. Catal. A: Gen.*, 224, **2002**, 219.

41 a) J. G. de Vries, Can. J. Chem., 79, 2001, 1086, b) M. T. Vandersall, R. A. Weinand, Pat. EP 1321450A2, 2003.

42 K. An, G. A. Somorjai, *ChemCatChem*, 10, **2012**, 1442.

43 H. Bönnemann, W. Brijoux, K. Siepen, J. Hormes, R. Franke, J. Pollmann, J. Rothe, *Appl. Organomet. Chem.*, 11, **1997**, 783.

44 H. Cong, J. A. Porco Jr, *ACS Catal.*, 2, **2012**, 65.

45 K. Dorfner, *Ion-exchangers*, W. De Gruyter, Berlin/New York, **1991**.

46 See commercially available resins in:
http://www.dowwaterandprocess.com/products/sac.htm

47   A. Guyot in D. C. Sherrington, P. Hodge (Eds.), *Synthesis and Separations Using Functional Polymers*, Wiley, New York, **1988**, 1.

48   B. Corain, P. Centomo, S. Lora, M. Kralik, *J. Mol. Catal. A: Chem.*, 204–205, **2003**, 755.

49   B. Corain, G. Schmid, N. Toshima (Eds.), *Metal Nanoclusters in Catalysis and Materials Science: The Issue of Size Control*, Elsevier B.V., **2008**.

50   F. Ancillotti, E. Pescarollo, M. Massi Mauri, *US patent 4039590*, **1977**; b) F. Ancillotti, M. Massi Mauri, E. Pescarollo, *J. Catal.*, 46, **1977**, 49; c) G. J. Huthchings, C. P. Nicolaides, M. S. Scurrell, *Catal. Today*, 15, **1992**, 23.

51   B. Corain, M. Zecca, K. Jěrábek, *J. Mol. Catal. A: Chem.*, 177, **2001**, 3.

52   K. Weissermel, H. Arpe, *Industrial Organic Chemistry*, 4th ed., Wiley-VCH, Weinheim, **2003**.

53   a) J. Wöllner, W. Neier, Bergbau und chemie (Homberg), *German patent 1260454*, **1966**; b) H. Giehring, Bergbau und chemie (Homberg), *German patent 1238453*, **1965**; c) J. Wöllner, Bergbau und chemie (Homberg), *German patent 1193931*, **1963**.

54   W. O. Haag, D. D. Whitehurst, *German patent 1800371*, **1969**; b) W. O. Haag, D. D. Whitehurst, *German patent 1800379*, **1969**; c) W. O. Haag, D. D. Whitehurst, *German patent 1800380*, **1969**.

55   M. Králik, V. Kratky, M. De Rosso, M. Tonelli, S. Lora, B. Corain, *Chem. Eur. J.*, 9, **2003**, 209.

56   S. V. Ley, C. Mitchell, D. Pears, C. Ramarao, J. Yu, W. Zhou, *Org. Lett.*, 5, **2003**, 4665; b) J. Yu, H. Wu, C. Ramarao, J. B. Spencer, S. V. Ley, *Chem. Commun.*, **2003**, 678.

57   D. Pears, S. C. Smith, *Aldrichimica Acta*, 38, **2005**, 23.

58   J. Wegner, S. Ceylan, A. Kirschning, *Chem. Commun.*, 47, **2011**, 4583.

59   a) V. Hessel, *Chem. Eng. Technol.*, 32, **2009**, 1655; b) R. L. Hartman, K.F. Jensen, *Lab Chip*, 9, **2009**, 2495; c) X.Y. Mak, P. Laurino, P.H. Seeberger, *Beilstein J. Org. Chem.*, **2009**, 5(19).

60   See for example: K. Geyer, J.D.C. Codee, P.H. Seeberger, *Chem.–Eur. J.*, 12, **2006**, 8434.

61   V. Hessel, presented at the 1st RSC/SCI *Symposium on Continuous Processing and Flow Chemistry*, 3rd–4th November **2010**.

62   a) B. Khanetsky, D. Dallinger, C.O. Kappe, *J. Comb. Chem.*, 6, **2004**, 884; b) W.S. Bremner, M.G. Organ, *J. Comb. Chem.*, 9, **2007**, 14.

2

Description of Experimental Techniques Used

2.1. OVERVIEW

The aim of this chapter is to briefly explain the experimental techniques that have been used to carry out a thorough characterization of the synthesized supported catalysts, likewise the equipments used in other sections of the current study such as catalytic testing are described. Explanation of continuous flow reactors and the chemical reactors used for medium/high pressure experiments in batch conditions is also provided. General notions are given with focus on most important aspects for the present work.

2.2. CATALYSTS CHARACTERIZATION TECHNIQUES

After nanoparticles are successfully synthesized, the first necessary step before any further application is characterization. Because of the small size of nanoparticles (< 100 nm), some conventional characterization techniques are no longer applicable. Judicious selection of characterization techniques is required for obtaining meaningful evaluation of nanoparticles on hand. Characterization of nanoparticles generally includes the following aspects: size, shape, morphology, crystal structure and composition. Each aspect can be characterized by multiple techniques, Table 2.1. summarizes the techniques that have been used in this study.[1]

Table 2.1. Nanoparticle characterization techniques.

Characteristics	Techniques
Size, shape, morphology	• Dynamic light scattering (DLS)
	Microscopy
	• Optical microscopy
	• Environmental Scanning Electron Microscopy (ESEM)
	• Transmission Electron Microscopy (TEM)
	• Scanning Transmission Electron Microscopy (STEM)
	X-ray
	• X-ray diffraction (XRD)
	• Small angle X-ray scattering (SAXS)
Crystal structure	• X-ray diffraction
	• Transmission electron Microscopy
Composition	• Energy dispersive X-ray Spectroscopy (EDS)
	• Inductively Coupled Plasma - Optical Emission Spectroscopy (ICP-OES)

Regarding the final catalyst, the location where the nanoparticles are placed in the support material, as well as its morphology, are other important parameters to study because of their potential influence in the catalysts efficiency. Next, the different techniques used for the characterization of the supported metal

nanoparticles (MNPs) and the final catalyst are described in detail, as well as the specific equipment employed for the analyses.

2.2.1. MICROSCOPIC TECHNIQUES

Microscopy is the discipline that uses microscopes to view objects. A microscope is an instrument that produces enlarged images of small objects, allowing the observer an exceedingly close view of minute structures at a scale convenient for examination and analysis. An image may be enlarged by many wave forms, including visible light, acoustic, X-ray, or electron beam, and be received by direct or digital imaging or by a combination of these methods. The magnifying power of a microscope is an expression of the number of times the object being examined appears to be enlarged and is a dimensionless ratio. It is usually expressed in the form 10× (for an image magnified 10-fold). The resolution of a microscope is a measure of the smallest detail of the object that can be observed.[2] Even though microscopy is the most straightforward technique for nanoparticle characterization, it is limited to only offering two dimensional projections of three dimensional objects.

2.2.1.1. Optical microscopy

The optical microscope, often referred to as the "light microscope", is a type of microscope that uses visible light and a system of lenses to magnify images of small samples. Optical microscopes can be simple, consisting of a single lens, or compound, consisting of several optical components in line. Single-lensed simple microscopes can magnify up to 300×, while compound microscopes can magnify up to 2000×. Images can be captured by photography through a microscope, a technique known as photomicrography.

This technique was used for the characterization of the bead-shaped polymer used as support for the immobilization of metal nanoparticles (MNPs). The optical microscope used to acquire the images was a Nikon Eclipse E600, equipped with

a 12 V 100 W LL halogen lamp. The images were acquired in reflectance mode using fibers optic as source. The magnification of the observations was in the range 1–20X. The software for the acquisition was Nikon ACT-1.

2.2.1.2. Electron microscopy

Alternatives to optical microscopy which do not use visible light but a beam of electrons in the image formation include scanning electron microscopy (SEM) and transmission electron microscopy (TEM). Historically, electron microscopes were developed due to the limited image resolution of optical microscopes, which is imposed by wavelength of visible light. Electron microscopes use electrons to illuminate a specimen and because electrons have a much smaller wavelength than light (0.02 Å and 4000 Å respectively) these microscopes can show much smaller structures.[3]

Electrons are one type of ionizing radiation, which is the general term given to the radiation capable of removing the tightly bond, inner-shell electrons from the attractive field of the nucleus by transferring some of its energy to individual atoms in the specimen. One of the advantages of using ionizing radiation is that a wide range of secondary signals arises from the specimen which can be collected by different types of detectors and analyzed to give different information about the sample. Some of these signals are summarized in Fig. 2.1.
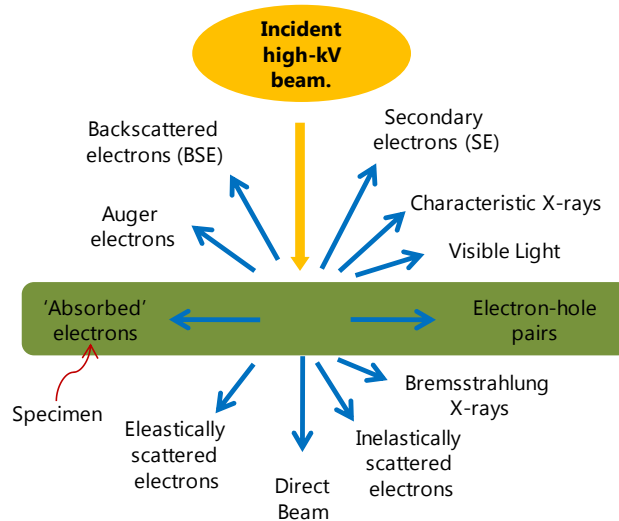
Fig. 2.1. Signals generated when a high-energy beam of electrons interacts with a thin specimen.

2.2.1.2.1. Environmental Scanning Electron Microscopy and Energy dispersive X-ray Spectroscopy

Environmental scanning electron microscope (ESEM) is a unique modification of the conventional scanning electron microscopy (SEM). While SEM operates with a modest vacuum ($\approx 10^{-3}$ Pa), ESEM is able to operate with gas pressures ranging between 10 Pa and 2700 Pa in the specimen chamber. This relaxed vacuum environment allows the examination of wet, oily and dirty specimens.

ESEM utilizes a gaseous secondary electron detector (GSED) that takes advantage of the gas molecules in the specimen chamber. The primary electron beam, operating between 10 kV and 30 kV, is generated from tungsten, lanthanum hexaboride, or field emission electron guns. When a primary electron beam strikes a specimen, it generates both backscattered and secondary electrons (see Fig 2.1.) that are collected for imaging of the sample topography. Backscattered electrons are energetic and are collected by a line-of-sight detector. The secondary electrons are low-energy and, as they emerge from the specimen, are accelerated towards the GSED by the electric field set up between the positive bias on the GSED and the grounded specimen stage. Conductive

coatings or low-voltage primary beams are needed to prevent surface charging under the electron beam.

Qualitative/Quantitative Analysis: In addition to the image-producing backscattered and secondary electrons that are generated when a primary beam strikes a specimen, there are also electron beam interactions that results in the generation of X-rays from the interaction volume (see Fig. 2.1.). The energy of the resulting X-rays is representative of the chemical composition within the interaction volume and can be measured by *Energy dispersive X-ray Spectroscopy (EDS)*, considered a qualitative method of compositional analysis. X-ray *counts* are plotted as a function of their energy, and the resulting peaks can be identified by element and line with standard X-ray energy tables.

ESEM can provide useful information about solid surfaces, in terms of composition and imaging, in a way that the conventional electron microscope cannot.[4]

In this Thesis, the above explained techniques were used for characterization of polymer supported nanoparticles made of palladium, rhodium, and gold; metal dispersion within the beads, composition and morphology of the support were also analyzed. ESEM measurements were performed on a FEI Quanta 200 microscope operating at 25 KeV accelerating voltage in the low-vacuum mode (1 torr) and equipped with an EDAX Energy Dispersive X-ray Spectrometer (EDS). X-ray maps were acquired on the same instrument using a 512x400 matrix, 25 KeV accelerating voltage and 350 μm horizontal full width.

2.2.1.2.2. Transmission Electron Microscopy and Scanning Transmission Electron Microscopy

Transmission electron microscopy is used to reveal sub-micrometre, internal fine structure in solids. The amount and scale of the information which can be extracted by TEM depends critically on four parameters; the resolving power of

the microscope (usually smaller than 0.3 nm); the energy spread of the electron beam (often several eV); the thickness of the specimen (typically about 100 nm), and the composition and stability.[5]

TEM uses transmitting electrons to obtain high magnification images of nanoparticles and measure particle size, shape and morphology. Since electrons are accelerated at a much higher voltage (100-400 KeV) than in SEM, the electron beam can be focus on a very small region to obtain high resolution images of nanoparticles (magnifying powers of more than 1,000,000×). The thin specimen is placed on a metal grid with carbon coating, by taking advantage of the contrast between the images of the nanoparticles and the carbon coating of the metal grid, nanoparticles can be quantified in size, size distribution and shape. In any case, both SEM and TEM techniques cannot distinguish composite nanoparticles if the image contrast from different compositions is small or if one composition fully coats the core particles of another composition.[1]

A scanning transmission electron microscope (STEM) is a type of electron microscopy in which the electron beam is focused into a narrow spot which is scanned over the sample, combining some working principles of TEM and SEM microscopes. The scanning of the beam across the sample makes STEM suitable for analysis techniques such as mapping by energy dispersive X-ray (EDX) spectroscopy, electron energy loss spectroscopy (EELS) and annular dark-field imaging (ADF). These signals can be obtained simultaneously, allowing direct correlation of image and quantitative data. Moreover, by using a STEM and a high-angle detector, it is possible to form atomic resolution images where the contrast is directly related to the atomic number (z-contrast image).

In the current research, TEM was used for size and size distribution characterization of polymer supported nanoparticles made of palladium, rhodium and gold while STEM techniques were used to characterize the polymer

supported colloidal Pd NPs synthesized in Chapter 6. TEM measurements were carried out using either a CM12 PHILIPS instrument at 100 keV accelerating voltage or a Leo 922 transmission electron microscope operating at 200 kV voltage, equipped with a built-in omega filter for electron energy loss spectroscopy (EELS). STEM analyses were performed in a Tecnai 20 microscope operating at 200 kV, equipped with Bright Field and Annular Dark Field modes.

Samples were prepared by crushing the catalysts in an agate mortar, followed by sonication in ethanol and deposition of the supernatant onto a graphite grid. Statistical nanoparticle size distribution analysis was typically carried out on 200-300 particles.

2.2.2. X-RAY TECHNIQUES

The use of X-ray methods in the field of materials analysis is now entering its seventh decade. X-ray photons are a form of electromagnetic radiation produced following the ejection of an inner orbital electron and subsequent transition of atomic orbital electrons from states of high to low energy. When a monochromatic beam of X-ray photons falls onto a given specimen three basic phenomena may result, namely absorption, scatter or fluorescence. The coherently scattered photons may undergo subsequent interference leading in turn to the generation of diffraction maxima. These three basic phenomena form the bases of three important X-ray methods: the absorption technique, which is the basis of radiographic analysis; the scattering effect, which is the basis of X-ray diffraction (XRD); and the fluorescence effect, which is the basis of XRF spectrometry.[6]

2.2.2.1. X-ray powder diffraction

X-ray powder diffraction (XRD), which derives its name from the fact that the specimen is typically in the form of a microcrystalline powder, is a rapid analytical technique primarily used for phase identification of a crystalline material that can

provide useful information on the crystal phase, lattice constant and average particle size of nanoparticles.[7]

X-ray diffraction is based on constructive interference of monochromatic X-rays and a crystalline sample. These X-rays are generated by a cathode ray tube, filtered to produce monochromatic radiation, collimated to concentrate, and directed toward the sample. The interaction of the incident rays with the sample produces constructive interference (and a diffracted ray) when conditions satisfy Bragg's Law ($n\lambda = 2d\sin\theta$).
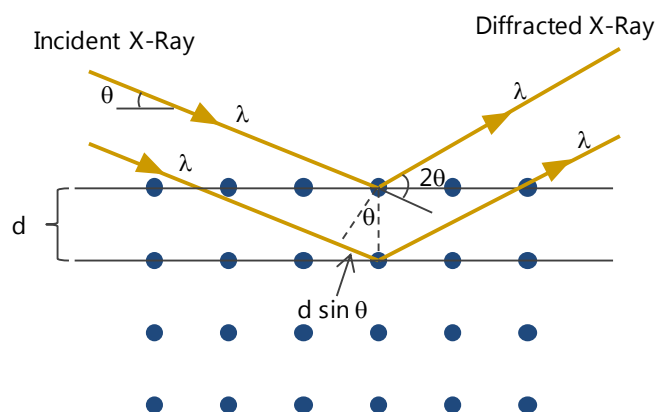

Fig. 2.2. Scheme of X-Ray diffraction from a cubic crystal lattice.

This law relates the wavelength of the X-rays (λ) to the diffraction angle (θ) and the spacing (d) of atomic planes.[8] These diffracted X-rays are then detected, processed and counted. By scanning the sample through a range of 2θ angles, all possible diffraction directions of the lattice should be attained due to the random orientation of the powdered material. Powder diffraction data are usually presented as a *diffractogram* in which the diffracted intensity is shown as function of the scattering angle 2θ. Each peak corresponds to diffraction from a particular set of interatomic planes whose spacing may be calculated from the Bragg equation, since we use X-Rays of known wavelength. This allows identification of the crystalline material because each one has a set of unique d-spacings.[9]

The XRD method is suitable to determine:

- crystal structures by analyzing the position and intensities of the diffraction peaks

- nanoparticle size by analyzing the peak profile (nanoparticles up to 100nm)[10]

In this study XRD was used for size characterization of polymer supported nanoparticles made of palladium and rhodium. XRD spectra were recorded with a PANanalytical XPERT PRO powder diffractometer, employing CuKα radiation (λ=1.54187 Å), a parabolic MPD-mirror and a solid state detector (PIXcel). The samples were subjected to measurement without grinding and prepared on a silicon wafer (zero background) that was rotating (0.5 rotations per second) during spectra acquisition. All XRD spectra were acquired at room temperature in a 2θ range from 4 to 95°, applying a step size of 0.0263° and a counting time of 77.5 seconds.

2.2.2.2. Small angle X-ray scattering

Small-angle X-ray scattering (SAXS) is a reliable and economic method for analyzing nanostructured materials. SAXS yields information such as particle sizes and size distributions, shape and orientation distributions in liquid, powders and bulk samples.[11] Any scattering process is characterized by a reciprocity law, which gives an inverse relationship between particle size and scattering angle. Particle dimensions (from 1 to 100 nm) are enormously large compared to the X-ray wavelength (e.g. the most frequently used CuK$_\alpha$ line of 1.54 Å) which makes the angular range of observable scattering correspondingly small.[12]

Conventional SAXS data (1D), collected by a point detector, such as a Kratky camera, are a curve of the scattered intensity versus the scattering angle. This kind of SAXS data can be used for samples either with isotropic structure or with

a particular orientation. SAXS data measured by two-dimensional detectors (2D) can reveal anisotropic features from specimens, such as from polymers, fibrous or layered materials, single crystals, and biomaterials.

The physical principle that rules SAXS technique is the observation of the coherent scattering from a sample as a function of the electron distribution in the sample. SAXS shows scattering angle (2θ) range from 0° up to roughly 2° or 3°. In a two-dimensional SAXS system, the scattered X-rays are measured in all 360° azimuthal angles simultaneously. The X-ray source used for SAXS can be a sealed tube or rotating anode generator (RAG). Small focal spots with high specific power loading on the target is preferred since long beam path, low divergence, and small beam size are typically required for SAXS, this is why collimation is the most critical part of a SAXS system since it defines the size, shape, and divergence of the X-ray beam. It also determines the resolution of a SAXS system.
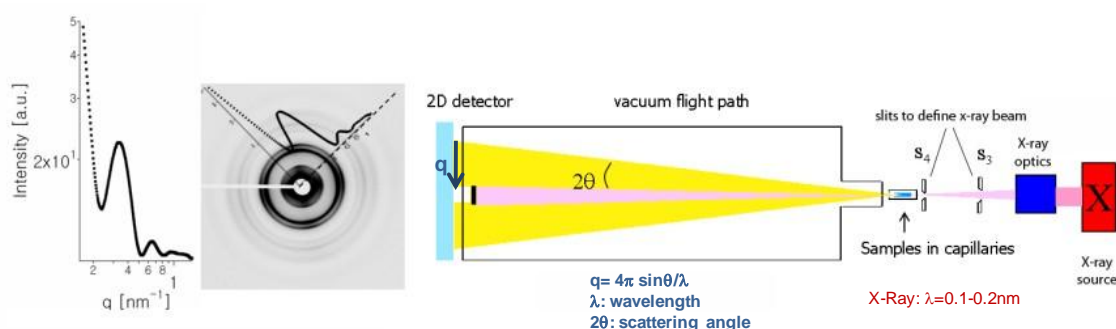

Fig. 2.3. Schematic representation of a SAXS set up.

In this work SAXS was used for size characterization of polymer supported palladium nanoparticles (Chapter 3). SAXS measurements were performed on a Hecus X-ray System GMBH Graz S3micro equipped with an ultra brilliant point microfocus source Gemix-Fox 3D (Xenoxs, Grenoble). The impinging radiation was the 1.54 Å CuK_α. The scattered X-rays were detected by a two-dimensional position sensitive detector with a sample-to-detector distance of 273 mm. The primary beam was masked by a 2 mm W filter, positioned so that the region of

scattering vectors q [Å^{-1}] was in the range 0.008<q<0.54. Here q has a modulus of $(4\pi/\lambda)\sin(\Theta/2)$ with λ the X-Ray wavelength and Θ the scattering angle. Samples were contained in a paste cell holder. The sample thickness was varied to have a transmittance around 0.8, measured as the area of the primary beam transmitted through the sample holder and a 1 mm Ni filter, without and with the sample. All measurements were collected at room temperature and with X-Ray source power of 12 W. The scattering profile was modelled with the empirical multiple level fit method developed by Beaucage, stopped at the second level plus a background term, to account for primary particles and their clusters. In order to be safely compared, the reduced data were normalized taking into account the acquisition time, the transmission and the source power.

2.2.3. DYNAMIC LIGHT SCATTERING

Dynamic light scattering (DLS) is a scattering method very useful for size and size dispersion analysis of colloidal suspensions. DLS uses visible light to hit the specimen and then measures the intensity autocorrelation function of light scattered from an ensemble of nanoparticles in solution. The particle size obtained is the hydrodynamic size and includes the ligand organic shell, so it will be larger than that observed in TEM which only visualizes the inorganic nanoparticle core. This is a useful technique to verify the organic shell thickness.[13]

This technique has been used to characterize colloidal palladium nanoparticles synthesized in Chapter 6 by using a Zetasizer Nano-S (Malvern) instrument in order to evaluate the average size of the stabilized particles in suspension.

2.2.4. INDUCTIVELY COUPLED PLASMA-OPTICAL EMISSION SPECTROMETRY

Inductively Coupled Plasma - Optical Emission Spectrometry (ICP-OES), also referred to as Inductively Coupled Plasma - Atomic Emission Spectroscopy (ICP-AES), is an analytical technique used for the detection of trace metals. Inductively

Coupled Plasma (ICP) methods have been widely used and have become very popular especially because of the possibility of multi-element analysis and their wide range of applications. By definition, plasma is a conducting gaseous mixture containing a significant concentration of cations and electrons. Argon ions, once formed in plasma, are capable of absorbing sufficient power from an external source (Radio Frequency) to maintain the temperature at a level at which further ionization sustains the plasma indefinitely. The argon plasma can reach temperatures as high as 10000 K.[14]

ICP-OES is based on the measurement of the light emitted by the elements that are part of a sample. Samples in solution are nebulized to produce an aerosol of fine droplets. A spray chamber is used to select only the smallest droplets for analysis. The selected droplets are swept into the centre of the plasma by an argon stream. The high temperature of the plasma supply energy to: vaporize solvent, eliminate sample matrix components and elevate atoms to their excited states. As atoms leave the plasma and cool, they relax leading to emission of light. The wavelengths of the emitted light are characteristic of the elements present, and the intensity proportional to their concentrations.[15] ICP-OES limits of detection for many metals lie in the range 1-100 ng/ml (ppb).[16]

In the developed work, this technique was used for the determination of metal content in the resin-supported catalyst as well as in the heterogeneous catalysis solutions to control the presence of leached metal. The measurements were done with a Varian 720ES instrument coupled with an autosampler Agilent SP3 at a sensitivity of 0.500 ppm for solid samples. Each resin-supported sample (50-100 mg) was treated in a microwave-heated digestion bomb (Milestone, MLS-200, 20 min.@ 220 °C) with concentrated HNO_3 (1.5 mL), 98% H_2SO_4 (2 mL), and 0.5 mL of H_2O_2 30%. After filtration, the solutions were analyzed. For the recovered solutions after catalysis, they were analyzed directly after 1:5 dilution in 0.1 M HCl.

2.3. GAS CHROMATOGRAPHY

Gas Chromatography (GC) is a common type of chromatography used in analytical chemistry for separation and analysis of volatile compounds.[17] The basic operating principle of GC involves volatilization of the sample in a heated inlet or injector of a gas chromatograph, followed by separation of the components of the mixture in a specially prepared column. Only those compounds that can be vaporized without decomposition are suitable for GC analysis. If the sample is non-volatile the techniques of derivatization and pyrolysis GC can be utilized.

A carrier gas (referred to as the mobile phase), usually an inert gas such as nitrogen or helium, is used to transfer the sample from the injector, through the column, and into the detector. The vast majority of columns used today are capillary tubes with a stationary phase coated on the inner wall. Separation of the components is determined by the distribution of each component between the mobile phase and the stationary phase. A component that spends little time in the stationary phase will elute quickly. After elution from the column, each component still in the carrier gas flows into a detector.[18,19]

In the current work GC analyses were extensively used in catalytic experiments to analyse conversion and selectivity after reaction. The analyses were performed with different equipments; Shimadzu GC-17A Gas Chromatograph equipped with a flame ionization detector and 50.0 m (0.25 mm ID, 0.25 μm FT) Lipodex-E type column, Shimadzu GC-2010 Gas Chromatograph equipped with a flame ionization detector and 30.0 m (0.25 mm ID, 0.25 μm FT) Varian VF-WAXms type column and SPB-1 type column.

2.4. GAS CHROMATOGRAPHY / MASS SPECTROMETRY

Gas chromatography / mass spectrometry (GC/MS) is the most ubiquitous analytical technique for the identification and quantification of organic substances in complex matrices. It is the synergetic combination of two powerful microanalytical techniques. The gas chromatography separates the components of a mixture in time, and the mass spectrometer provides information that aids in the structural identification of each component. The advantage is that after component separation, mass spectra of individual substances can be obtained for qualitative and quantitative purposes. GC/MS can provide a complete mass spectrum from a few femtomoles of an analyte; ideally this spectrum gives direct evidence for the nominal mass and provides a characteristic fragmentation pattern or "chemical fingerprint" that can be used as the basis for identification along with the gas chromatograph retention time.[18]

In this Thesis GC/MS analyses were performed on two different equipments; Shimadzu QP2010S spectrometer equipped with a 30.0m (0.25 mm ID, 0.25 μm FT) Varian VF-WAXms capillary column, and Shimadzu QP5000 equipped with a 30.0m (0.25 mm ID, 0.25 μm FT) WCOT fused silica capillary column coated with CP-Wax 52CB.

2.5. NUCLEAR MAGNETIC RESONANCE SPECTROSCOPY

Nuclear Magnetic Resonance (NMR) is a spectroscopic technique that relies on the magnetic properties of the atomic nucleus. When placed in a strong magnetic field, certain nuclei resonate at a characteristic frequency (*resonant frequency*) in the radio frequency range of the electromagnetic spectrum. Slight variations in this resonant frequency give us detailed information about the molecular structure in which the atom resides.[20] Many of the most common elements found

in organic molecules (H, C, N, P) have at least one isotope that is a NMR active nucleus (when either the atomic number or the atomic mass is odd, or both are odd, the nucleus has magnetic properties and is said to be spinning, e.g. ^{1}H, ^{13}C, ^{15}N, ^{31}P). These isotopes behave as if the positively charged nucleus was spinning on an axis. The spinning charge creates a magnetic field so, when placed in a strong external magnetic field, the magnetic nucleus try to align with it.[21]

The resonant frequency is not only a characteristic of the type of nucleus but also varies slightly depending on the position of that atom within a molecule. This subtle variation, in the order of one part in a million, is called the *chemical shift* (δ) and provides detailed information about the structure of molecules. Different atoms within a molecule can be identified by their chemical shift. A graph of the resonant frequencies over a very narrow range of frequencies centered on the fundamental resonant frequency of the nucleus of interest is called *spectrum*, and each peak in the spectrum represents a unique chemical environment within the molecule being studied.

About one half of micromole of a pure molecule in 0.5 ml of solvent is required for this non-destructive test. The intensity of NMR signals is directly proportional to concentration. Only X-ray crystallography can give a comparable kind of detailed information on the precise location of atoms and bonds within the molecule.

NMR spectroscopy was used in the characterization of products after catalytic reactions when detection by GC was not possible. ^{1}H and ^{13}C{^{1}H} NMR spectra were recorded on a Bruker Avance DRX-400 spectrometer operating at 400.13 and 100.61 MHz, respectively. Chemical shifts are relative to tetramethylsilane as external reference.

2.6. CHEMICAL REACTOR EQUIPMENTS

A chemical reactor is an equipment unit where chemical transformations take place to generate a desirable product at a specified production rate, using a given chemistry. The reactor configuration and its operating conditions are selected to achieve certain objectives such as maximizing the profit of the process, minimizing the generation of pollutants, while satisfying several design and operating constraints (safety, controllability, availability of raw materials, etc). Usually, the performance of a chemical reactor plays a pivotal role in the operation and economics of the entire process.[22]

2.6.1. BATCH REACTORS

A batch reactor, as its name states, is a non-continuous and perfectly mixed closed vessel where a reaction takes place.[23] Reactants are charged to the system, rapidly mixed, and rapidly brought up to the temperature so that operating conditions are well defined. Batch reactors are the most common type of industrial reactor, heat and mass transfer limitations may emerge upon scale-up but are rarely important in the laboratory. A batch reactor has no input or output of mass after the initial charging. The amounts of individual components can change due to reaction but not due to flow into or out of the system.[24]

Batch reactors were extensively used during this Thesis for testing the developed catalysts. Reactions under a controlled pressure of hydrogen were performed using either a non-metallic Büchi Miniclave® (up to 10 bar and 50 mL internal volume) or a stainless steel autoclave (up to 80 bar and 20 mL internal volume) constructed at ICCOM-CNR (Firenze, Italy) and equipped with a magnetic stirrer, a Teflon® inset and a pressure controller for high pressures. The use of inert reactors for the catalytic tests ensures that no catalytic contributions come from their metallic components.
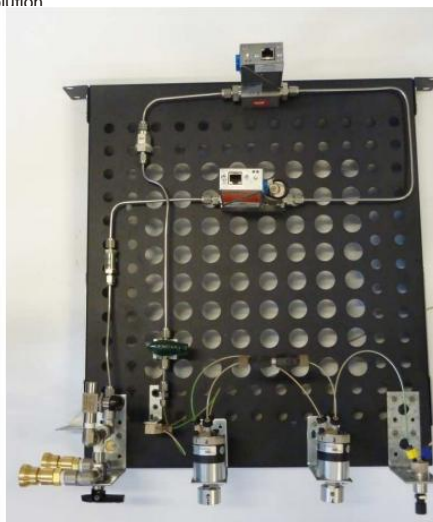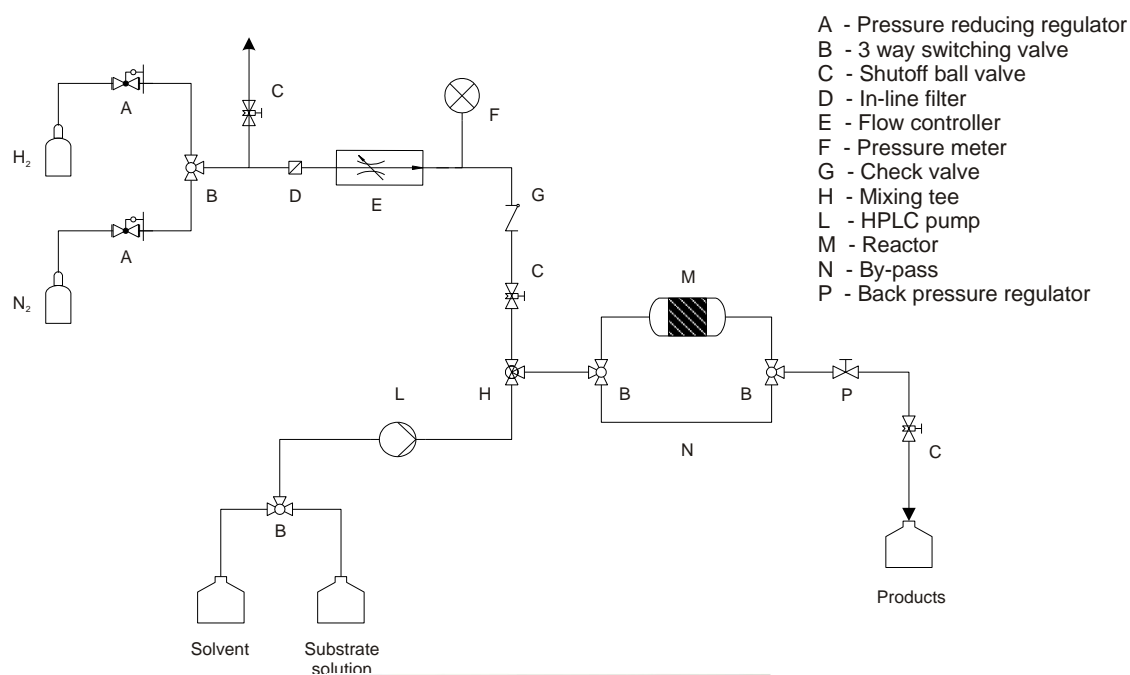
Fig. 2.4. Stainless steel autoclave constructed at ICCOM-CNR (left) and non-metallic Büchi Miniclave® (right).

2.6.2. CONTINUOUS FLOW REACTORS

Flow reactors, also known as continuous reactors, function with a reaction media being "carried" in a flowing stream through a reactor. In order to maintain the desired stoichiometry, reagents are continuously fed into the reactor, traverse through the reaction zone and exit as a continuous stream of product(s). This reactor configuration is used widely in the chemical industry and is now finding application in new areas of pharmaceutical industry. Flow reactors are designed in a variety of shapes, lengths, diameters and materials of construction.[25] The potential benefits of continuous reactors are increased reaction rates, solventless reactions, enhanced mixing and the ability to effectively remove heat produced by the reaction, due to increased heat transfer capacity and defined concentration profiles. The ability to control residence time within the reaction zone allows for greater control of products distributions and operating conditions. A further advantage is that *miniaturized flow reactors* can be designed to have reduced reactor volumes, physical footprint and energy requirements when compared with their batch reactor counterparts. Miniaturized flow reactors are referred to as nano-, micro-, meso-, macro- (mm) scale reactors, depending on their dimension,

being microfluidic (i.d. 10-500 μm) and mesofluidic (500 μm-several mm i.d) reactors, the most used bench-sized flow devices.[26]

In this Thesis, catalytic flow hydrogenations were carried out using a packed-bed mesofluidic flow reactor constructed at Istituto di Chimica dei Composti Organo Metallici, Firenze (Italy) shown in Scheme 2.1.

A - Pressure reducing regulator
B - 3 way switching valve
C - Shutoff ball valve
D - In-line filter
E - Flow controller
F - Pressure meter
G - Check valve
H - Mixing tee
L - HPLC pump
M - Reactor
N - By-pass
P - Back pressure regulator

Scheme 2.1. Schematic view (top) and image of the core (bottom) of the continuous-flow, high-pressure reactor system used.

The system was designed to allow for a simultaneous flow of substrate solution and hydrogen gas (up to 40 bar pressure) through a reactor tube containing the

heterogeneous catalyst. The reactor was completely inert, as all wet parts were made of PEEK, PFA or PFTE. The flow of the substrate solution was regulated by an Alltech® model 426 HPLC pump in PEEK. A constant flow of hydrogen gas was adjusted by a flow controller BRONKHORST HI-TEC model F200CV-002-RGD-11-V-MFC. The hydrogen pressure in the reactor was monitored by a BRONKHORST HI-TEC P502C-AGD-11-V-6K0R-EPC meter. The concurrent flows of gas and liquid were driven through a T-shaped PEEK mixer to ensure efficient gas dispersion. The mixed hydrogen-substrate solution stream was introduced in the reactor through a 6-port Rheodyne mod. 9060 switching valve in PEEK. The solid catalyst was pre-packed into a commercial 3 mm inner diameter Omnifit® glass column, equipped with 10μm PE frits at the entrance of the catalyst bed to ensure an optimum flow distribution.

REFERENCES

1 K. Lu, *Nanoparticulate Materials: Synthesis, Characterization, and Processing*, John Wiley & Sons Inc., Hoboken, New Jersey, **2012**.

2 Information obtained from the official website of Encyclopædia Britannica (*http://www.britannica.com/*), Retrieved Oct. **2012**.

3 D.B. Williams, C. Barry Carter, *Transmission Electron Microscopy: A Text Book for Materials Science,* Springer, New York, **2009**.

4 H. Czichos, T. Saito, L.E. Smith (Eds), *Handbook of Materials Measurement Methods*, Springer, Wurzburg, **2006**.

5 P. Goodhew, *General Introduction to Transmission Electron Microscopy* in *Aberration-Corrected Analytical Transmission Electron Microscopy* (Ed R. Brydson), John Wiley & Sons Ltd., Chichester, UK, **2011**.

6 R.A. Meyers, *Encyclopedia of Analytical Chemistry*, John Wiley & Sons Ltd., Chichester, **2000**.

7 B. Corain, B. Schmid, N. Toshima, *Metal nanoclusters in catalysis and materials science* in *The issue of size control*, Elsevier B.V., Amsterdam, **2008**.

8 C. Suryanarayana, M. Grant Norton, *X-Ray diffraction. A practical approach*, Plenum Press, New York, **1998**.

9 E. Lifshin, *X-Ray Characterization of Materials*, Wiley-VCH, Weinheim, **1999**.

10 M. Hosokawa, K. Nogi, M. Naito, T. Yokoyama (Eds), *Nanoparticle Technology Handbook*, Elsevier, Amsterdam, **2012**.

11 B.B. He, *Small-Angle X-Ray Scattering* in *Two-Dimensional X-Ray Diffraction*, John Wiley & Sons, Inc., Hoboken, New Jersey, **2009**.

12 O. Glatter, O. Kratky, *Small Angle X-Ray Scattering*, Academic Press Inc., London, **1982**.

13 R.L. Johnston, J. Wilcoxon, *Metal Nanoparticles and Allows*, Vol. 3, Oxford, Elsevier, **2012**.

14 A. Postawa, *Best Practise Guide on Sampling and Monitoring of Metals in Drinking Water*, IWA Publishing, London, **2012**.

15 D. Barceló, *Sample Handling and Trace Analysis of Pollutants*, Vol. 21, *Techniques, Applications and Quality Assurance*, Elsevier Science B. V., Amsterdam, **2000**.

16 J.E. Girard, *Principles of Environmental Chemistry*, Jones and Bartlett Publishers, Sudbury, MA, **2010**.

17 H.M. McNair, J.M. Miller, *Basic Gas Chromatography*, John Wiley & Sons Inc., Hoboken, New Jersey, **2009**.

18 O.D. Sparkman, Z.E. Penton, F.G. Kitson, *Gas Chromatography and mass spectrometry; a practical guide*, Elsevier Inc., Oxford, **2011**.

19 R.L. Grob, E.F. Barry, *Modern Practice on Gas Chromatography*, John Wiley & Sons Inc., Hoboken, New Jersey, **2004**.

20 N.E. Jacobsen, *NMR Spectroscopy Explained : Simplified Theory, Applications and Examples for Organic Chemistry and Structural Biology,* John Wiley & Sons Inc., Hoboken, New Jersey, **2007**.

21 J.B. Lambert, E.P. Mazzola, *Nuclear Magnetic Resonance Spectroscopy; an introduction to principles, applications and experimental methods*, Prentice Hall, Upper Saddle River, New Jersey, **2003**.

22 U. Mann, *Principles of Chemical Reactor Analysis and Design; new tools for industrial chemical reactor operations*, John Wiley & Sons Inc., Hoboken, New Jersey, **2009**.

23 O. Levenspiel, *Chemical Reaction Engineering* 3rd ed., John Wiley & Sons, New York, **1999**.

24 E. Bruce Nauman, *Chemical Reactor Design, optimization and scaleup* 2nd ed., John Wiley & Sons Inc., Hoboken, New Jersey, **2008**.

25   W. Zhang, B.W. Cue (Eds), *Green techniques for organic synthesis and medicinal chemistry*, John Wiley & Sons, Ltd, Chichester, UK, **2012**.

26   J. Wegner, S. Ceylan, A. Kirschning, *Chem. Comm*. 47, **2011**, 4583.

3

Polymer Supported Metal Nanoparticles:

Synthesis and Optimization

3.1. OVERVIEW

This chapter describes the experimental work carried out, particularly it covers the synthesis and characterization of polymer supported metal nanoparticles used as catalysts in hydrogenation and oxidation reactions. With the aim of designing the optimized methodology that leads to a catalytic system featured by the highest activity and stability, an in depth investigation was accomplished. Resin supported Pd based catalysts and the hydrogenation of probe substrates were taken as point of reference to evaluate the effect that several modifications related to the support and the activation of the catalytic species could have on the final performance of these systems. The standardized method was then extended to the synthesis of other noble metal nanoparticles such as rhodium and gold.

3.2. INTRODUCTION

The research in the field of fine chemicals synthesis by solid supported metal nanoparticles (MNP) catalysts attracts increasing interest due to the possibility to couple high activity with ease of preparation, catalyst reuse and continuous processing,[1,2] thus offering a green and cost-effective alternative to homogeneous and conventional heterogeneous catalysts in an industrial segment blemished by the highest *E*-factors.[3,4]

A variety of porous materials have been used as the support media for the preparation of catalytic active nanoparticles made of noble metals, with Ru, Rh, Pd, Pt and Au being the most studied. Much attention has been paid to inorganic supports; metal oxides like silica, alumina, titania or ceria are commonly employed.[5] In the field of organic supports, powder activated charcoal base-catalysts have become very popular,[6] nevertheless the use of ion exchange resin has been somewhat less studied, maybe owing to the fact that the work mechanism in the swollen state is not well known yet.

The proposal of cross-linked functional polymers as supports for metal nanoparticles to be employed in catalysis dates back to 1968, when Wöllner and Neir patented the use of cross-linked strongly acidic polymers as acidic supports for Pd^0 nanoparticles.[7] This preparation gave rise to a bifunctional catalyst (Bayer catalysts OC 1038) with acid and metal centres that was used for the chemoselective synthesis of the industrial solvent methyl isobutyl ketone (MIBK) from acetone and dihydrogen (Scheme 3.1.), with a global production of several million kilograms per year.[8]
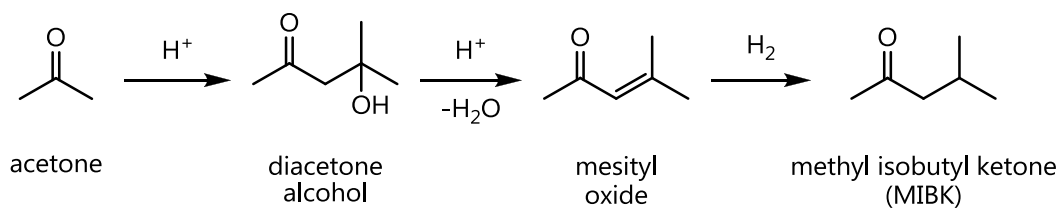
Scheme 3.1. Schematic representation of the one-pot synthesis of MIBK.

The scientific community didn't dedicate too much effort to the study of these systems as demonstrated by the few publications in next years. Some examples are Pt^0 supported on a macroreticular sulphonic resin for the chemoselective synthesis of acteone,[9] Pd^0 supported on polybenzimidazole for the reduction of aliphatic and aromatic nitrocompounds,[10] or Pt^0 and ultrafine Rh particles immobilized on a polyacrylamide for the hydrogenation of functional olefins.[11] Lately, the promising catalytic use of gold has brought some examples of Au NPs supported onto ion exchange resins with different functionalities for their use in oxidation reactions.[12] Except for the pioneering work of Corain on the immobilization and characterization of Pd^0 nanoclusters onto gel-type functional polymers,[13] and the use of Amberlyst®-supported systems,[14] ion-exchange resins were poorly explored as far as catalysts production and reuse is concerned.[7,15]

In general terms, purification and separation processes likely still represent the most important industrial application of ion-exchange resins at present. However, the number of industrial processes developed in the recent years based on metal catalysts supported on resins indicates this as an emerging class of catalysts. These applications include the synthesis of methyl tert-butyl ether MTBE (EC Erdölchemie Process), the reduction of dioxygen level in water from ppm to ppb (Bayer catalysts K 6333 and VP OC 1063), and etherification-hydrogenation of mixtures of insaturated hydrocarbons to give blends of alkanes and branched ethers for the manufacture of green petrol without lead (BP Etherol Processs). Biffis *et al.*[16] described a chemoselective catalyst for the hydrogenation of 2-ethyl-

anthraquinone (EAQ) to 2-ethylanthrahydroquinone (EAHQ), which is a key step in the current industrial synthesis of hydrogen peroxide.

Compared to other solid supports for catalytically active species, ion exchange resins show several inherent advantages. In fact, they are:

- commercial, low cost products

- available in several chemical and physical modifications

- able to stabilize MNPs due to the dual effect of charged functional groups (electrostatic stabilization) and porosity (steric stabilization)[17]

- reasonably resistant from a chemical, mechanical and thermal point of view

- easy to handle

- easily integrable in reactor equipments.

Particularly, low-cross linked resins (typical 0.5 - 4 % crosslinkage) develop a microporous (gel) structure when swollen in the appropriate solvent, which makes them particularly suitable to accommodate nano-sized metal particles.[18]

Prompted by the above considerations and by the experience of the group in this research field,[19] it was carried out an in-depth investigation on the performance of heterogeneous catalysts based on palladium nanoparticles embedded into gel-type ion-exchange resins, and the factors affecting this, whose results are shown in following sections.

3.3. PREPARATION OF POLYMER-SUPPORTED PALLADIUM CATALYSTS

A sketch of the ion-exchange resins used in this work is reported in Scheme 3.2. The resins were gel type (2% divinylbenzene as cross-linker), either strong cation-exchange (i.e. containing sulfonic groups, DOWEX® 50WX2) or strong anion-exchange (trimethylbenzyl ammonium group, DOWEX® 1X2), and with bead dimensions ranging from 38 to 300 μm. All resins were commercially available at low-cost (from 0.1 to 0.7 €/g). Strong cation-exchange resins were used in their protonated form as manufactured, or converted into the parent lithium salt,[20] in order to suppress acid-catalyzed side reactions (see Chapter 4 / Section 4.4.3.) when used as support (e.g. acetalizations, dehydrations, condensations, transesterifications).[21]

$$X = SO_3^-, CH_2N(CH_3)_3^+$$
$$Y = H^+, Li^+, Cl^-$$
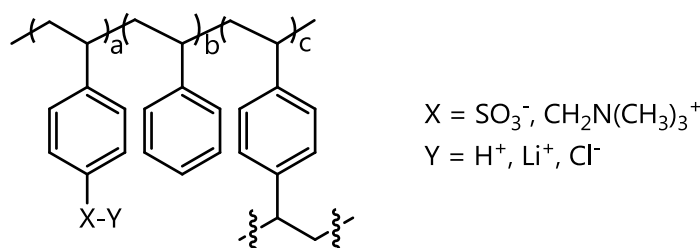
Scheme 3.2. Sketch of the resin used.

The resins were metallated to palladium(II) species by a straightforward ion exchange procedure involving stirring of the resin in the presence of an appropriate amount of palladium salt in water. The salts employed are listed in Table 3.1.

Table 3.1. Palladation of ion-exchange resins.

Metal precursor	Price (€/g)	Metal Loading [wt%]	Metal Uptake (%)
$Pd(NO_3)_2$	65	1.00	67
$[Pd(CH_3CN)_4(BF_4)_2]$	170	1.25	89
K_2PdCl_4	40	1.00	92

Pd(NO$_3$)$_2$ and [Pd(CH$_3$CN)$_4$(BF$_4$)$_2$] were employed in conjunction with cation exchange resins and K$_2$PdCl$_4$ with anion exchange resins. A typical [mmol Pd] / [meq ion exchange capacity] ratio of (1 / 33) was used to afford 1 and 1.25 wt% Pd loading, corresponding to different metal uptake depending on the precursor used, in any case fully compared with that of previously reported systems.[22]

The metallated resins were then converted into palladium(0)-containing polymers using different procedures: i) isolation after reduction with NaBH$_4$ in water, ii) isolation after reduction with H$_2$ in methanol, iii) generation *in-situ* under the conditions of catalytic hydrogenations; i.e. 0.8-1 bar H$_2$, methanol, excess of substrate, room temperature. The synthetic procedure for the preparation of the isolated species is shown in Fig. 3.1., both for cationic and anionic exchangers. Irrespective of the synthetic method, XRD and TEM analyses showed the presence of Pd^0 nanoparticles into the polymers (see Section 3.4).

Importantly, the *in-situ* synthesis of supported Pd NPs was possible only in the case of Pd^{2+} onto strong cation-exchange resins. Indeed, no appreciable reduction of resin-PdCl$_4^{2-}$ species by H$_2$ in methanol was detected within reasonable timeframes.[23] This finding is consistent with the higher reduction potential of "naked" Pd^{2+} ions as compared to PdCl$_4^{2-}$ anions.[24]

Previously reported methods for the preparation of supported Pd NPs onto cation-exchange resins involved the isolation of the product after a two-step metallation / reduction procedure, either by thermal reduction of immobilized [Pd(NH$_3$)$_4$]$^{2+}$ ions (eventually followed by high temperature treatment with H$_2$ or NaBH$_4$),[14a,b,25] or by sodium borohydride reduction of immobilized Pd(OAc)$_2$.[26]
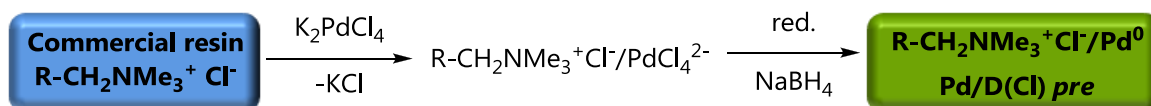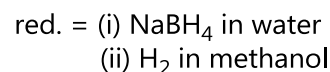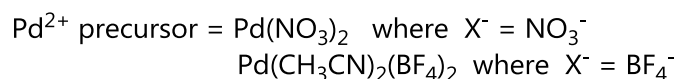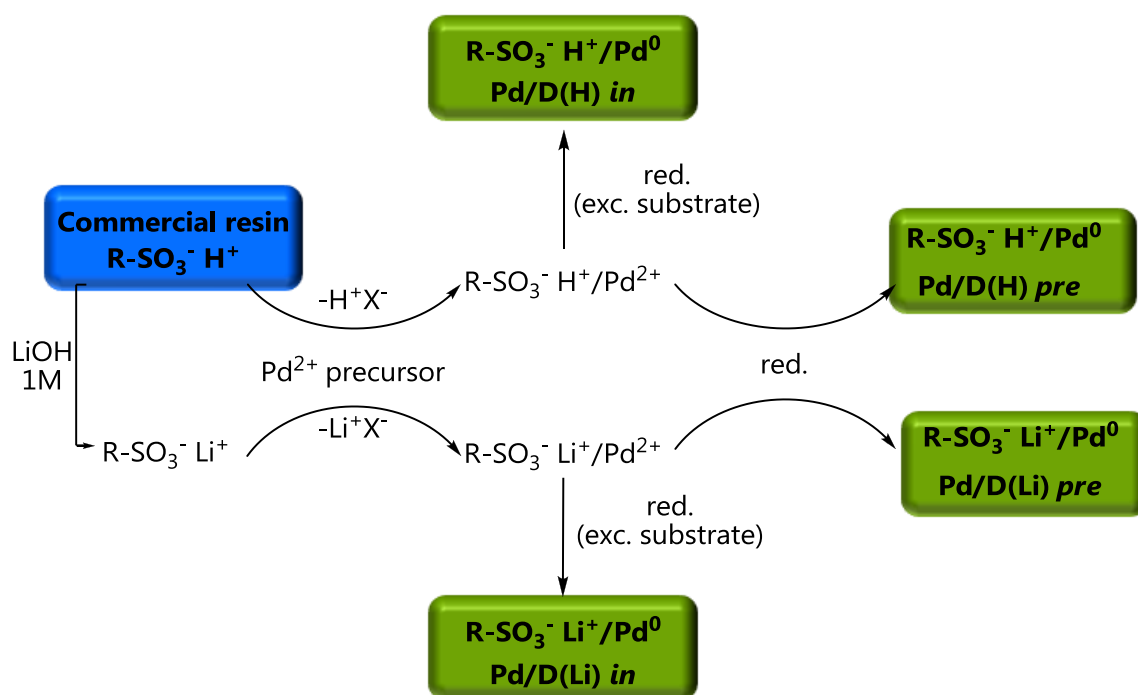
Fig. 3.1. Scheme of the synthetic procedure for the preparation of supported palladium nanoparticles onto cation-exchange resins (top) and anion-exchange resins (bottom).

Table 3.2. lists all the resin-supported Pd^0 species prepared in the present work. The catalysts have been named with the label [Pd/D(X) *"preparation" "n"*] where D is Dowex resin, X is the ionic form of the resin (H : protonated, Li : lithiated, Cl : chlorated), "preparation" means when the active specie has been formed (*pre*: *prior* to use -isolated-, *in*: *in situ*, under catalytic conditions) and "n" is the catalyst number.

Table 3.2. Supported palladium catalysts prepared.

Abbrev.	Catalyst label	Resin (exchanger, ionic form, mesh)	Metal precursor	Preparation method	Pd[a] wt%
Pd/D(Li) *pre*	Pd/D(Li) *pre* 1	Sulfonic, Li$^+$, 50-100	Pd(NO$_3$)$_2$	Isolated, NaBH$_4$ in H$_2$O	1.2
	Pd/D(Li) *pre* 2		Pd(NO$_3$)$_2$	Isolated, H$_2$ in CH$_3$OH	1.2
	Pd/D(Li) *pre* 3		Pd(NO$_3$)$_2$	Isolated, H$_2$ in CH$_3$OH	5.0
	Pd/D(Li) *pre* 4		Pd(CH$_3$CN)$_4$(BF$_4$)$_2$]	Isolated, H$_2$ in CH$_3$OH	1.2
Pd/D(H) *pre*	Pd/D(H) *pre* 5	Sulfonic, H$^+$, 50-100	Pd(NO$_3$)$_2$	Isolated, H$_2$ in CH$_3$OH	1.3
	Pd/D(H) *pre* 6		Pd(CH$_3$CN)$_4$(BF$_4$)$_2$]	Isolated, H$_2$ in CH$_3$OH	1.2
Pd/D(Cl) *pre*	Pd/D(Cl) *pre* 7	Trimethylbenzyl ammonium, Cl$^-$, 50-100	K$_2$PdCl$_4$	Isolated, NaBH$_4$ in H$_2$O	1.1
Pd/D(Li) *in*	Pd/D(Li) *in* 8	Sulfonic, Li$^+$, 50-100	Pd(NO$_3$)$_2$	Prepared in situ[b]	1.3
	Pd/D(Li) *in* 9		Pd(NO$_3$)$_2$	Prepared in situ[b]	5.1
	Pd/D(Li) *in* 10		Pd(CH$_3$CN)$_4$(BF$_4$)$_2$]	Prepared in situ[c]	1.3
	Pd/D(Li) *in* 11	Sulfonic, Li$^+$, 200-400	Pd(NO$_3$)$_2$	Prepared in situ[b]	1.1
Pd/D(H) *in*	Pd/D(H) *in* 12	Sulfonic, H$^+$, 50-100	Pd(NO$_3$)$_2$	Prepared in situ[b]	1.5
	Pd/D(H) *in* 13		Pd(CH$_3$CN)$_4$(BF$_4$)$_2$]	Prepared in situ[c]	1.2

[a] wt% Pd loading from AAS. [b] 0.8 bar H$_2$, CH$_3$OH, excess of substrate, rt. [c] 1 bar H$_2$, CH$_3$OH, excess of substrate, rt.

3.4. CHARACTERIZATION OF POLYMER-SUPPORTED PALLADIUM CATALYST

All Pd-containing resins were characterized in the solid state by a combination of microscopic and scattering techniques employing the equipments described in Chapter 2. Palladium loading was obtained from ICP-OES (Table 3.2.). The appearance of the ion-exchange resins before and after palladiation and reduction is shown in the optical microscope images reported in Fig. 3.2.
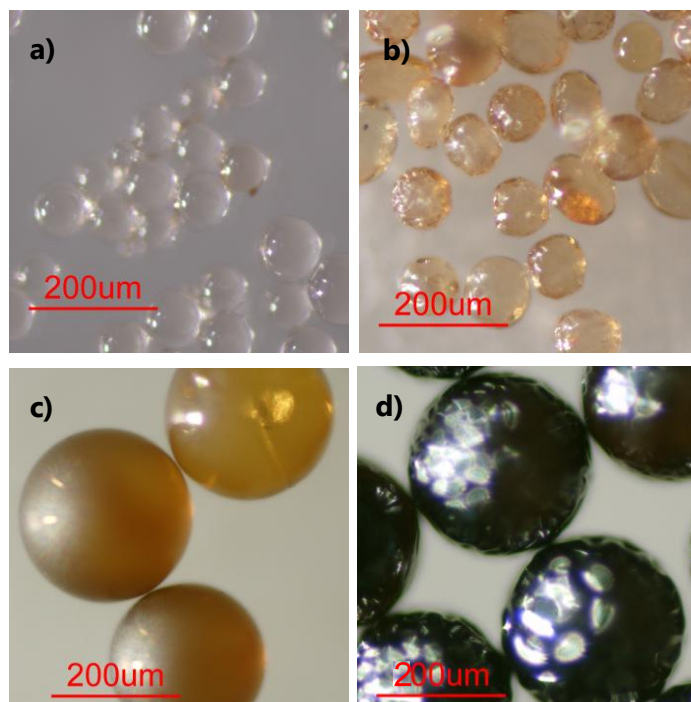
Fig.3.2. a) Dowex® 50WX2: R-SO$_3^-$ H$^+$ (H$^+$, 200-400 mesh); b) R-SO$_3^-$Li$^+$/Pd^{2+} (200-400 mesh, 1 wt% Pd); c) R-SO$_3^-$Li$^+$/Pd^{2+} (50-100 mesh, 1 wt% Pd); d) R-SO$_3^-$Li$^+$/Pd^0 (50-100 mesh, 1 wt% Pd).

ESEM analysis showed that the resin beads are not affected by metallation, reduction or use in catalysis, since no signs of breakage or cracking were detected anyhow. This fact justifies the intact recovery of the resins at any preparations stage and after their use in successive catalytic runs. A typical ESEM image of the lithiated resin before, D(Li), and after metallation, Pd/D(Li) *pre*, are reported in Fig. 3.3. EDS maps recorded on sections of Pd-containing beads proved the metal to be evenly distributed within the solid support. A representative example is shown in Fig. 3.4. in which palladium, carbon and sulphur maps are reported for comparison. This evidence indicates that the solvent diffuses thoroughly into and out the bead during the immobilization procedure, thus allowing good site accessibility to all soluble reactants.[27] Consistently with previous reports, no significant depletion of the metal was observed within the support upon reduction or use of the Pd-resins in catalysis, at least for resins with 1 and 1.25 wt% metal loading.[28]
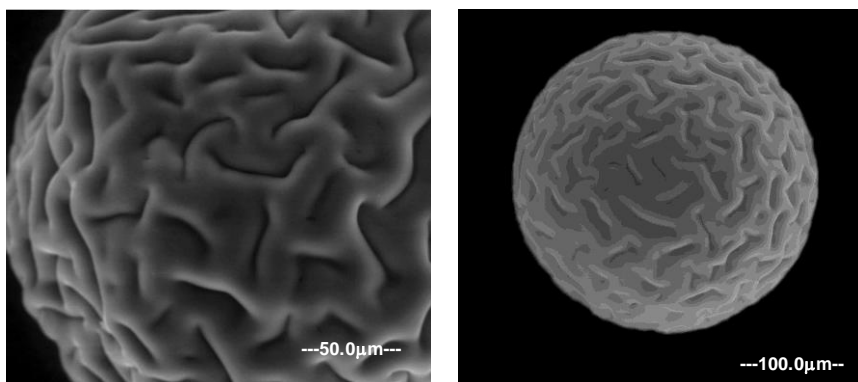
Fig. 3.3. ESEM image (secondary electrons). (left) DOWEX® 50WX2 after lithiation D(Li); and (right) after subsequent metallation D/Pd(Li) *pre*, (Li$^+$, 50-100 mesh, Pd(NO$_3$)$_2$, 1 wt% Pd, H$_2$ reduction, before use in catalysis).
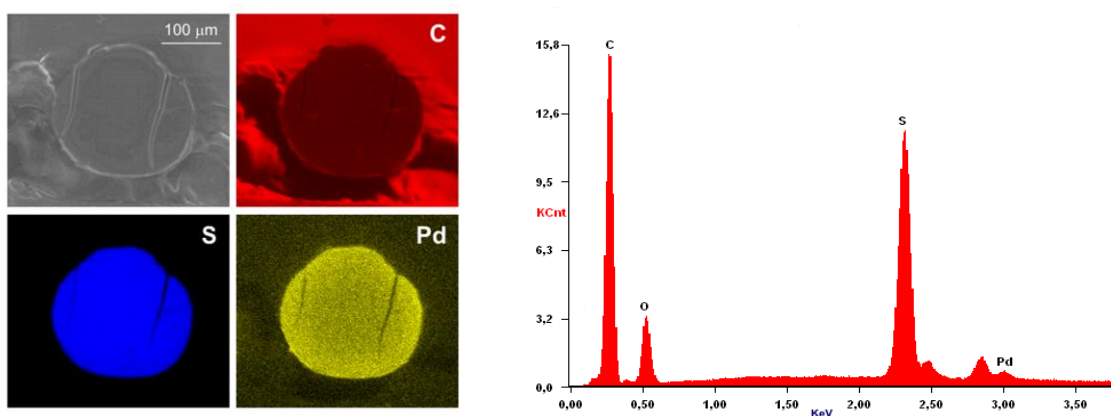

Fig. 3.4. (left) ESEM image (1 torr, 25 KeV, 800 magnifications) and EDS maps of an equatorial section of D/Pd(Li) *pre* catalyst bead (Li$^+$, 50-100 mesh, Pd(NO$_3$)$_2$, 1 wt% Pd, H$_2$ reduction). Top left: secondary electrons image; top right: carbon map (C Kα1); bottom left: sulphur map (S Kα1); bottom right: palladium map (Pd Lα1). (Right) EDS microanalysis; X-ray *counts* are plotted as a function of their energy, the present elements are identified.

The size of Pd NPs was determined by TEM, XRD and SAXS analysis. Table 3.3. summarizes the average values obtained on representative samples prepared under the conditions described in the Experimental Section, before and after use in catalysis. TEM measurements were generally consistent with those obtained from XRD and SAXS, within the experimental errors. Embedded spheroidal Pd NPs, with a mean diameter of 3.4 and 3.2 nm were observed by TEM, on samples recovered after catalytic hydrogenation when [Pd(CH$_3$CN)$_4$(BF$_4$)$_2$] and Pd(NO$_3$)$_2$

were used as metal precursors respectively. According to the reducing agent, nanoparticles sizes of 3.7 and 5.3 nm (TEM), were found on samples isolated after H_2 and $NaBH_4$ treatment respectively. Typical TEM images and the corresponding NPs size distribution are shown in Fig. 3.5. and in Fig. 3.6.

Table 3.3. Size of the supported Pd NPs prepared.[a]

Catalyst	Pd precursor	Reducing agent	Before catalysis			After catalysis[b]		
			TEM	XRD	SAXS	TEM	XRD	SAXS
Pd/D(Li) *in*	$[Pd(CH_3CN)_4(BF_4)_2]$	H_2	-	-	-	3.4	2.5	2.7
Pd/D(Li) *in*	$Pd(NO_3)_2$	H_2	-	-	-	3.2	3.3	3.1
Pd/D(Li) *pre*	$Pd(NO_3)_2$	H_2 [c]	3.7	2.2	2.6	3.9	3.4	3.6
Pd/D(Li) *pre*	$Pd(NO_3)_2$	$NaBH_4$	5.3	3.8	4.0	6.0	4.8	4.8

[a] Diameter in nm. SAXS data report the geometrical diameters. Resin type: sulfonic, Li^+, 50-100 mesh, 1 wt% Pd. [b] Reaction conditions: methanol, rt, substrate **2** : Pd =220:1 molar ratio, H_2 flow pressure 0.8bar, substrate concentration 0.17M, after 5 cycles of complete substrate conversion. [c] H_2 flow, pressure 0.8bar.
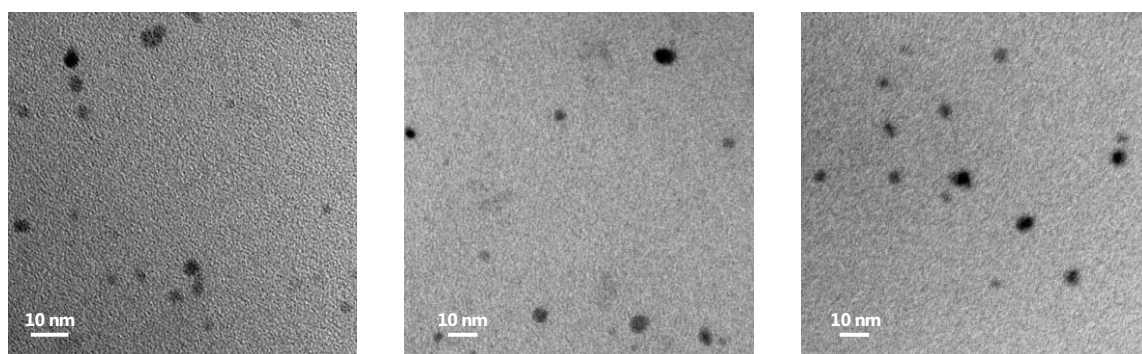

Fig 3.5. TEM images of supported Pd NPs obtained from $Pd(NO_3)_2$ and H_2 reduction (Table 3.3): (left) Pd/D(Li) *in*, (center) Pd/D(Li) *pre* before use in catalysis, (right) Pd/D(Li) *pre* recovered after catalysis.

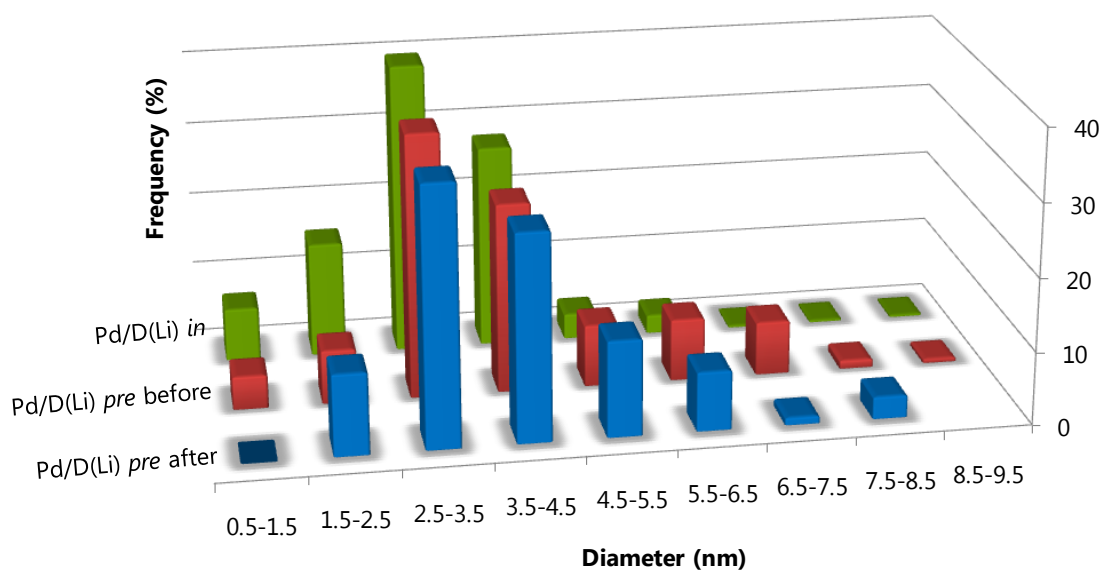**Fig. 3.6.** Size distribution from TEM analysis of resin-embedded Pd NPs, before and after use in catalysis (1 wt% Pd/D(Li), 50-100 mesh, $Pd(NO_3)_2$, H_2 reduction).

With regard to palladium precursor, no significant differences have been noticed in the particle mean diameter (Table 3.3.). On the other hand, Fig. 3.7. shows the size distribution of Pd NPs starting from $[Pd(CH_3CN)_4(BF_4)_2]$ with 90% of the nanoparticles concentrated in the range (2 - 5 nm), unlike $Pd(NO_3)_2$ that leads to the formation of 42% of the clusters within the range of (2.5 - 3.5nm). The corresponding XRD pattern that can be seen too in Fig 3.7., shows one diffraction peak at a 2 theta value of 39.95° which corresponds to a reflection caused by the plane (111) of Pd. The peak is broad and poorly defined, as befits the size of small particles. Due to the low amount of palladium (1.25 wt%), diffraction peaks at 46.80° and 67.90° (less intense) corresponding to (200) and (220) planes are not detected. The interplanar spacing calculated from the diffractogram applying Bragg's Law is 0.225nm, indicating that the crystal structure of Pd nanoparticles is face-centered cubic, according to previously published works.[29]
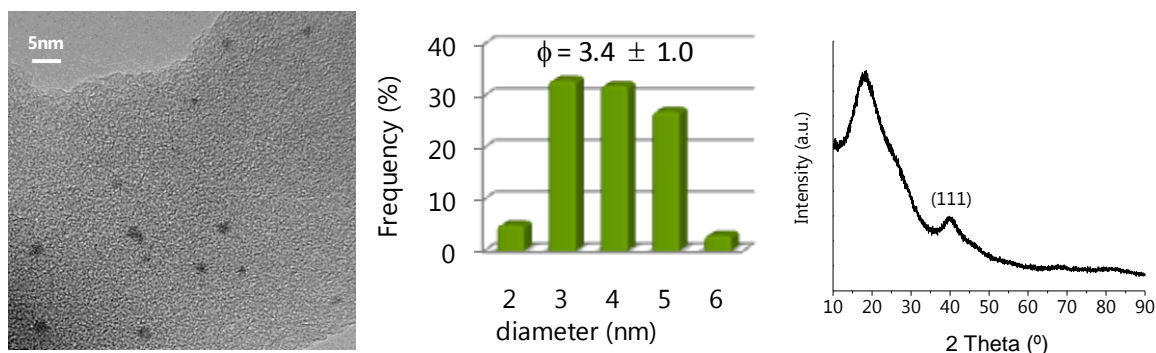
Fig 3.7. (left) TEM image of 1.25 wt% Pd/D(Li) *in* catalyst (50-100 mesh, [Pd(CH$_3$CN)$_4$(BF$_4$)$_2$] precursor,) recovered after catalysis, (center) Size distribution from TEM analysis, (right) XRD diffractogram form the same catalysts.

XRD analyses allowed to notice that Pd NPs dimension is affected by the exchanger group contained in the stabilizing polymer. The cationic exchange resin can accommodate clusters 20% smaller than the anionic resin. It must be considered that a different exchanger group also implies different ionic form and palladium precursor. Regarding palladium loading, the mean diameter of the particles is not significantly affected. Fig 3.8. shows the diffractograms obtained from different samples with the corresponding values collected in Table 3.4.
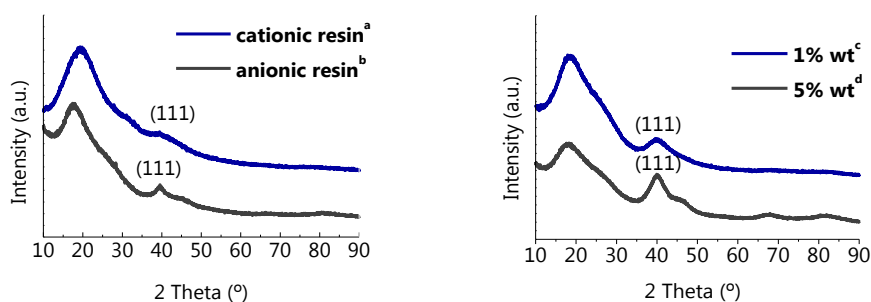

Fig. 3.8. XRD diffractograms for supported Pd NPs samples indicated in Table 3.4.

Table 3.4. Size of the supported Pd NPs according to XRD measurements.

Diameter (nm)			
Exchanger group		Palladium loading	
Cationic[a]	Anionic[b]	1 wt%[c]	5 wt%[d]
3.8	4.5	2.2	2.5

[a] Pd/D(Li) *pre* 1, [b] Pd/D(Li) *pre* 7, [c] Pd/D(Li) *pre* 2, [d] Pd/D(Li) *pre* 3

65

A representative example of SAXS spectrum is reported in Fig. 3.9. in which the excess of Pd/D(Li) *pre* scattering intensity with respect to the scattering due to the unmetallated resin is plotted. A pattern is clearly observable which can be ascribed to the higher electron density of the Pd nanoparticles with respect to the matrix they are dispersed in. The scattered spectrum is characterized by a low-q clustering part and an intermediate to high-q part, attributable well-defined primary particles. The profile was fitted with a model function in which the variable parameters are the geometrical radius of the primary spherical particles and the polydispersity (see 'Experimental').[30] Within these assumptions, the medium-high q part of the spectra was very well interpreted yielding e.g. a radius of 1.3 nm for the Pd/D(Li) *pre* samples obtained by H_2 reduction, in very good agreement with TEM and XRD results.
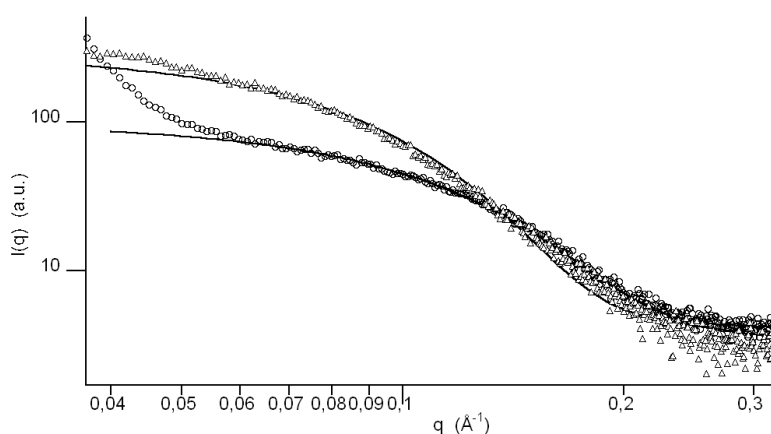

Fig 3.9. SAXS differential spectra of Pd/D(Li) *pre* resin (Li^+, 50-100 mesh, $Pd(NO_3)_2$, 1 wt% Pd, H_2 reduction) before (○) and after (△) use in catalysis, obtained by subtraction of the scattering intensity due to the metal-free matrix. Solid lines represent the best-fit data.

The SAXS spectra are consistent with the coagulation of the primary particles (e.g. from 2.6 to 3.6 nm), but they also allow highlighting further subtle structural differences. Indeed, the degree of aggregation of the primary particles into clusters, clearly evidenced by the low-q upturn observed before catalysis, diminishes as a consequence of the Pd NPs enlargement after catalyst use (Fig.

3.9). Growth of polymer-supported Pd nanoparticles upon use in catalysis was previously demonstrated by EXAFS measurements.[31]

The dimensional data obtained confirm that ion-exchange resins are able to stabilize small Pd NPs with a narrow size distribution. The values are in overall agreement with those on comparable gel-type functionalized polymers,[32] taking into account that dimensions, distribution and dispersion of Pd NPs are strongly dependent from the synthetic experimental conditions (temperature, concentration of the reducing agent), with metal crystallites obtained by hydrogen reduction usually smaller than those prepared by sodium borohydride.[33] On the contrary, there are other factors that seem not to have a great influence, i.e. metal precursor and metal loading.

On the basis of the data reported in Table 3.3. and from previous arguments, it can be confirmed the incipient Pd NPs generated under catalytic conditions are smaller than those obtained in the corresponding Pd^0-resin by pre-reduction. It could be speculate that an "excess of substrate stabilizing effect" might be responsible for the restricted growth of Pd nanoparticles under *in situ* conditions.[34]

In the next section, a deep study of the performance of the catalysts synthesized and characterized will be carried out. The hydrogenation reaction of reference substrates will be used as a model reaction to gain insights into the system that will help to the election of the best catalytic system in terms of activity and stability.

3.5. ANALYSIS OF PARAMETERS THAT INFLUENCE THE CATALYSTS PERFORMANCE

The great variety of Dowex® polymeric resins and the additional variations that can be introduced in the synthesis of catalytic active species allowed for the preparation of a whole set of catalysts (Table 3.2.). In order to evaluate how these modifications could affect the final effectiveness of the catalyst, hydrogenation reactions of the probe substrates shown in Scheme 3.3. were carried out.
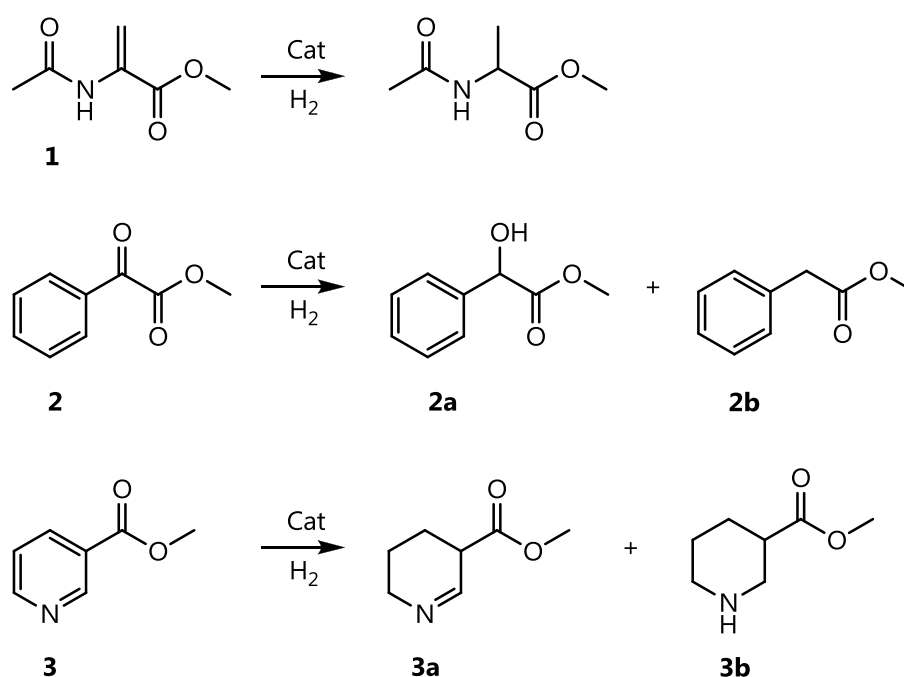
Scheme 3.3. Sketch of the probe substrates tested in hydrogenation reactions.

All supported catalysts prepared were highly active in hydrogenation reactions under very undemanding conditions, *i.e.* room temperature, (0.8 - 1) bar H_2 pressure, albeit with remarkable differences depending on the catalyst preparation method. The catalysts could be quantitatively recovered by simple decantation and reused by addition of identical amounts of substrate solution under hydrogen. In order to estimate the activity and stability of the different catalysts upon recycling, few experiments were carried out in this respect.

3.5.1. PREPARATION METHOD

The Pd^0-containing resins were used as catalyst precursors in hydrogenation reactions under batch conditions, either as isolated, pre-reduced species or prepared *in-situ*. In the latter case, the Pd^{II}-resins were directly added to the substrate solution under nitrogen, before the mixture was exposed to the desired H$_2$ pressure, which was taken as the start time of the catalytic reaction. Regardless the substrate, the isolated catalysts Pd/D(Li) *pre* were more active when Pd NPs were obtained by H$_2$ reduction instead of by NaBH$_4$ treatment. Representative results are reported in Table 3.5. for the hydrogenation of methyl 2-acetamidoacrylate **1**. This finding is consistent with the smaller dimensions, hence with the higher surface area, of the particles synthesized using hydrogen compared to those obtained from borohydride (see Table 3.3)[35] Minor differences in activity were observed for the catalysts obtained by reduction under a static atmosphere or by a flow of hydrogen, nevertheless the latter procedure was significantly simpler (see Experimental Section). No catalytic activity was shown by the H$_2$-stable Pd^{II}-anionic resins.

Table 3.5. Activity of the pre-reduced catalysts Pd/D(Li) *pre* in the hydrogenation of **1**.[a]

Catalyst	Reducing agent	Yield (%)	TOF (h^{-1}) [b]
Pd/D(Li) *pre* 1	NaBH$_4$	56.3	767
Pd/D(Li) *pre* 2	H$_2$ [c]	87.4	1180

[a] Reaction conditions: methanol, r.t., substrate : Pd = 450 : 1 molar ratio, H$_2$ pressure 0.8 bar, substrate concentration 0.17 M, 1 wt% Pd/D(Li) catalyst (50-100 mesh, Pd(NO$_3$)$_2$ precursor), 20 min. [b] TOF = mol product / mol Pd x h. [c] 2 bar static atmosphere.

Most importantly, under the same reaction conditions, the activity of the *in situ* prepared catalysts Pd/D *in* was invariably higher than that of the corresponding pre-reduced Pd^0 species Pd/D *pre*. This trend is graphically represented in Fig. 3.10 that reports the catalytic results obtained in the hydrogenation of **1** using Pd/D type catalysts.
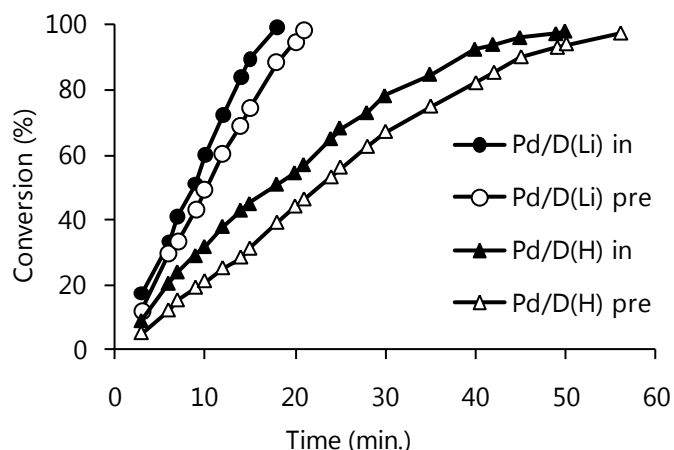
Fig. 3.10. Hydrogenation reaction of **1** using 1.25 wt% Pd/D catalysts (50-100 mesh, [Pd(CH$_3$CN)$_4$(BF$_4$)$_2$] precursor). Reaction conditions: methanol, r.t., substrate : Pd = 250 : 1 molar ratio, H$_2$ pressure 1 bar, substrate concentration 0.17 M.

Although it cannot be given a definitive explanation for the above behaviour with regard to pre-reduced and *in situ* formed catalysts (Pd/D *pre*, Pd/D *in*), one could hypothesize that the dimension of the Pd particles may play a role. Indeed, assuming the smaller size of the Pd NPs formed under catalytic conditions (see Section 3.4. / Table 3.3.), a more active Pd nanocatalyst can be rationalized in that case. On the other hand, despite the time required to reduce supported Pd^{2+} to Pd^0, no induction period was observed in hydrogenation reactions for Pd/D *in* catalysts.[36,37] The representative example reported in Fig. 3.10. indicates that when Pd/D *in* catalysts are used, Pd reduced species featured by very high catalytic activity must be in operation since the early hydrogenation reaction stages, albeit in minimal amounts. Indeed, previous reports claim that functionalized polymers are able to stabilize monovalent or mixed-valence metastable Pd species whose reactivity is higher than that of conventional Pd^0.[38] These species are often referred as "Pd$^{\delta+}$" or "Pd clusters".[39] It may be assumed that the fast, partial reduction of Pd^{2+} to the catalytically active metastable Pd$^{\delta+}$ species is actually responsible for both the absence of induction period and for the enhanced activity of the *in situ* prepared catalysts, compared to that of the pre-reduced catalysts.[25]

In order to analyze the activity and stability of Pd/D type catalysts upon recycling, the hydrogenation of methyl benzoylformate **2** was preformed. Fig 3.11. reports the data obtained for the first six cycles.
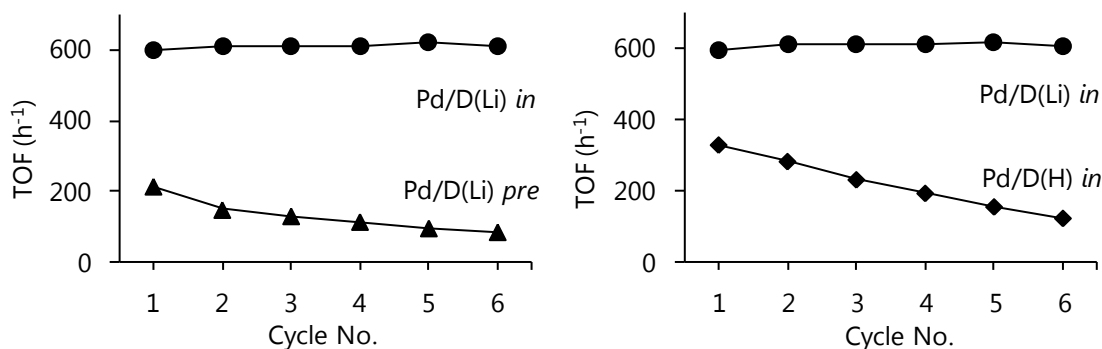

Fig. 3.11. Hydrogenation of **2**; recycle of 1 wt% Pd/D catalyst (50-100 mesh, Pd(NO$_3$)$_2$ precursor). Reaction conditions: methanol, rt, H$_2$ pressure 0.8 bar, substrate : Pd = 220:1 molar ratio, substrate concentration 0.17M, duration of each cycle 20min. Selectivity to **2a** > 99.5%. No Pd detected in solution by ICP-OES. (left) comparison between Pd NPs formed *in situ* Pd/D(Li) *in* (●) and *prior* to use Pd/D(Li) *pre* (▲), catalysts obtained by 2bar H$_2$ reduction; (right) comparison between protonated form Pd/D(H) *in* (♦) and lithiated form Pd/D(Li) *in* (●).

A perusal of the recycle data disclosed in Fig 3.11. shows that: i) irrespective of the cycle, the *in-situ* prepared catalysts were invariably more active than the corresponding isolated, pre-reduced species, ii) the *in-situ* catalysts showed pretty constant activity upon recycle, whereas the isolated catalysts slowly deactivated. In short, supported Pd catalysts obtained under catalytic conditions are not only more reactive, but also more stable, compared to the corresponding pre-reduced species. Quantitative data on the deactivation of functional polymer-supported Pd catalysts are rather poor in the literature.[40] Activity decay of pre-reduced catalysts upon recycle can be tentatively ascribed to the agglomeration of Pd NPs during catalysis (see *e.g.* Table 3.3).[41] Nevertheless, deactivation due to degradation of the polymeric support or to metal leaching in solution can be ruled out under the present experimental conditions.[14b,42] An explanation for the better reusability of the *in-situ* formed catalysts is not evident, though a

possibility is that the resin-Pd^{2+} ions act as a "reservoir" of the highly active Pd$^{\delta+}$ species which are continuously "fed" to the catalysts. The process takes place in presence of the substrate, which further prevents NPs agglomeration. From a different point of view, it could be said that a slow nucleation of Pd^{0} seeds occurs in the presence of the substrate, resulting in a constant catalyst activity upon recycle, compared to preformed Pd^{0}.[43,44]

3.5.2. IONIC FORM

Palladium was immobilized onto strong cation exchange resins in both protonated and lithiated form. The performance of Pd-based catalysts supported onto the lithiated resin Pd/D(Li) was invariably higher than that of the analogous catalysts supported onto the protonated resin Pd/D(H), specially in the hydrogenation of **1**, whose results are reported in Fig 3.10.

Compared to the corresponding protonated or pre-reduced species, the benchmark D/Pd lithiated catalyst showed up to 4 times higher efficiency under the same experimental conditions, thus confirming the beneficial effect of the resin lithiation and the generation of the active species under catalytic conditions. The contribution of homogeneous-phase catalysts can be ruled out, as neither was detected Pd leached in solution by ICP-OES, nor catalytic activity of the solutions recovered after catalysis (Maitlis test,[45] see Experimental Section).[46]

Regarding the activity of Pd NPs immobilized onto strong cation-exchange resins bearing either H^{+} or Li^{+} counterions, from the experimental data showed in Fig. 3.10., it can be concluded that lithiated resin-supported catalysts resulted to be more active compared to the corresponding protonated derivatives. Unlike previous observations on the hydroxylation of benzene by Amberlyst-supported Pd catalysts, no acceleration effects by the acid sites were detected.[14c,d,47] The higher efficiency of Li^{+} resins can be attributed to their better swelling because of the high solvation of lithium.[20,48]

With regard to the stability of the catalyst according to the ionic form when cation exchange resins are used, Fig. 3.10. shows that lithiated resin-supported catalysts were not only more active but also more stable upon recycle, significant lower conversions and an activity decay by *ca.* 50% after 6 cycles were observed for the H$^+$ resin. Catalyst deactivation using protonated resins, at least for the hydrogenation of **2**, may be ascribed to catalysts poisoning due to the degradation of acid sensitive substrates. Indeed, the use of protonated resins resulted in significant amounts of by-products due to concurrent solid acid-catalyzed reactions, *e.g.* formation of ketals, acetals (Chapter 4 / Section 4.4.3.). This behaviour was exploited by others to engineer multifunctional solid catalysts.[14,49,50] Based on our results, the presence of acidic groups was not a requisite for Pd-catalyzed hydrogenation reactions. By contrast, use of lithiated resins allowed for the obtainment of the desired products with higher selectivities.

3.5.3. BEAD DIMENSION

Hydrogenation experiments were scrutinized using catalysts embedded in resins of bead size 50-100 and 200-400 mesh. The results obtained for the recycle of Pd/D(Li) *in* catalysts in the hydrogenation of **2** under the same reaction conditions, are reported in Fig. 3.12. as example. Use of smaller beads invariably resulted in higher productivity, thus indicating that the kinetic of the hydrogenation reaction is affected by internal mass transfer limitations, *i.e.* by the diffusion inside the beads.[51] Despite of this result, resins of larger size were preferably used in the present work, due to their easier separation and reuse.
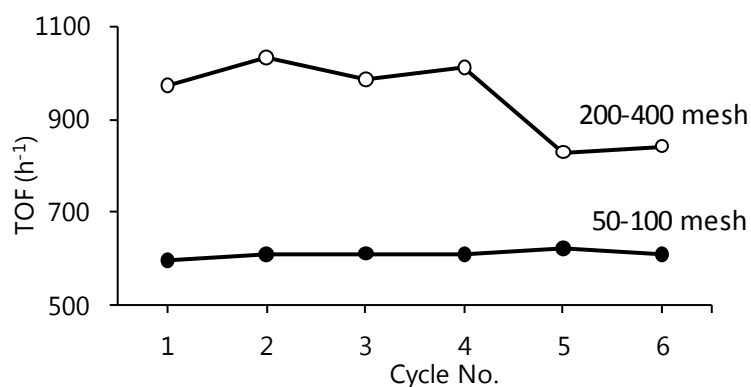
Fig. 3.12. Hydrogenation of **2**: reuse of 1 wt% Pd/D(Li) *in* catalysts (Pd(NO$_3$)$_2$ precursor) using Dowex® with different bead size. Reaction conditions: methanol, H$_2$ pressure 0.8 bar, r.t, substrate : Pd = 220 : 1 molar ratio, substrate concentration 0.17 M, orbital stirring 150 rpm. (●) 50-100 mesh, (○) 200-400 mesh. TOF (h^{-1}) at 90% conversion. Selectivity to **2a** > 99.5 %.

3.5.4. EXCHANGER GROUP

Palladium NPs supported onto ion-exchange resins with either cationic (sulfonic) or anionic (trimethylbenzyl ammonium) functionalities were tested as catalysts under the same experimental conditions. The analysis was limited to catalysts obtained after NaBH$_4$ reduction to keep identical additional parameters. In no case the anionic resin- catalysts showed higher activities compared to the cationic-supported counterparts, as is shown in Fig 3.13.
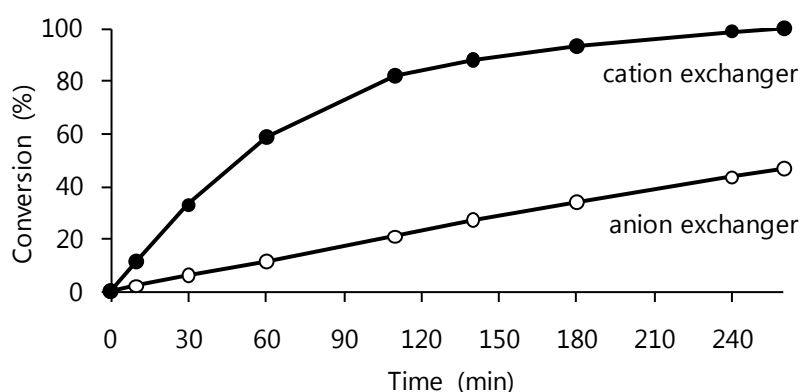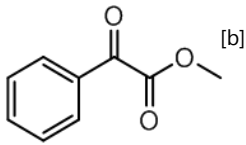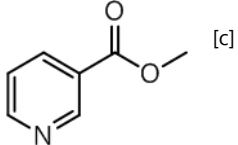

Fig 3.13. Hydrogenation of **2** by cation and anion-exchange resins-supported Pd^0 catalysts. Reaction conditions: methanol, H$_2$ pressure 0.8 bar, r.t., substrate : Pd = 220 : 1 molar ratio, substrate concentration 0.17 M. 1 wt% Pd/D catalysts (50-100 mesh, NaBH$_4$ reduction). (●) lithium sulfonate exchanger (○) trimethylbenzyl ammonium chloride exchanger.

74

The obtained result, the unavoidable use of NaBH$_4$ and the need of a two-step synthetic procedure, induced us not to explore further the anionic resin-based catalysts.

3.5.5. PALLADIUM LOADING

Pd NPs supported onto cation exchange resins were prepared with different palladium loadings. Polymer supported catalysts with 1 and 5 wt% Pd loading were tested in the hydrogenation of **2** and methyl nicotinate **3**, which results are presented in Table 3.6. The different loading did not make any distinction in the activity of the catalysts when keeping constant the ratio substrate/palladium, not even in the hydrogenation of the heteroaromatic compound where very similar conversions were reached under identical reaction conditions. These results, previously reported for palladium onto several supports,[52] indicate that there is no significant change in the specific surface area of the Pd particles in this Pd-loading range, what can be confirmed with the comparable dimensions of the clusters (see Fig. 3.8 and Table 3.4 for characterization) found for Pd NPs synthesized by this method (see Section 3.3.).

Table 3.6. Hydrogenation reactions of **2** and **3** by polymer supported Pd catalysts with different Pd content.[a]

Pd loading (wt%)	Conversion (%)	
	[b]	[c]
1	33.4	26.9
5	33.6	34.1

[a] React. conditions: Pd/D(Li) catalysts (50-100 mesh, Pd(NO$_3$)$_2$ precursor), substrate : Pd = 230 : 1 molar ratio, substrate concentration 0.17 M. [b] Catalyst Pd/D(Li) *in*, r.t., H$_2$ pressure 0.8 bar, 5 min. [c] Catalyst Pd/D(Li) *pre* obtained by 2 bar H$_2$ reduction, 40 C, H$_2$ pressure 4 bar, 24h.

3.6. OTHER FACTORS AFFECTING THE CATALYST ACTIVITY

The effect of other factors such as the solvent and the H_2 pressure in which the catalytic hydrogenation is performed was also evaluated. To this purpose, hydrogenation reactions using different solvents and pressures were performed in order to optimize the reaction conditions for the developed catalysts (Chapter 4 / Section 4.3.)

3.7. SYNTHESIS AND CHARACTERIZATION OF POLYMER SUPPORTED RHODIUM CATALYSTS

After the deep study carried out to evaluate the impact that several modifications in the preparation method could have in the activity, stability and lifetime of polymer supported Pd catalysts, and established that the optimized synthesis entails the use of the cation exchange resin in the lithiated form with MNPs reduced *in situ*, under catalytic conditions, the developed method was broadened to other metals. Particularly, it was applied in the synthesis of polymer supported rhodium nanoparticles (Rh NPs).

3.7.1. PREPARATION OF POLYMER SUPPORTED Rh CATALYSTS

A sketch of the ion-exchange resin used in the immobilization of Rh NPs is reported in Scheme 3.2. The resin was gel type (2% divinylbenzene as cross-linker), strong cation-exchange (containing sulfonic groups, DOWEX® 50WX2) and with bead dimensions ranging from 150 to 300 μm. In a first step, strong cation-exchange resins were converted into the parent lithium salt, then metallated to rhodium(I) species by a straightforward ion exchange procedure involving stirring of the resin in the presence of an appropriate amount of rhodium salt in methanol. A typical [mmol Rh] / [meq ion exchange capacity] ratio of (1 / 33) was used to afford 1.4 wt% Rh loading corresponding to 100% metal

uptake. The metallated resins were then converted into rhodium(0)-containing polymers by reduction i) with 1 bar H_2 in methanol or ii) *in-situ* under the conditions of catalytic hydrogenations; 1 bar H_2, methanol, excess of substrate, room temperature. The synthetic procedure is shown in Fig. 3.16. The characterization of the catalyst by XRD and TEM techniques showed the presence of Rh^0 nanoparticles into the polymers (see Section 3.7.2.).
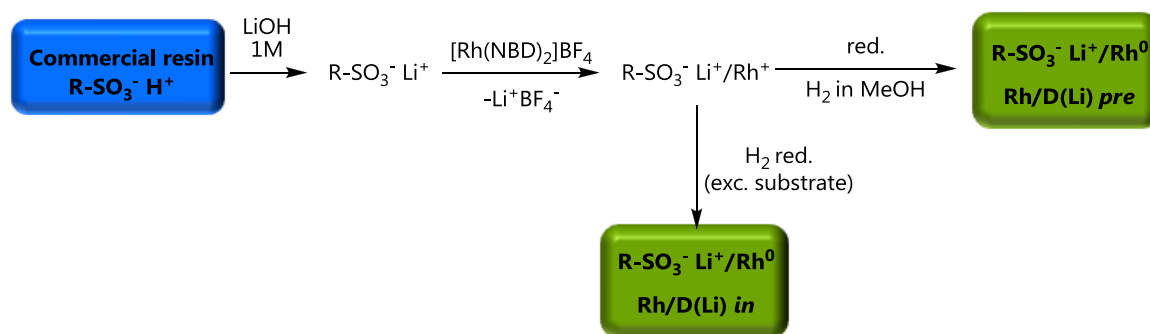

Fig. 3.16. Scheme of the synthetic procedure for the preparation of supported rhodium nanoparticles onto cation-exchange resins.

Following the proposed route, the preparation of polymer supported nanoparticulated rhodium catalyst can be achieved by a two-step synthetic procedure. To date, there are no examples reported for the preparation of supported Rh NPs onto ion exchange resins and the examples where rhodium nanoparticles are immobilized onto polymeric supports are limited. Zahmakiran *et al.*[53] have lately reported the one-step synthesis of polymer supported Rh NPs in organic medium, however the hazardous hydrazine is used as reducing agent of the rhodium(I) precursor.

3.7.2. CHARACTERIZATION OF POLYMER SUPPORTED Rh CATALYSTS

In identical way that the previous Pd based catalysts, all polymer supported Rhodium catalysts were characterized in the solid state by using the same microscopic and scattering techniques. Rhodium loading was analyzed by ICP-OES obtaining a value of 1.4 wt% Rh.

EDS maps recorded on sections of Rh-containing beads showed the metal to be located mainly in the edge of the bead giving place to a perfect egg-shell distribution. A representative example is shown in Fig. 3.17.
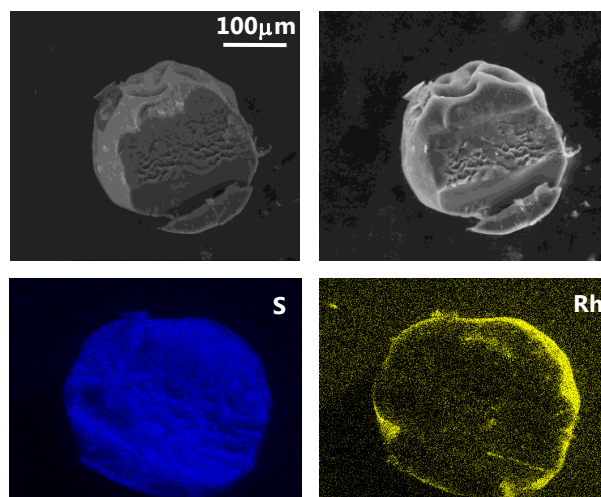

Fig. 3.17. ESEM image (1 torr, 25 KeV, 800 magnifications) of an equatorial section of 1.4 wt% Rh/D(Li) catalyst (50-100 mesh). Top left: back scattered image; top right: secondary electrons image; bottom left: sulphur map (S Kα1); bottom right: rhodium map (Rh Lα1).

A possible explanation to the peripherical distribution of rhodium within the bead could be related to the reduction step. Apparently, the reduction with H$_2$ would not be fast enough to prevent the diffusion of ions Rh$^+$ already fixed inside the bead from the core towards the periphery of the resin particle, potentially pulled out by the Rh$^+$ concentration gradient associated with the reduction of Rh$^+$ to Rh^0. In agreement with this, EDS microanalysis showed the concentration of rhodium inside the bead to be 10 times lower than in the edge. This phenomenon was also described by Corain and co-workers in the H$_2$ reduction of Pd NPs supported on cationic exchange resins.[27]

The size of Rh NPs was determined by TEM and XRD analysis, representative results are showed in Fig. 3.18. These results demonstrate that in the case of rhodium, NP's dimension is not affected by the formation of metallic rhodium *in situ* or *prior* to use. The corresponding XRD pattern shows one diffraction peak at

a 2 theta value of 41.50° which corresponds to a reflection caused by the plane (111) of Rh. The peak is broad and poorly defined, as befits the size of small particles. As previously mentioned for the palladium based catalysts, due to the low amount of rhodium (1.4 wt%) and the small nanoparticle size, no other diffraction peaks are detected. The interplanar spacing calculated from the diffractogram applying Bragg's Law is 0.217nm, indicating that the crystal structure of Rh nanoparticles is face-centered cubic, according to previously published works.[54]
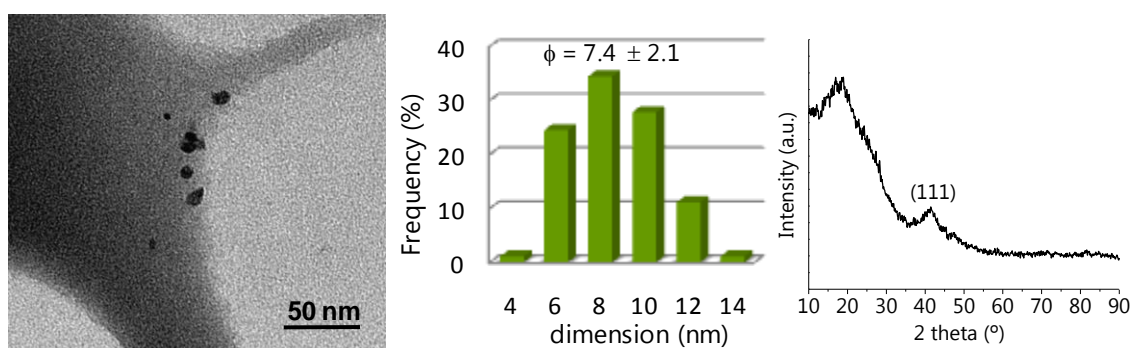

Fig. 3.18. (left) TEM image of 1.4 wt% Rh/D(Li) catalyst, (center) Size distribution from TEM analysis, (right) XRD diffractogram form the same catalysts.

However, data obtained from TEM and XRD were slightly different. A mean diameter of 7.4 nm was obtained for Rh NPs by TEM, while the size shown by XRD was 2.5 nm. The fact that Rh is mainly located in the edge of the bead could favour a possible aggregation of the nanoparticles that can be seen as a whole particle with TEM (a more local technique), but they contribute as single nanoparticles in XRD. In any case, the dimensional data obtained confirmed again that ion-exchange resins are able to accommodate small NPs.

3.7.3. EFFECT OF THE FORMATION OF Rh NPs *IN SITU*

As previously reported for Pd NPs (see Section 3.5.2), Rh NPs supported onto cation exchange resin turned out to be more active when nanoparticles are obtained *in situ*, under catalytic conditions, as can be corroborated with the

hydrogenation of **1**, which results are shown in Fig. 3.19. From XRD characterization data, it was confirmed that whether NPs are formed *in situ* or pre-reduced, the mean size falls within the range (2.5 - 2.7 nm), moreover not aggregation of clusters was either detected during the catalytic reaction. Therefore, it cannot be resorted to the stabilizing effect by the substrate to explain the different performance in catalysis in this case. A hypothetical explanation could be the contribution of rhodium(I) species to hydrogenation process, which catalytic behavior has been extensively reported.[55] Given that Rh NPs formed *in situ* are more efficient, the catalytic activity could be the result of two contributions: rhodium particles formed since the very beginning (ca. 10 min, see Experimental) and the rhodium(I) species not reduced yet, that working together give rise to a more active catalyst.
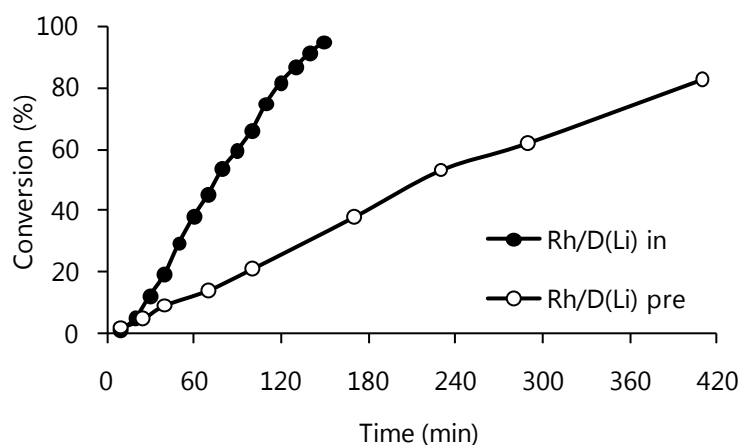

Fig. 3.19. Hydrogenation of **1** with 1.4 wt% Rh/D(Li) catalyst (50-100 mesh). Reaction conditions: methanol, rt, H_2 pressure 1 bar, substrate : Pd = 250:1 molar ratio, substrate concentration 0.17M. No Rh detected in solution by ICP-OES. (●) catalyst formed *in situ* Rh/D(Li) *in*, (○) catalyst formed *prior* to use Rh/D(Li) *pre*.

3.8. SYNTHESIS AND CHARACTERIZATION OF POLYMER SUPPORTED GOLD CATALYSTS

Having established the validity of the method to immobilize and stabilize metal nanoparticles, it was applied in the synthesis of gold nanoparticles. In this case, anion exchange resins were used for metallation and subsequent reduction with $NaBH_4$ due to the stability of the supported gold (III) species to molecular hydrogen.

3.8.1. PREPARATION OF POLYMER SUPPORTED Au CATALYSTS

A sketch of the ion-exchange resin used is reported in Scheme 3.2. The resin was gel type (2% divinylbenzene), strong anion-exchange (trimethylbenzyl ammonium group, DOWEX® 1X2), and with bead dimensions ranging from 150 to 300 μm. The resin was metallated to gold(III) species by a straightforward ion exchange procedure involving stirring of the resin in the presence of an appropriate amount of gold salt in water. A [mmol Au] / [meq ion exchange capacity] ratio of (1 / 100) was used to afford 0.7 wt% Au loading corresponding to 100% metal uptake. The metallated resins were then converted into gold(0)-containing polymers by reduction with $NaBH_4$ in water. The synthetic procedure is shown in Fig. 3.20.
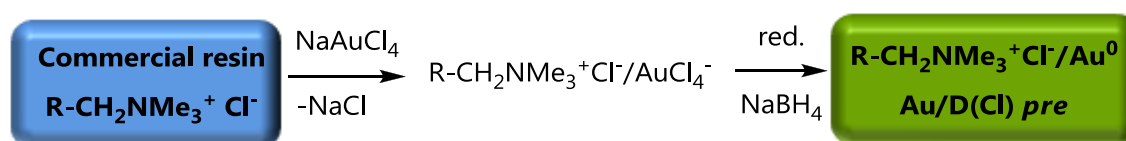

Fig. 3.20. Scheme of the synthetic procedure for the preparation of supported gold nanoparticles onto anion-exchange resins.

3.8.2. CHARACTERIZATION OF POLYMER SUPPORTED Au CATALYSTS

Au supported catalysts were characterized by TEM (Fig. 3.21.) with a mean diameter showed by this technique of 4.4 nm. Regarding the size distribution, 45% of the nanoparticles were smaller than 4 nm, what means than more than 50% were over the critical size of gold nanoparticles for catalytic applications.[56]
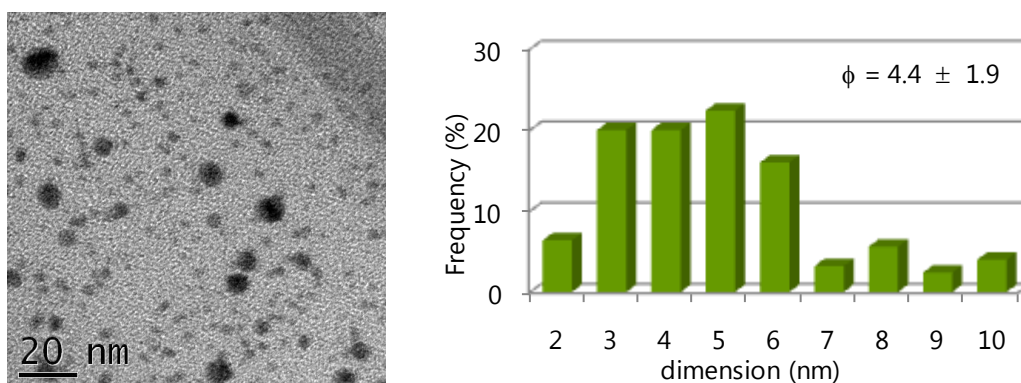

Fig. 3.21. (left) TEM image of 0.7 wt% Au/D(Cl) *pre* (right) Size distribution from TEM analysis,

3.9. CONCLUSIONS

A synthetic strategy was developed for the preparation of metal nanoparticles supported onto ion exchange resins used as heterogeneous catalysts for hydrogenation and oxidation reactions. The process is featured by simplicity and versatility, what makes it easily applicable to different resins and metals.

A systematic investigation was carried out showing that an appropriate selection of starting materials (cation exchange resin, lithiated form, simple metal cations) allows for the preparation of polymer supported Pd or Rh hydrogenation catalysts with no need nor benefits of pre-reduction steps.

The proposed synthetic method fulfils many of the requirements for catalysts utilized in the fine chemicals industry:

- it uses cheap and commercially available materials (ion-exchange resins),

- the solid catalyst is directly generated in one-pot in the flask used for the catalytic reaction, with no need of pre-reduction nor isolation steps,

- the procedure is "green" and easy, requiring H_2 as clean reagent and avoiding any excess of hazardous reducing agent (borohydrides, hydrazine), harsh or long conditioning steps, toxic stabilizers or elaborate apparatuses,

- durable hydrogenation catalysts are obtained featuring better performance in terms of activity and stability, compared to the corresponding pre-reduced species,

- the catalyst does not require any particular care of handling or storage.

Compared to commercial Pd/C catalysts, the devised system offers the clear advantages of a lower-impact process,[57] and the easiness of recycling. Since Pd/C is usually provided as a powder, it is very difficult to reuse it in practice, while it may also clog or poison the reactor used.

Notably, the synthetic approach described, while satisfying most Principles of Greener Nanomaterial Production,[58] affords a solid catalyst whose metal leach accomplish to the specification limits for residues of metal catalysts according to EMEA.[59]

3.10. EXPERIMENTAL

General information

Unless otherwise stated, all reactions and manipulations were routinely performed under nitrogen atmosphere by using standard Schlenk techniques. DOWEX® 50WX2 - 100 (H^+ form, 2% cross-linked, gel-type, 50-100 mesh [150-

300 µm] bead size, 4.8 meq/g exchange capacity), DOWEX® 50WX2 - 400 (H$^+$ form, 2% cross-linked, gel-type, 200-400 mesh [38-75 µm] bead size, 4.8 meq/g exchange capacity) strong cation-exchange resins and DOWEX® 1X2 - 100 (Cl$^-$ form, 2% cross-linked, gel-type, 50-100 mesh [150-300 µm] bead size, 3.5 meq/g exchange capacity) strong anion-exchange resin were obtained from Aldrich. The palladium precursors $Pd(NO_3)_2$, $[Pd(CH_3CN)_4(BF_4)_2]$, K_2PdCl_4 were also obtained from Aldrich, while the rhodium precursor $[Rh(NBD)_2](BF_4)$ was procured from Alfa Aesar, all of them were used as received without any further purification.

The synthesized catalysts were characterized by using the different techniques explained in detail in Chapter 2. ESEM (Environmental Scanning Electron Microscopy) was utilized to assess the stability of the polymer, whilst EDS (Energy Dispersive X-ray Spectrometer) helped to observe the distribution of metal within the bead as well as to analyse qualitatively the composition. TEM (Transmision Electron Microscopy), XRD (X-ray Diffraction) and SAXS (Small-Angle X-ray Scattering) were used to evaluate the dimension of the clusters, while the size distribution was investigated by TEM. Reactions under a controlled pressure of hydrogen were performed using either a non-metallic Büchi Miniclave® (up to 10 bar) or a stainless steel autoclave constructed at ICCOM-CNR (Firenze, Italy) described in Chapter 2. The catalytic solutions were analyzed by GC and GC-MS equipments. The metal content in the resin-supported catalysts was determined by ICP-OES (Inductively Coupled Plasma – Optical Emission Spectrometry). This technique was also applied for the quantification of leached metal content in the heterogeneous catalysis solutions recovered after reaction.

Preparation of the resins

The following operations were performed in air atmosphere. The commercial resins were washed prior of use to remove incidental impurities. 20 g of cation exchange resin were washed with refluxing deionised water for 2 h and with refluxing methanol for 1 h using a Soxhlet apparatus. After cooling down to room

temperature, the resin was washed sequentially with dichloromethane (3 x 100 ml), methanol (3 x 100 ml) and diethyl ether (3 x 100 ml). Then, it was dried in a stream of nitrogen and stored under nitrogen.

Preparation of polymer supported MNPs

Palladium was immobilized onto the cationic resin in two different states; i) *R-SO$_3^-$H$^+$*: commercial resin previously washed as abovementioned, ii) *R-SO$_3^-$Li$^+$*: commercial resin previously washed as abovementioned and subsequently treated with lithium hydroxide. Henceforth, palladation and reduction steps follow the same procedure.

<u>Lithiation of strong cation-exchange resin *R-SO$_3^-$H$^+$*</u>: 5 g of the protonated form of the commercial resin purified as above were added to a 1M solution of lithium hydroxide (150 ml) in air atmosphere. The mixture was stirred at 150 rpm at room temperature for 24 h using an orbital stirrer. The resin obtained was placed in a glass filter and washed repeatedly with deionised water (3 x 100 ml) until neutral pH of the washings. Then, it was washed with methanol (3 x 100 ml) and diethyl ether (3 x 100 ml) and dried in a stream of nitrogen. The lithiated resin *R-SO$_3^-$Li$^+$* obtained as white beads was stored under nitrogen.

<u>Polymer Supported Palladium (II) species:</u> In a typical procedure, 1 g of dry cation-exchange resin (*R-SO$_3^-$H$^+$* or *R-SO$_3^-$Li$^+$*) was added into a flask containing a degassed solution of i) palladium nitrate dihydrate (38.7 mg, 0.145 mmol, ratio Pd/sulfonic groups = 1/33) in deionized water (55 ml), or ii) tetrakis(acetonitrile)palladium(II) tetrafluoroborate (64 mg, 0.145 mmol, ratio 1/33, 55ml deionized H$_2$O). The mixture was stirred at room temperature for 24 h using an orbital stirrer. The resin obtained was transferred into a glass filter via a Teflon tube under nitrogen and washed sequentially with deionised water (3 x 50 ml), methanol (3 x 50 ml) and diethyl ether (3 x 50 ml) before being dried in a stream of nitrogen overnight. The palladiated resins obtained as orange (*R-SO$_3^-$*

Li^+/Pd^{2+}) and brownish (*R-SO$_3^-$H$^+$/Pd^{2+}*) beads were stored under nitrogen in the dark. ICP-OES analysis showed the resins to contain an average loading of 1 wt% Pd (67% metal uptake when Pd(NO$_3$)$_2$ 2H$_2$O was used as precursor) and 1.25 wt% Pd (89% metal uptake for [Pd(CH$_3$CN)$_4$(BF$_4$)$_2$]). A similar procedure was adopted for the preparation of the resins with a 5 wt% Pd loading, except that 1 g of dry resin was added to a solution of palladium nitrate dihydrate (159.8 mg, 0.600 mmol, ratio Pd/sulfonic groups = 1/8) in deionised water (100 ml). In the case of the anion-exchange resin, 1 g of dry chlorinated resin was added to a solution of potassium tetrachloropalladate (II) (34.6 mg, 0.106 mmol, ratio Pd/ammonium groups = 1/33) in deionized water (50 ml). The resin was then treated as previously described, to afford the palladiated orange resin with 1 wt% Pd loading corresponding to 92% metal uptake. The metallated resin was stored under nitrogen in the dark.

Polymer Supported Rhodium (I) species: In a typical procedure, 1 g of dry cation-exchange resin (*R-SO$_3^-$Li$^+$)* was added into a flask containing a degassed solution of bis(norbornadiene)rhodium(I) tetrafluoroborate (54.4 mg, 0.145 mmol, ratio Rh/sulfonic groups = 1/33) in methanol (55 ml). The mixture was stirred at room temperature for 24 h using an orbital stirrer. The resin obtained was transferred into a glass filter via a Teflon tube under nitrogen and washed sequentially with deionised water (3 x 50 ml), methanol (3 x 50 ml) and diethyl ether (3 x 50 ml) before being dried in a stream of nitrogen overnight. The Rh content resin obtained as pale yellow beads (*R-SO$_3^-$Li$^+$/Rh$^+$*) was stored under nitrogen in the dark. ICP-OES analysis showed the resin to contain an average loading of 1.4 wt% Rh which indicates 100% of metal uptake.

Polymer Supported Metal (0) species: four different methods were used. ***a) Reduction with NaBH$_4$***: solid NaBH$_4$ (55.0 mg, 1.45 mmol) was slowly added to 0.5 g of 1 wt% palladium(II)-resin in 30 ml of deionized water at 0 °C. The resin became immediately black. The suspension was then stirred at 160 rpm at room

temperature for 3h, using an orbital stirrer. The resin obtained was transferred into a glass filter via a Teflon tube under nitrogen and washed with deionized water (5 x 75 ml), methanol (3 x 75 ml) and diethyl ether (3 x 75 ml), and was dried in a stream of nitrogen overnight. The product, obtained as black beads, was stored under nitrogen in the dark. **b) *Reduction with a static atmosphere of H$_2$*:** 0.5 g of metallated resin were placed into a non-metallic autoclave under nitrogen. 30 ml of methanol were then added via a Teflon tube under nitrogen. Nitrogen was replaced by hydrogen with three cycles 2 bar H$_2$/ normal pressure, the autoclave was finally charged with 2 bar H$_2$. The mixture was kept at room temperature for 1 h with orbital stirring at 160 rpm. The resin became slowly black. After that time, the autoclave was depressurized and the resin obtained was washed by decantation with degassed methanol (3 x 75 ml) and diethyl ether (3 x 75 ml), before it was dried in a stream of nitrogen for 2 h. The autoclave was then opened and the resin transferred into a glass filter where it was dried under a stream of nitrogen overnight. **c) *Reduction with a flow of H$_2$*:** For the reduction in the absence of substrate, 50 mg of metallated resin was suspended in 12 ml of methanol under nitrogen. Hydrogen gas was bubbled at 1 bar at room temperature for 1 h under orbital stirring at 160 rpm. The resin became slowly black (ca. 20 min for Pd, ca. 10 min for Rh). After that time, the resin was whether c1) isolated or c2) immediately used in catalysis. In the first case (c1), the resin was transferred into a glass filter under nitrogen via a Teflon tube, it was washed with methanol (3 x 30 ml), diethyl ether (3 x 30 ml) and then dried in a stream of nitrogen overnight. The product, obtained as black beads, was stored under nitrogen in the dark. In the second case (c2), the methanolic solution was decanted and without further washing step, the substrate solution was added under H$_2$ atmosphere. **d) *Reduction in-situ with an excess of substrate*:** 50 mg of resin supported metal (n+) were swollen in a methanolic solution of the substrate 0.17M contained into a flask, then a flow of 1 bar H$_2$ was bubbled at room temperature for 1 h under orbital stirring at 160 rpm. The resin became

slowly black (ca. 20 min for Pd, ca. 10 min for Rh).

Polymer Supported Gold (0) species In a typical procedure, 1 g of dry anion-exchange resin (R-$CH_2NMe_3{}^+Cl^-$) was added into a flask containing a degassed solution of sodium tetrachloroaurate(III) dehydrate (13.9 mg, 0.035 mmol, ratio Au/ammonium groups = 1/100) in deionized water (25 ml). The mixture was stirred at room temperature for 2 h using an orbital stirrer, the resin became wine colour. After that, the solution was removed to be analyzed by ICP-OES to determine Au loading (by difference) and a new solution of $NaBH_4$ (39.7 mg, 1.05 mmol) in 25 ml deionized water was added. From here on, it proceeded as abovementioned for $NaBH_4$ reduction method. The Au content resin obtained as wine colour beads (R-$CH_2NMe_3{}^+Cl^-/Au^0$) was stored under nitrogen in the dark.

Hydrogenation reactions in batch mode, catalyst recycling

Low pressure: All the hydrogenation reactions were performed in a 100 ml flask using very mild conditions at 1bar of H_2 and room temperature. The experimental procedure shows slight differences depending on the catalytic specie used. ***a) Polymer Supported MNPs formed in excess of substrate***: In a typical experiment, 50 mg of the resin supported metal (n+) specie was added into a flask containing a degassed solution of the substrate 0.17M. A flow of hydrogen gas was bubbled at 1 bar and 15 mL/min at room temperature, using an orbital stirrer at 160 rpm. This was taken as the start time of the reaction. The resin became slowly black (ca. 20 min.). After the desired time, the solution was completely removed under a stream of hydrogen using a gas-tight syringe. A sample of this solution (0.5 μl) was used for GC (product yield), GC-MS (product identification) and ICP-OES analysis (metal leaching), while the remaining aliquot was used for the Maitlis test (catalyst leaching test, see below). A fresh solution of the substrate was then transferred under hydrogen via a gas-tight syringe into the flask containing the recovered supported catalyst. The mixture was stirred at 160 rpm and room temperature under hydrogen flow and, after the desired time,

the mixture was treated as described above. The same recycling procedure was used in the subsequent hydrogenation cycles. After use in catalysis, the solid catalyst was washed with methanol (3 x 10 ml) and diethyl ether (3 x 10 ml), dried in a stream of nitrogen overnight and stored under nitrogen for later characterization. Catalyst leaching test: an additional portion of the substrate was added under hydrogen to the clear solution recovered after the first and subsequent cycles, hydrogen was then bubbled through the solution at room temperature for 1h and the mixture analyzed by GC for conversion measurement.

b) Polymer Supported MNPs formed in absence of substrate: In a typical experiment, 50 mg of the resin supported metal (0) specie was added into a flask containing a degassed solution of methanol (12ml) and left it swollen. A portion of the substrate was added under N_2 flow to reach a final concentration of 0.17M. A flow of hydrogen gas was then bubbled at 1 bar and 15 mL/min at room temperature under orbital stirrer at 160 rpm. This was taken as the start time of the reaction. After the desired time, the methanol solution was completely removed under a stream of hydrogen using a gas-tight syringe. From here on, it proceed as abovementioned.

Medium/High pressure: In a typical experiment, the supported catalyst precursor, either resin-Palladium(0) or resin-Palladium(II) (50 mg, ca. 1 wt% Pd ca. 0.005 mmol of palladium), was placed under nitrogen into a metal-free autoclave. A degassed solution of substrate (1.04 mmol) in methanol (6 ml) was transferred under nitrogen via a Teflon tube into the autoclave. Nitrogen was replaced by hydrogen with three cycles pressurization/depressurization. The autoclave was finally charged with the desired pressure of hydrogen and then stirred at room temperature at 160 rpm, using an orbital stirrer. After the desired time, the reactor was depressurized and the solution was removed under a stream of hydrogen using a gas-tight syringe. From here on, it proceed as abovementioned.

REFERENCES

1   a) H. Cong, J. A. Porco, *ACS Catal.,* 2, **2012**, 65; b) J. M. Campelo, D. Luna, R. Luque, J. M. Marinas, A. A. Romero, *ChemSusChem,* 2, **2009**, 18; c) A. Fukuoka, P. L. Dhepe, *Chem. Rec.,* 9, **2009**, 224; d) N. Semagina, L. Kiwi-Minsker, *Catal Rev.,* 51, **2009**, 147.

2   a) D. Astruc (Ed)*, Nanoparticle and Catalysis*, Wiely-VCH, Weinheim, **2007**; b) D. J. Cole-Hamilton, R. P. Tooze (Eds), *Catalyst Separation, Recovery and Recycling; Chemistry and Process Design*, Springer, Dordrecht, **2006**; c) R. A. Sheldon, H. van Bekkum (Eds), *Fine Chemicals Through Heterogeneous Catalysis*, Wiley-VCH, Weinheim, **2001**.

3   a) German Catalysis Society, *Roadmap for catalysis research in Germany*, March **2010**; b) R. A. Sheldon, I. Arends, U. Hanefeld, *Green Chemistry and Catalysis*, Wiley-VCH, Weinheim, **2007**.

4   a) W. J. W. Watson, *Green Chem.*, 14, **2012**, 251; b) C. Lucarelli, A. Vaccari, *Green Chem.*, 13, **2011**, 1941.

5   a) G. Glaspell, H. M. A. Hassan, A. Elzatahry, V. Abdalsayed, M. S. El-Shall, *Top. Catal.*, 47, **2008**, 22; b) S. Senkan, M. Kahn, S. Duan, A. Ly, C. Ledholm, *Catal. Today*, 117, **2006**, 291; c) A. Barau, V. Budarin, A. Caragheorgheopol, R. Luque, D. J. Macquarrie, A. Prelle, V. S. Teodorescu, M. Zaharescu, *Catal. Lett.*, 124, **2008**, 204; d) A. Sandoval, A. Gomez-Cortes, R. Zanella, G. Diaz, J. M. Saniger, *J. Mol. Catal. A: Chem.*, 278, **2007**, 200; e) M. Haruta, *Chem. Rec.*, 3, **2003**, 75.

6   a) V. Bethmont, C. Montassier, P. Marecot, *J. Mol. Catal. A: Chem.*, 152, **2000**, 133; b) C. Pham-Huu , N. Keller , G. Ehret , L. J. Charbonnière , R. Ziessel , M. J. Ledoux , *J. Mol. Catal. A: Chem.*, 170, **2001** ,155.

7   J. Wöllner, W. Neir, Bergbau und chemie (Homberg), German Patent 1260454, **1968**.

8   *Methyl Isobutyl Ketone Product Information*, The Dow Chemical Company, Form No. 327-00032-0405, June **2002**.

9   J. M. Tibbitt, B. C. Gates, J. R. Katzer, *J. Catal.,* 38, **1975**, 505.

10   N. Li, J. M. J. Fréchet, *J. Chem. Soc. Chem. Commun*., **1985**, 1100.

11   M. Ohtaki, M. Komiyama, H. Hirai, N. Toshima, *Macromolecules*, 24, **1991**, 5567.

12   T. Ishida, S. Okamoto, R. Makiyama, M. Haruta, *App. Catal. A: Gen.,* 353, **2009**, 243

13   a) B. Corain, M. Zecca, P. Canton, P. Centomo, *Phil. Trans. R. Soc. A,* 368, **2010**, 1495; b) M. Zecca, P. Centomo, B. Corain in *Metal Nanoclusters in Catalysis and Materials Science*, Eds: B. Corain, G. Schmid, N. Toshima, Elsevier, Amsterdam, **2008**, 201.

14   a) T. Seki, J. D. Grunwaldt, A. Baiker, *Chem. Commun.* **2007**, 3562; b) T. Seki, J. D. Grunwaldt, N. van Vegten, A. Baiker, *Adv. Synth. Catal.* 350, **2008**, 691; c) W. Laufer, W. F. Hoelderich, *Chem. Commun.*, **2002**, 1684; d) W. Laufer, J. P. M. Niederer, W. F. Hoelderich, *Adv. Synth. Catal.*, 344, **2002**, 1084; e) A. M. Raspolli Galletti, C. Antonetti, V. De Luise, M. Martinelli, *Green Chem.*,14, **2012**, 688.

15   G. Gelbard, *Ind. Eng. Chem. Res.*, 44, **2005**, 8468.

16   A. Biffis, R. Ricoveri, S. Campestrini, M. Kralik, K. Jeřábek, B. Corain, *Chem. Eur. J.* 8, **2002**, 2962.

17   a) B. Corain, K. Jeřábek, P. Centomo, P. Canton, *Angew. Chem. Int. Ed.*, 43, **2004**, 959; b) H. Bönnemann, R. M. Richards, *Eur. J. Inorg. Chem.*, **2001**, 2455; c) A. Roucoux, J. Schulz, H. Patin, *Chem. Rev.*, 102, **2002**, 3757; d) L. S. Ott, R. G. Finke, Coord. Chem. Rev., 251, **2007**, 1075.

18   a) B. Corain, M. Zecca, K. Jeřábek, *J. Mol. Catal.*, 177, **2001**, 3; b) M. Králik, A. Biffis, *J. Mol. Catal.*, 177, **2001**, 113.

19   a) P. Barbaro and F. Liguori, *Chem. Rev.,* 109, **2009**, 515; b) P. Barbaro, *Chem. Eur. J.,* 12, **2006**, 5666.

20   P. Barbaro, C. Bianchini, G. Giambastiani, W. Oberhauser, L. Morassi Bonzi, F. Rossi, V. Dal Santo, *Dalton Trans.*, **2004**, 1783.

21 a) M. A. Harmer, *Industrial Processes Using Solid Acid Catalysts* in Handbook of Green Chemistry and Technology, J. Clark and D. Macquarrie (Eds), Blackwell Science, Oxford, **2002**, pp 86; b) I. Tóth and B. E. Hanson, *J. Mol. Catal.,* 71, **1992**, 365.

22. M. Kralik, M. Hronec, S. Lora, G. Palma, M. Zecca, A. Biffis, B. Corain, *J. Mol. Catal. A: Chem.*, 97, **1995**, 145.

23 Cationic palladiated resins are redox stable to dihydrogen in methanol up to 5 bar. See also: M. Kralik and D. Gasparovicova in *Proceedings of the CHISA 2000 Special Symposium on Chemical Technology for Sustainable Future*, 27–31 August **2000**, Prague.

24 S. G. Bratsch, *J. Phys. Chem. Ref. Data* 18, **1989**, 1.

25 Induction periods were previously reported for the hydrogenation of cyclohexene by preformed Pd NPs onto functional polymers and were attributed to the reduction of residual amounts of palladium(II) acetate in the catalyst precursor. See: P. Centomo, M. Zecca, M. Kralik, D. Gasparovicova, K. Jeřábek, P. Canton, B. Corain, *J. Mol. Catal. A Chem.,* 300, **2009**, 48.

26 a) M. Zecca, R. Fišera, G. Palma, S. Lora, M. Hronec, M. Králik, *Chem. Eur. J.,* 6, **2000**, 1980; b) G. Bombi, S. Lora, M. Zancato, A. A. D'Archivio, K. Jeřábek, B. Corain, *J. Mol. Cat. A: Chem.*, 194, **2003**, 273; c) D. Belli, A. A. D'Archivio, L. Galantini, S. Lora, A. Biffis, B. Corain, *J. Mol. Catal. A: Chem.*, 157, **2000**, 173; d) A. Primavera, M. Zecca, B. Corain, *J. Mol. Catal.,* 108, **1995**, 131; e) Y. Nakao, K. Kaeriyama, *J. Colloid Interface Sci.*, 131, **1989**, 186.

27 B. Corain, M. Králik, *J. Mol. Cat. A: Che.,* 173, **2001**, 99.

28 a) R. Fisera, M. Kralik, J. Annus, V. Kratky, M. Zecca, M. Hronec, *Collect. Czech. Chem. Commun.*, 62, **1997**, 1763; b) M. Zecca, M. Kralik, M. Boaro, G. Palma, S. Lora, M. Zancato, B. Corain, *J. Mol. Catal. A: Chem.,* 129, **1998**, 27.

29 (a) H. Hirai, Y. Nakao, N. Toshima, *J. Macromol. Sci. Chem.*, 6, **1979**, 727. (b) H. Choo, B. He, K.Y. Liew, H. Liu, J. Li, *J. Mol. Catal. A: Chem.*, 244, **2006**, 217, (c) S-W. Kim, J. Park, Y. Jang, Y. Chung, S. Hwang, T. Hyeon, *Nano Lett.,* 3, **2003**, 1289. (d) Y. Xiong, J. Chen, B. Wiley, Y. Xia, *J. Am. Chem. Soc.*, 127, **2005**, 7332.

30 Schulz distribution: G. V. Z. Schulz, *Phys. Chem. Abt. B,* 43, **1939**, 25.

31 T. B. Lin, D. L. Chung, J. R. Chang, *Ind. Eng. Chem. Res.,* 38, **1999**, 1271.

32 a) R. H. Grubbs, L. C. Kroll, *J. Am. Chem. Soc.,* 93, **1971**, 3062; b) C. Burato, P. Centomo, G. Pace, M. Favaro, L. Prati, B. Corain *J. Mol. Catal. A: Chem,.* 238, **2005**, 26; c) A. Biffis, A. A. D'Archivio, K. Jerabek, G. Schmid, B. Corain, *Adv. Mater.*, 12, **2000**, 1909; d) B. Corain, P. Centomo, M. Zecca, *Chim. Ind.* (Milan), 86, **2004**, 114; e) F. Artuso, A. A. D'Archivio, S. Lora, K. Jerabek, M. Kralik, B. Corain, *Chem. Eur. J.*, 9, **2003**, 5292.

33 a) M. C. Daniel, D. Astruc, *Chem. Rev.,* 104, **2004**, 293; b) M. G. Warner, J. E. Hutchison, *Synth., Funct. Surf. Treat. Nanopart.*, **2003**, 67; c) N. R. Jana, X. Peng, *J. Am. Chem. Soc.,* 125, **2003**, 14280; d) D. L. Hanson, J. R. Katzer, B. C. Gates, G. C. A. Schuit, H. F. Harnsberger, *J. Catal.*, 32, **1974**, 204.

34 a) G. Grochola, I. K. Snook, S. P. Russo, *J Chem Phys.*, 129, **2008**, 154708; b) K. Philippot, B. Chaudret, *C.R. Chimie,* 6, **2003**, 1019.

35 a) G. A. Somorjai, J. Y. Park, *Angew. Chem. Int. Ed.,* 47, **2008**, 9212; b) D. Yu. Murzin, *Catal. Sci. Technol.* 1, **2011**, 380.

36 Reduction of resin-supported Pd^{2+} by H$_2$ in methanol at room temperature was accomplished in *ca.* 30-60min (see 'Experimental'). See also: R. Fisera, M. Kralik, J. Annus, V. Kratky, M. Zecca, M. Hronec, *Collect. Czech. Chem. Commun.*, 62, **1997**, 1763.

37 By contrast, large induction periods were previously reported for reactions catalyzed by *in-situ* formed, un-supported Pd NPs. See for example: a) L. Durán Pachón, C. J. Elsevier, G. Rothenberg, *Adv. Synth. Catal.,* 348, **2006**, 1705; b) M. T. Reetz, E. Westermann, *Angew. Chem. Int. Ed.*, 39, **2000**, 165.

38 a) Z. M. Michalska, B. Ostaszewski, J.Zientarska, J. W. Sobczak, *J. Mol. Catal. A: Chem,.* 129, **1998**, 207; b) V. A. Semikolenov, V. A. Likhotobov, P. A. Zhdan, A. P. Shelepin, I. Yu. Ermakov, *Kinet. Katal.,* 21, **1980**, 429.

39   a) S. M. Huang, L. Wang, B. L. He, *React. Polym.,* 16, **1991-1992**, 93; b) Z. Karpinski, *Adv. Catal.*, 37, **1990**, 45.

40   The recycle of sulfonated resin-supported Pd^0 pre-reduced catalysts was previously reported for the hydrogenation of cyclohexene in: a) M. Kralik, V. Kratky, P. Centomo, P. Guerriero, S. Lora, B. Corain, *J. Mol. Catal. A: Chem.,* 195, **2003**, 219, b) see Ref 13a.

41   a) G. A. Somorjai, *Introduction to Surface Chemistry and Catalysis*, Wiley, New York, **1994**; b) A. Rouocoux, J. Schulz, H. Patin, *Chem. Rev.,* 102, **2002**, 3757.

42   M. Kralik, B. Corain, M. Zecca, *Chem. Papers,* 54, **2000**, 254.

43   T. Leisenr, C. Rosche, S. Wolf, F. Granzer, L. Wöste, *Surf. Rev. Lett.,* 3, **1996**, 1105.

44   The concept of "catalytic reservoir" was already adopted to justify the catalytic behaviour of supported Pd NPs, although for different reactions. See: a) J. G. de Vries, *Dalton Trans.,* **2006**, 421; b) A. M. Trzeciak, J. J. Ziólkowski, *Coord. Chem. Rev.,* 251, **2007**, 1281; c) M. T. Reetz, J. G. de Vries, *Chem. Commun.,* **2004**, 1559.

45   J. P. Collman, K. M. Kosydar, M. Bressan, W. Lamanna, T. Garrett, *J. Am. Chem. Soc.,* 106, **1984**, 2569.

46   Unless otherwise stated, Pd leaching in solution was below the ICP-OES detection limit, i.e. 0.006 ppm. It was previously reported that Pd^0 species are hardly leached from ion-exchange resins, see also Ref 13a

47   J. T. Miller, B. L. Mojet, D. E. Ramaker, D. C. Koningsberger, *Catal. Today,* 62, **2000**, 101.

48   R. Selke, K. Häupke, W. Krause, *J. Mol. Catal.,* 56, **1989**, 315.

49   a) J. M. Tibbitt, B. C. Gates, J. R. Katzer, *J. Catal.,* 38, **1975**, 505; b) M. C Wissler, U. Jagusch, B. Sundermann, W. F. Hoelderich, *Catal. Today,* 121, **2007**, 6.

50   Z. Karpiński, S. N. Gandhi, W. M. H. Sachtler, *J. Catal.,* 141, **1993**, 337.

51   a) A. Drelinkiewicz, A. Knapik, A. Waksmundzka-Góra, A. Bukowska, W. Bukowski, J. Noworól, *React. Fun. Poly*. 68, **2008**, 1059; b) A. El Kadib, R. Chimenton, A. Sachse, F. Fajula, A. Galarneau, B. Coq, *Angew. Chem. Int. Ed.* 48, **2009**, 4969; c) D. De Vos, M. Dam, B. F. Sels, P. A. Jacobs, *Chem. Rev.* 102, **2002**, 3615; d) Y. Ono, *J. Catal.,* 216, **2003**, 406.

52   a) S. Mahmoud, A. Hammoudeh, S. Gharaibeh, J. Melsheimer, *J. Mol. Catal. A: Chem.,* 178, **2002**, 161; b) T. Kubota, H. Ogawa, Y. Okamoto, T. Misaki, T. Sugimura, *Appl. Catal A: Gen.,* 437 – 438, **2012**, 18.

53   S. Karahan, M. Zahmakiran, S. Özkar, *Chem Commun.,* 48, **2012**, 1180.

54   A.J. Bruss, M.A. Gelesky, G. Machado, J. Dupon, *J. Mol. Catal. A: Chem.,* 252, **2006**, 212.

55   a) R. H. Grubbs, L. C. Kroll, *J. Am. Chem. Soc.,* 93, **1971**, 3062; b) U. Nagel, J. Leipold *Chem. Ber.,* 129, **1996**, 815; c) C. Bianchini, M. Frediana, F. Vizza, *Chem. Commun.,* **2001**, 479.

56   F. Pinna, A. Olivo, V. Trevisan, F. Menegazzo, M. Signoretto, M. Manzoli, F. Boccuzzi, *Catal. Today*, **2012**, doi:10.1016/j.cattod.2012.01.033.

57   a) R. Mozingo, *Palladium Catalysts* in *Org. Synth*. Coll. Vol. 3, **1955**, 685; b) *Vogel's Textbook of Practical Organic Chemistry*, 5th ed, **1989**, 452-460.

58   a) J. A. Dahl, B. L. S. Maddux, J. E. Hutchison, *Chem. Rev.* 107, **2007**, 2228; b) W. W. Weare, S. M. Reed, M. G. Warner, J. E. Hutchison, *J. Am. Chem. Soc.* 122, **2000**, 12890.

59   European Agency for the Evaluation of Medicinal Products *Note for guidance on specification limits for residues of metal catalysts*, EMEA/CHMP/SWP/4446/2000, February 2008.

4

Catalytic Reactions in Batch Mode

4.1. OVERVIEW

This chapter covers the analysis of the catalysts prepared in terms of activity, selectivity and reusability. Hydrogenation reactions of model substrates were performed with palladium and rhodium based systems evaluating their performance in reactions relevant to the synthesis of fine chemicals. A comparison with the state of art was also carried out, when possible. Selectivity to partial hydrogenation products of hydrocarbons with multiple C=C and/or C≡C bonds was studied with close attention to the synthesis of the leaf alcohol *cis*-3-hexen-1-ol, since it is an important compound in the fragrance industry,[1] and to the hydrogenation of 1,5-cyclooctadiene. The chemo-selectivity to double bond hydrogenation in the presence of other functional groups was also tested. Finally, the oxidation reaction of furfural was carried out to evaluate the activity of gold based catalyst.

4.2. INTRODUCTION

The application of catalytic methods to the large-scale production of complex molecules, such as agrochemicals and pharmaceuticals, is continuously increasing due to a more environmentally concerned legislation.[2] In order to achieve greener industrial processes, catalysts should be highly active, selective and recyclable under mild reaction conditions. In the special case of hydrogenation and oxidation reactions, the use of clean alternative reagents, i.e. hydrogen and oxygen respectively, can decrease the high E-factors that rule the fine chemicals sector.[3].

Catalytic hydrogenations in the fine chemicals industry are usually carried out with heterogeneous catalysts, whereas homogeneous catalysts are typically applied for highly selective transformations, particularly enantioselective reductions. Among the heterogeneous systems, palladium-based catalysts are the most versatile and widely applied.[4] On the other hand, selective oxidation reactions constitute industrial core technologies for converting bulk chemicals into useful products.[5] With the late discovery of gold as a very active catalyst,[6] the use of gold based heterogeneous catalysts represents a very promising system for oxidation processes.

One of the major problems in synthesis of fine chemicals is related to the chemo-, regio-, stereo- or enantio-selective transformation of organic molecules. Various types of hydrogenation reactions are required in several manufacturing processes towards valuable products in fine industry.[7] For example, selective hydrogenation of hydrocarbons with multiple C=C and/or C≡C bonds to achieve partial hydrogenation products is a highly desired and challenging process in the pharmaceutical, agrochemical and petrochemical industries.[8] Particularly, the stereo- and chemo- selective hydrogenation of alkenes and alkynes in the presence of other functional groups is of fundamental importance in the synthesis of food additives, flavors and fragrances.[9,10] Partial hydrogenation

reactions are also crucial in industrial polymerization processes to achieve the complete elimination of alkynes and dienes from alkene feedstocks.[11]

In general, a drawback in hydrogenation of alkynes by metal catalysts is overhydrogenation with formation of fully saturated alkane products, since the second hydrogenation step (alkene to alkane) is generally faster than the first (alkyne to alkene).[12] However, as long as some of the starting alkyne remains in the reaction mixture, selectivity can be high since the alkynes bind more strongly to the metal surface.[13] The most widely used and selective commercial catalysts for this reaction is the Lindlar catalyst, based on Pd supported on $CaCO_3$ and doped with Pb.[14]

Several papers have been published in which polymer supported catalyst were used in selective transformations. With regard to hydrogenation of α,β-unsaturated carbonyl compounds, J. Aumo *et al* reported a Pd polymer-supported fiber catalyst used in the hydrogenation of citral, an important compound in the perfumery industry, finding the selectivity to citronellal (mono-unsaturated ketone) to be higher than in the case of Pd/C catalyst.[15]

The first example of a polymer-supported gold catalyst was provided by Shi, Deng *et al*,[16] who used a cation exchange resin as a polymer support after pre-treatment with NaOH for the impregnation with $HAuCl_4$. The obtained catalyst was applied to the formation of urea and carbamates from amines using carbon monoxide and molecular oxygen. The most recent example of polymer-supported gold catalysts came from Kobayashi and co-workers,[17] who developed recyclable polystyrene-based copolymer-microencapsulated gold nanocatalysts. They examined the oxidation of 1-phenylethanol under almost the same reaction conditions as employed by Corma and co-workers[18] with Au/CeO_2, and found the polymer catalysts to be 60% more active than the analogous metal oxide, highlighting the competitive alternative regarding to the support that polymers offer to the extensively used metal oxides.

In order to evaluate the performance of the developed catalysts in important reaction types for the synthesis of fine chemicals, hydrogenation and oxidation reactions of model molecules were studied. The proposed examples were carefully analysed and compared with similar systems already described in literature.

4.3. OPTIMIZATION OF REACTION CONDITIONS

To assure an ideal participation of the developed catalysts in hydrogenation reactions, the best reaction conditions were scrutinized. In this regard, the effect of the reaction media (solvent) and the H_2 reaction pressure on the catalyst's activity was analyzed.. Hydrogenations reactions with probe substrates, methyl 2-acetamidoacrylate **1** and methyl benzoylformate **2** (Scheme 4.1.) were carried out to optimize the catalytic conditions for this kind of catalysts
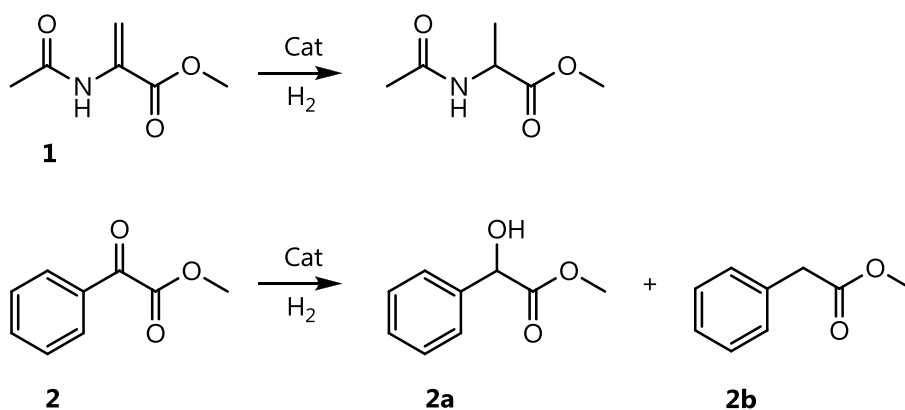
Scheme 4.1. Sketch of the probe substrates tested for optimization of the reaction conditions.

4.3.1. SOLVENT

A typical feature of ion-exchange resin-supported catalysts is that their activity is ruled by the swelling of the support in the reaction solvent.[19] Accordingly, water or methanol are the most appropriate in the case of gel-type resins. It was investigated the catalytic activity and the reusability of the supported Pd species

catalyzing either in pure water, pure methanol or in a mixture methanol : water = 3 : 1 (v/v). For further confirmation, the reaction was also performed in THF. Representative results for the hydrogenation of **1** and **2** are reported in Table 4.1. and Fig. 4.1, respectively.

Table 4.1. Solvent effect in the hydrogenation of **1**: activity and leaching test.[a]

Solvent	TOF (h^{-1})	Conversion (%)	
		Catalytic reaction	Recovered solution[b]
H_2O	624	69.3[c]	30.0[e]
MeOH	1238	91.7[d]	0.0[f]
THF	0	0.0	0.0

[a] React. conditions: 1 wt% Pd/D(Li) *in* catalyst (50-100 mesh, $Pd(NO_3)_2$ precursor), r.t., substrate : Pd = 450 : 1 molar ratio, H_2 pressure 0.8 bar, substrate concentration 0.17 M. [b] Solution recovered after decantation of the catalyst and kept for 60 min under under 1 bar H_2 pressure. [c] 30 min. [d] 20 min. [e] 1.8 ppm Pd in solution by ICP-OES. [f] No Pd detected in solution.
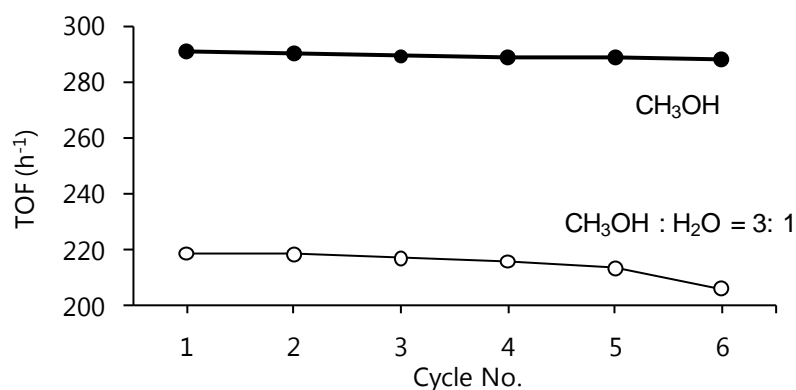
Fig. 4.1 Solvent effect in the hydrogenation of **2**; catalyst recycle. Reaction conditions: H_2 pressure 0.8 bar, r.t., substrate : Pd = 220 : 1 molar ratio, substrate concentration 0.17 M, 1 wt% Pd/D(Li) *pre* catalyst (50-100 mesh, $Pd(NO_3)_2$ precursor, obtained by 2 bar H_2 reduction), conversions > 93.5%. (●) solvent CH_3OH, duration of each cycle 45min. (o) solvent CH_3OH:H_2O 3:1, duration of each cycle 60 min.

Regardless of the substrate or the catalyst preparation method, the presence of water in the reaction solution invariably caused both a decrease in the catalyst activity and a loss of productivity upon reuse compared to pure methanol, moreover the solutions recovered after each cycle showed significant amounts of palladium leached (> 1 ppm), as well as a residual catalytic activity. This indicates

that the activity loss of the supported catalyst can be safely ascribed to the leach of catalytically active Pd species in solution in those cases. Deactivation of polymer-supported Pd catalysts due to dissolution of metal crystallites was previously reported for the hydrogenation of nitroaromatics as a consequence of oxidative side-reactions.[20] With respect to THF, no activity was detected when used as a solvent,. The hydrophilic resin was not able to swell in the organic solvent what prevented the access to the catalytic sites within the micropores.

4.3.2. H_2 PRESSURE

Hydrogenation reactions were carried out at different hydrogen pressures. Representative results for the hydrogenation of **2** are reported in Fig. 4.2. As a general observation, an increase of the H_2 pressure in the range 1-8 bar caused an increase of the overall catalyst activity up to reach a *plateau,* whilst promoting the formation of fully hydrogenated species. In the case of the hydrogenation of **2** using Pd/D(Li) *in* type catalysts, nearly constant conversions were obtained above *ca.* 4 bar, whereas the selectivity to the alcohol product **2a** decreased from 96.6 to 88.4%, on passing from 1 to 8 bar H_2. A similar dependence from the total reaction pressure was previously described for the hydrogenation of cyclohexene by macroporous resin-supported Pd catalysts and attributed to mass transport limitation of gaseous H_2.[21]
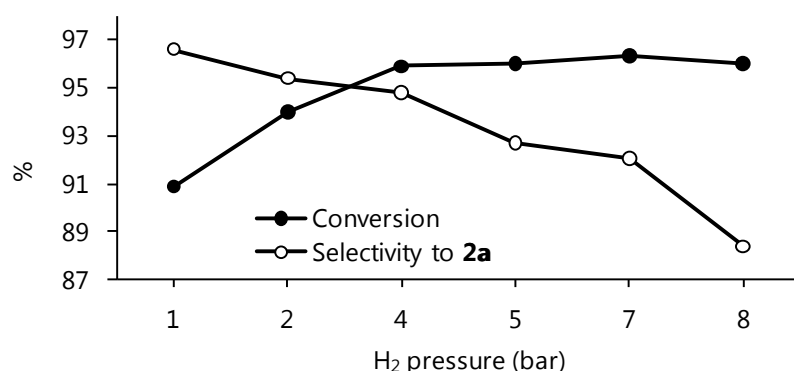
Fig. 4.2. Catalytic hydrogenations of **2** under 1 - 8 bar H_2 pressure. Reaction conditions: methanol, 1 wt% Pd/D(Li) *in* catalyst (50-100 mesh, Pd(NO$_3$)$_2$ precursor), r.t., substrate : Pd = 250 : 1 molar ratio, time 15 min, substrate concentration 0.1 M.

4.4. HYDROGENATION REACTIONS WITH Pd NPS

Having established that the optimal reaction conditions for Pd/D type catalysts in hydrogenation reactions are methanolic solutions and H_2 pressure of 1 bar, an in depth investigation was carried out with regard to activity and selectivity.

4.4.1. HYDROGENATION OF C=C BONDS

Carbon–carbon double bonds are among the more readily hydrogenated functional groups that may be converted to the corresponding saturated hydrocarbons under mild conditions (low hydrogen pressure and room temperature). In order to get a first evaluation of the activity of the catalysts developed in the present work, the hydrogenation of cyclohexene **4** was carried out (Table 4.2.).

Table 4.2. Hydrogenation of cyclohexene **4** with Pd/D(Li) type catalysts.[a]

Entry	Substrate	Selectivity (%)[b]	Catalyst	Ratio S/C	t (h)	Conv. (%)	TOF (h^{-1})[c]
4		96.2	Pd/D(Li) *in*	350	1.5	99.4	234
		95.4	Pd/D(Li) *pre*	350	0.83	97.3	414

[a] React. conditions: methanol, 1bar H_2, r.t., 1.25 wt% Pd/D(Li) catalyst (50-100 mesh, [Pd(CH$_3$CN)$_4$(BF$_4$)$_2$] precursor) substrate concentration 0.17 M, [b] Selectivity to the product @ specified conversion. [c] TOF = mol product / mol Pd x h.

Following the standardized procedure described in Chapter 3, Pd/D(Li) *in* type catalysts were initially used. However, the reaction rate was slower than expected, what induced to think that the possible coordination of Pd^{2+} species to the double bond prevents the reduction to Pd^0, the catalytic active component of the solid catalyst. Indeed, differently from what previously noticed (see Chapter 3 / Section 3.5.1.), the activity for *pre*-reduced species was 50% higher than for *in situ* activated catalysts, what can be graphically seen in Fig. 4.3.
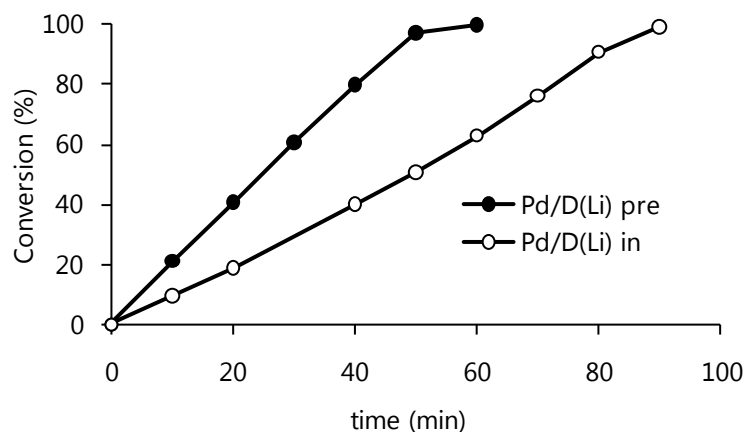
Fig. 4.3. Hydrogenation of cyclohexene **4** with 1.25 wt% Pd/D(Li) catalyst (50-100 mesh, [Pd(CH$_3$CN)$_4$(BF$_4$)$_2$] precursor). React. conditions: methanol, 1bar H$_2$, r.t., substrate concentration 0.17 M, substrate : Pd = 350 : 1 molar ratio.

In addition to the expected formation of cyclohexane, small amounts of benzene *ca.* 4% were detected. This finding was previously reported for the palladium-catalyzed hydrogenation of cyclohexene, which was attributed to the disproportionation of cyclohexene to cyclohexane and benzene mediated by Pd, irrespective of the presence of hydrogen gas.[22,23]

Rare examples are reported in the literature for the hydrogenation of **4** using comparable systems. P. Centomo *et al.*[24] proposed a number of catalysts with Pd supported onto gel type, functional acrylic polymers. Using slightly harder conditions (5.5 bar H$_2$) the sulfonic functionalized resin showed TOF of *ca.* 650h^{-1} while the one with carboxylic groups gave TOF of *ca.* 430h^{-1}. In any case, pretty comparable results with those obtained using the catalysts here presented. It should be notice that Pd immobilized onto different supports, namely carbon or metal oxides, has been reported with higher turnover frequency values.[25]

4.4.2. SELECTIVITY TO PARTIAL HYDROGENATION PRODUCTS. THE SPECIAL CASE OF 3-HEXYN-1-OL

Selectivity in partial hydrogenation reactions to synthesize mono-enes is of fundamental importance in fine chemicals production. Due to its extraordinary chemoselectivity and activity, Pd, especially supported on carbon, is the most satisfactory and widely used catalyst compared to the other Group VIII transition metals Pt, Rh, Ru and Ni. Palladium catalyzes selectively the semi-hydrogenation of dienes to the mono-alkenes, being this the preferred pathway compared to complete saturation. However, besides this advantageous feature, one must be aware that Pd is able to catalyze competitive reactions such as *cis/trans* isomerization, double bond migration and it can induce hydrogenolysis of other functional groups, that can affect importantly the selectivity of the processes.

The selectivity of Pd/D(Li) type catalysts in partial hydrogenation of hydrocarbons with multiple C=C or C≡C bonds under very mild conditions (1 bar H_2 and r.t.) was demonstrated by performing the hydrogenation of 1,5-cyclooctadiene (1,5-COD, **5**), 1,5,9-dodecatriene (1,5,9-CDT, **6**) and 3-hexyn-1-ol (**7**). Representative results are summarized in Table 4.3. The sketch of the tested substrates in catalytic reactions is reported in Scheme 4.2.

The catalysts showed to be selective for partial hydrogenation with excellent to good selectivities to the mono-hydrogenated product. The reduction of 1,5-COD **5** was achieved with 96.7% selectivity to the mono-ene **5a** at 98.5% conversion, for 3-hexyn-1-ol **7**, 98.1% of the alkene was obtained (98.1% of which was the *cis*-isomer **7a**) at 73.2% conversion. Minor amounts of fully hydrogenated products (**5b**, **7c** <2.4%) were observed for both substrates. The hydrogenation of 1,5,9-CDT **6** was slightly less selective producing the diene **6a** (isomers mixture) with 83.2% selectivity at 78.2% conversion.
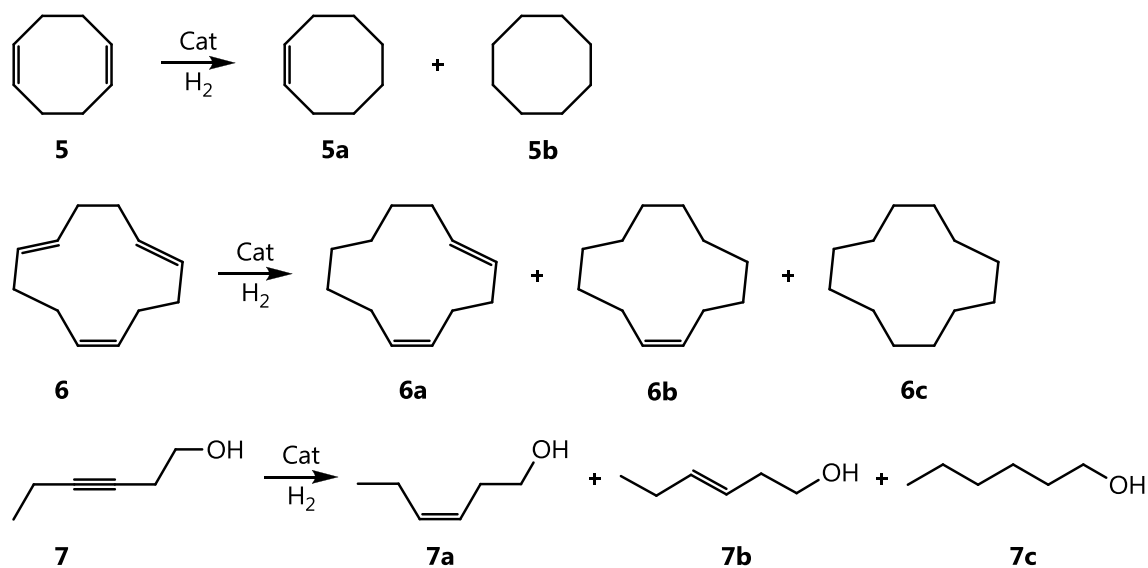
Scheme 4.2. Sketch of the substrates tested in hydrogenation reactions of hydrocarbons with multiple C=C or C≡C bonds.

Table 4.3. Hydrogenation reactions of hydrocarbons with multiple C=C or C≡C bonds by Pd/D(Li) type catalysts under batch conditions.[a]

Entry	Substrate	Selectivity (%)[d]		Ratio S/C	t (h)	Conv. (%)	TOF (h⁻¹)[e]
5 [b]			96.7	350	0.8	98.5	418
6 [b]			83.2	350	1.25	78.2	222
7 [c]			98.2	350	1.0	91.0	322

[a] React. conditions: methanol, 1bar H_2, r.t., 1.25 wt% Pd/D(Li) catalyst (50-100 mesh), [Pd(CH$_3$CN)$_4$(BF$_4$)$_2$] precursor. [b] Pd/D(Li) *pre* catalyst, substrate concentration 0.17 M, [c] Pd/D(Li) *in* catalyst, substrate concentration 0.19M. [d] Selectivity to the product @ specified conversion. [e] TOF = mol product / mol Pd x h.

As abovementioned, the coordination of Pd^{2+} to the double bounds hampers the formation of Pd NPs within reasonable timeframes. In fact, long induction times were observed in the hydrogenation of **5** using Pd/D(Li) *in* catalysts (18% conversion after 3 h), unlike Pd/D(Li) *pre* catalysts, as it can be seen from Fig. 4.4.
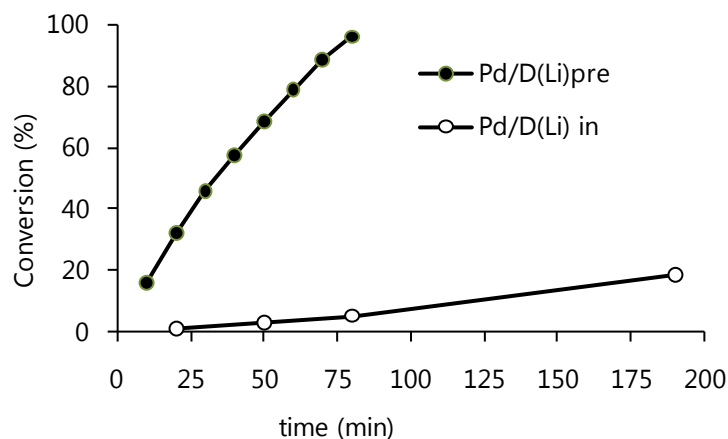

Fig. 4.4. Hydrogenation of 1,5-COD **5** with 1.25 wt% Pd/D(Li) catalyst (50-100 mesh, [Pd(CH$_3$CN)$_4$(BF$_4$)$_2$] precursor). React. conditions: methanol, 1bar H$_2$, r.t., substrate concentration 0.17 M, substrate : Pd = 350 : 1 molar ratio.

It must be noted that in the first stages of the hydrogenation of **5**, small amounts of isomerization product 1,4-COD are detected, that, however, disappear upon reaction progress (see Fig. 4.5.). A graphic representation of the hydrogenation of **6** is also shown in Fig. 4.5. where **6** and **6a** (-diene) are mixtures of isomers. From the reaction progress it can be seen that the selectivity can be tailored, that is, if the reaction is stopped after 75 min., the selectivities to **6a** and **6b** (-ene) are 83.2 and 13.9% respectively, highlighting the possibility of reducing mainly one double bond. However, if the desired product is cyclododecene **6b**, an interesting chemical for the production of musk fragrances and perfumes with a woody note, one could further hydrogenate to increase the amount of this product, as the trend indicates, up to 35.7% if the reaction is stopped at 120 min.
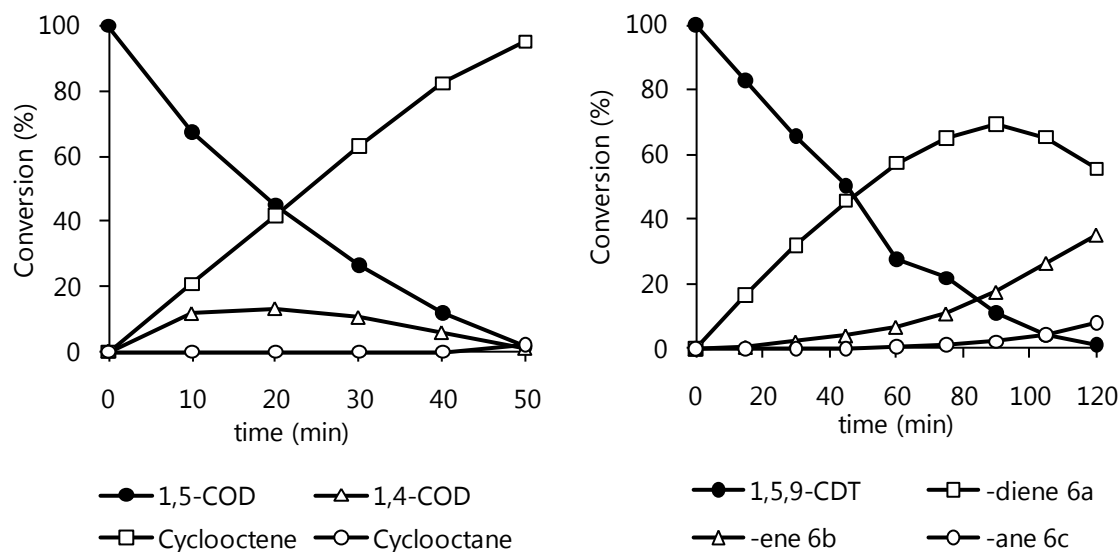
Fig. 4.5. Hydrogenation of 1,5-COD **5** (left) and 1,5,9-CDT **6** (right) with 1.25 wt% Pd/D(Li) *pre* catalyst (50-100 mesh, [Pd(CH$_3$CN)$_4$(BF$_4$)$_2$] precursor). React. conditions: methanol, 1bar H$_2$, r.t., substrate concentration 0.17 M. substrate : Pd = 350 : 1 molar ratio.

Concerning the selective hydrogenation of alkynes, this reaction is of utmost importance in the synthesis of fine chemicals, such as food additives, flavours, fragrances, pharmaceutical or agrochemical substances.[26] The main goal is to avoid overhydrogenation to C-C single bond and, in the case of non-terminal alkynes, is to obtain the highest possible conversion and selectivity to the (Z)-alkene.[27] The hydrogenation of 3-hexyn-1-ol is an industrially relevant process since *cis*-3-hexen-1-ol is the active component of leaf fragrance. Having established that the developed catalysts Pd/D(Li) *in* are efficient (TOF = 322 h^{-1}) and selective for this reaction, the reusability of the catalyst in term of activity and selectivity upon recycling, was then evaluated (Fig. 4.6.).
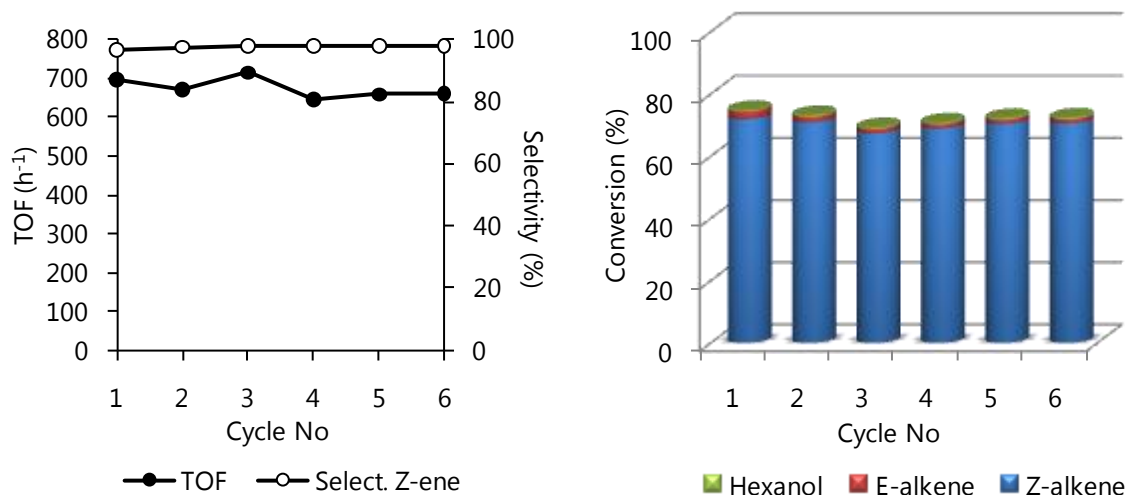
Fig. 4.6. Recycle of Pd/D(Li) *in* catalyst in the hydrogenation of **7**. left) TOFs (on overall conversion indicated in right figure) and Selectivity = **7a**/(**7a**+**7b**)x100; right) Conversion upon recycling. Reaction conditions: methanol, 1.25 wt% Pd/D(Li) *in* catalyst (50-100 mesh, [Pd(CH$_3$CN)$_4$(BF$_4$)$_2$] precursor), substrate concentration 0.19M, r.t., 1 bar H$_2$, substrate : Pd = 390 : 1 molar ratio, time 26 min.
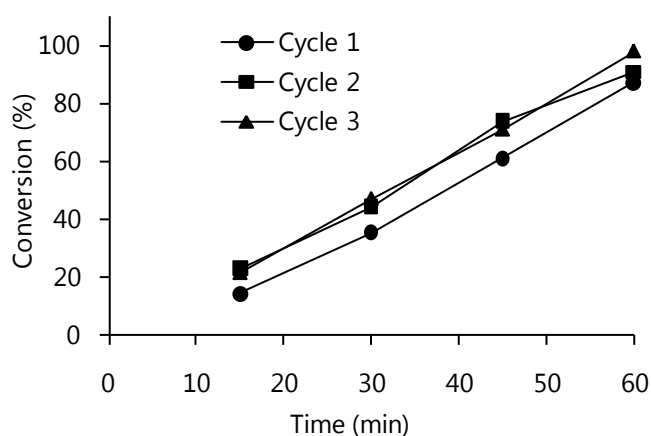

Fig. 4.7. Recycle of Pd/D(Li) *in* catalyst in the hydrogenation of **7**. Conversion upon recycling. Reaction conditions: methanol, 1.25 wt% Pd/D(Li) *in* catalyst (50-100 mesh, [Pd(CH$_3$CN)$_4$(BF$_4$)$_2$] precursor), substrate concentration 0.17M, r.t., 1 bar H$_2$, substrate : Pd = 350 : 1 molar ratio.

Catalyst recovery and reuse was quantitatively possible by simple decantation, showing negligible activity and selectivity decay upon recycle. This is graphically shown in Fig. 4.6. and in Fig. 4.7., in which the catalyst performance and the reaction progress in the hydrogenation **7** upon recycle are reported, respectively**.**

105

Metal leaching in solution was below the ICP-OES detection limit in all cycles, while the absence of catalytic activity of the recovered reaction solutions proved that the catalyst was truly heterogeneous,[28] thus ruling out the contribution of homogeneous species. The alkene selectivity was > 96.0% for all cycles, > 97% of which was the leaf alcohol *cis*-3-hexen-1-ol **7a**. The catalyst retained > 95 % of its starting efficiency after ca. 2.6 h use, which corresponds to a TON of *ca.* 1700 for the product **7a**.

The leaf alcohol *cis*-3-hexen-1-ol **7a** is manufactured with *ca.* 97% selectivity@99% conversion by a batch process using the Lindlar catalyst (5% Pd + 2-3% Pb on $CaCO_3$), with a production of about 400 t/y.[29] Despite the slightly higher selectivity of the industrial process, the catalyst described in the present work provides clear advantages in terms of environmental impact, by avoiding potential contamination by toxic Pb, and reusability. The activities and/or the selectivities obtained in the hydrogenation of **7** using our catalysts also compare favourably with those reported for Pd onto charcoal and hydrotalcite.[30] To this purpose, the commercial 5 wt% Pd/C was tested under similar reaction conditions (Fig. 4.8.)
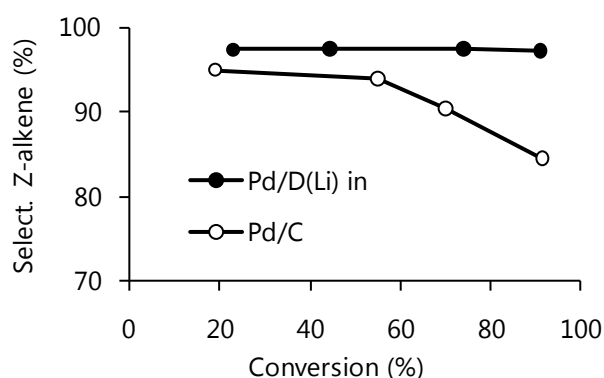

Fig. 4.8. Hydrogenation of 3-hexyn-1-ol **7** with (•) 1.25 wt% Pd/D(Li) *in* (50-100 mesh, [Pd(CH_3CN)$_4$(BF_4)$_2$] precursor), substrate concentration 0.17M, substrate : Pd = 350 : 1 molar ratio, and (o) 5 wt% Pd/C, substrate concentration 0.5M, substrate : Pd = 250 : 1 molar ratio. Reaction conditions: methanol, r.t., H_2 pressure 1 bar. Selectivity = **7a**/(**7a**+**7b**)x100.

In no case, the commercial catalyst was more selective than Pd/D(Li) type catalyst which showed constant selectivity regardless the conversion, unlike Pd/C that exhibited high selectivity to the *cis*-isomer at low conversion but it decreased significantly as conversion increased.

4.4.3. SELECTIVITY TO C=C IN THE PRESENCE OF C=O BONDS

Selective hydrogenation of carbon–carbon double bonds in unsaturated carbonyl compounds plays an important role in the synthesis of fine chemicals on a multi-ton scale via heterogeneous catalysis.[31] To this purpose, the hydrogenation reaction of various substrates combining alkene and carbonyl functionalities was performed, including benzylidenactone **8**, isophorone **9** and carvone **10**, whose results are summarized in Table 4.4.

**Table 4.4.** Hydrogenation reactions of unsaturated carbonyl compounds by Pd/D(Li) type catalysts.[a]

Entry	Substrate	Selectivity (%)[d]	Ratio S/C	t (h)	Conv. (%)	TOF (h⁻¹)[e]
8 [b]		83.7	250	0.3	99.2	774
9 [c]		74.3	175	1.5	88.6	105
10 [c]		45.3	175	1.0	95.3	169

[a] React. conditions: methanol, substrate concentration 0.17 M. [b] 1 wt% Pd/D(Li) *in* catalyst (50-100 mesh, Pd(NO$_3$)$_2$ precursor), 0.8 bar H$_2$. [c] 1.25 wt% Pd/D(Li) *pre* catalyst LiCl post-treatment (50-100 mesh, [Pd(CH$_3$CN$_4$)(BF$_4$)$_2$ precursor], 1bar H$_2$. [d] Selectivity to the product @ specified conversion. [e] TOF = mol product / mol Pd x h.

From the data obtained, it can be confirmed the synthesized Pd/D(Li) type catalyst show good selectivities to the reduction of double bond in the presence of carbonyl groups reaching values as high as 83.7% in the case of

benzylidenacetone. This behaviour can be justified in terms of greater affinity of Pd for –C=C- than for -C=O- bonds.[32] The selectivity drops for isophorone to 74.3% and goes down to 45.3% for carvone hydrogenation. This loss of selectivity can be ascribed to the presence of different parallel reactions that will be explained below.

The hydrogenation of benzylidenactone **8** (Scheme 4.3.) was performed for several rounds affording the C=C hydrogenation product **8a** in *ca.* 84% constant yield upon recycle, together with *ca.* 10% saturated alcohol **8b** and *ca.* 6 % of the fully hydrogenated product **8d** (Fig. 4.9.). No traces of the C=O hydrogenation product **8c** were detected and no amount of Pd leached in solution was detected by ICP-OES in any cycle.
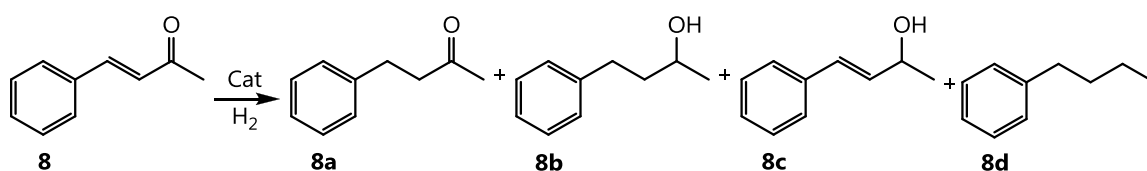
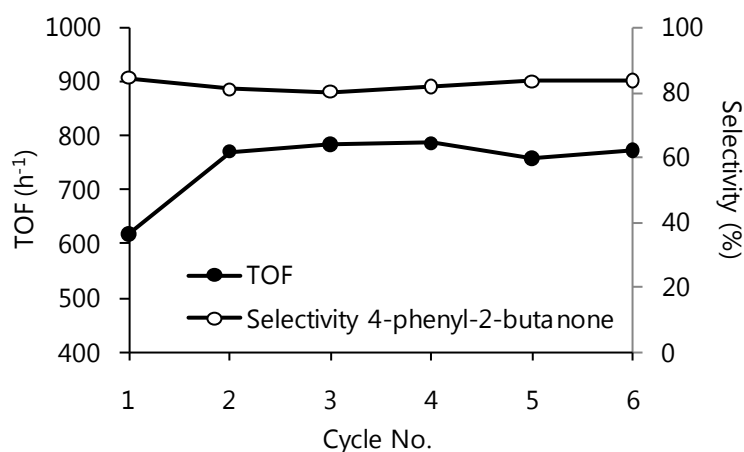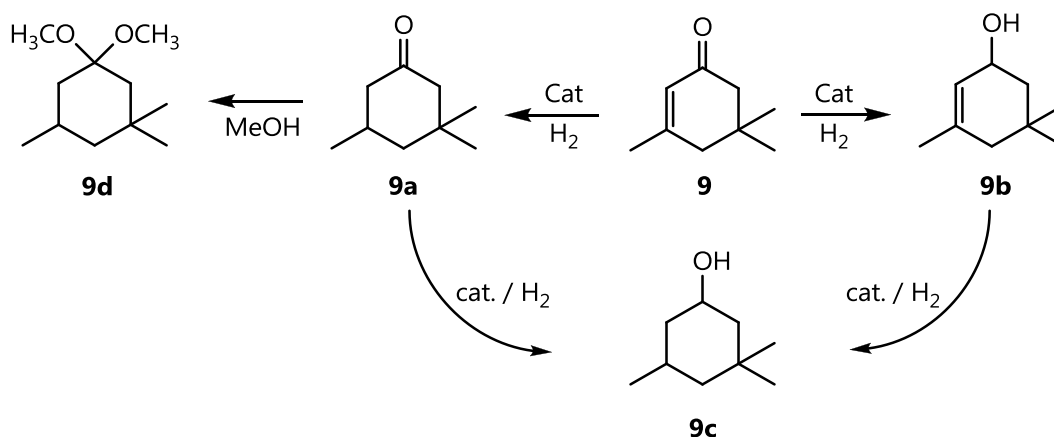**Scheme 4.3.** Reaction scheme of the hydrogenation of benzylidenacetone **8**.

Fig. 4.9. Recycle of 1 wt% Pd/D(Li) *in* catalyst (50-100 mesh, (Pd(NO$_3$)$_2$ precursor). in the hydrogenation of **8**: TOFs (on overall conversion) and selectivities. Reaction conditions: methanol, r.t., H$_2$ pressure 0.8 bar, substrate : Pd = 220 : 1 molar ratio, time 15 min. Selectivity = **8a**/(**8a**+**8b**+**8c**+**8d**)x100.

The hydrogenation of isophorone **9** (Scheme 4.4.) has been reported in the asymmetric version.[33] Considering that asymmetric hydrogenation reactions are the further scope for this kind of catalysts, it was a meaningful substrate to start with.

Scheme 4.4. Reaction scheme of the hydrogenation of isophorone **9** including all possible products; **9a**: dihydorisophorone, **9b:** homomenthol, **9c**: : isophorol and the parallel reaction of acetilization to give **9d**.

As can be seen in Fig. 4.10. (left), the hydrogenation of isophorone with Pd/D(Li) *in* catalyst was 100% chemoselective to dihydroisophorone since no alcohols were detected at the first stage and neither after the consumption of the substrate, when the saturated ketone could undergo further hydrogenation. Nevertheless, an important amount of the acetal product **9d** was found from the very beginning that reached up to. 40%. This acid-catalyzed side reaction was probably a consequence of a residual acidity coming from the support (see Chapter 3 / Section 3.3.) without forgetting that methanol was the solvent used in the reaction (Scheme 4.5.). In order to suppress the remaining acidity, an additional treatment with LiCl was done to the catalyst Pd/D(Li) *pre* prior to use, to remove all the protons by exchange with lithium. The results (Fig. 4.10., right) showed that indeed the formation of acetal decreased 37% in comparison with the catalyst without treatment. It should be noticed that acetilization side

reactions have been already reported for hydrogenation of α,β-unsaturated carbonyl compounds when an alcohol is used as solvent.[15]
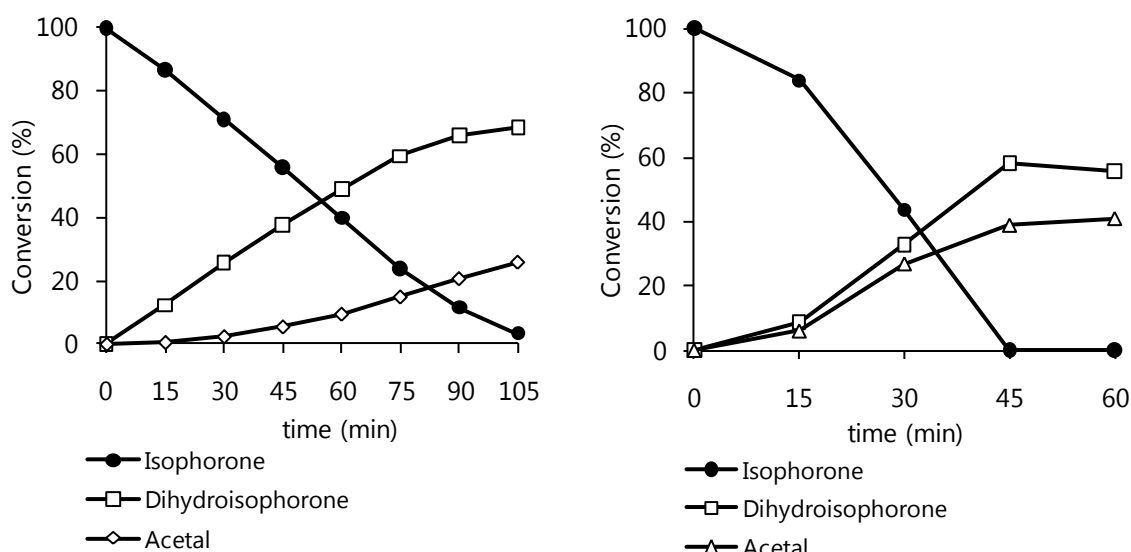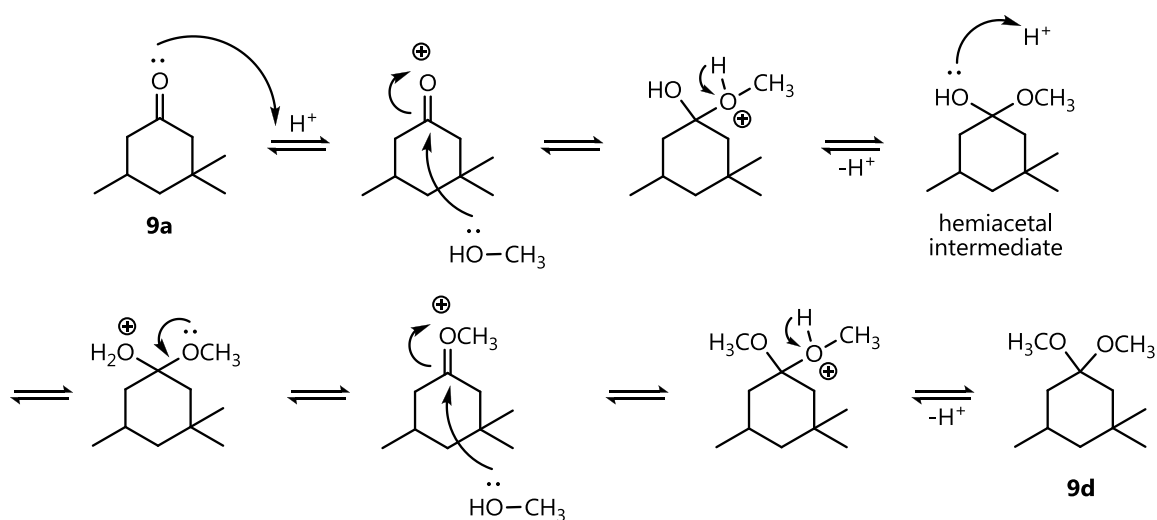

Fig. 4.10. Hydrogenation of isophorone **9** with 1.25 wt% Pd/D(Li) catalyst (50-100 mesh, [Pd(CH$_3$CN)$_4$(BF$_4$)$_2$] precursor). Reaction conditions: methanol, r.t., substrate : Pd = 175 : 1 molar ratio, H$_2$ pressure 1 bar, substrate concentration 0.17 M. (left) Pd/D(Li) *in* catalyst (right) Pd/D(Li) *pre* catalyst LiCl post-treatment.

**Scheme 4.5.** Acid-catalyzed acetal formation mechanism.

Regarding the activity of the catalyst, the reaction was slower for *pre*-reduced species (105 *vs* 45 min to reach total conversion), what corroborates again (see Section 3.5.1.) the beneficial effect of generating the active species under catalytic

conditions. Notwithstanding, the election of *pre*-reduced species this time was commitment since a washing with LiCl in the presence of Pd^{2+} would take them away from the polymer through ion exchange by lithium.

The selective hydrogenation of isophorone **9** was previously reported by different groups in $scCO_2$. Hitzler *et al.*[34] performed the reaction with a palladium catalyst (5% Pd/Deloxan®) obtaining 100% of dihydroisphorone at complete conversion however, high reaction temperature (200°C) was required. On the other hand, T. Sato *et al.*[35] presented two palladium catalysts; 5% Pd/C and 5% Pd/Al_2O_3, that allowed obtaining total selectivity to the saturated ketone but conversions did not go beyond 5 and 15% respectively and the pressure of hydrogen amounted to 10 bar. Recently, M. Lakshmi Kantam *et al.*[36] have reported a nanopalladium catalyst (LDH-Pd^0) that under mild conditions produces ketone with 94% yield after 2.5h.

The last of the substrates studied in this section, carvone **10**, represents a suitable probe molecule since it has three functional groups that are capable of being hydrogenated: a -C=O- group, and endocyclic -C=C- group and an exocyclic –C=C-. In the Scheme 4.6., all the possible routes that carvone can undergo during a hydrogenation process are presented.

Carvone was nearly complete hydrogenated after 1 hour under very mild conditions (1 bar H_2, r.t.) by using Pd/D(Li) *pre* catalyst LiCl post-treatment as in the previous example, so the formation of acetals could be avoided. The results are shown in Fig. 4.11.
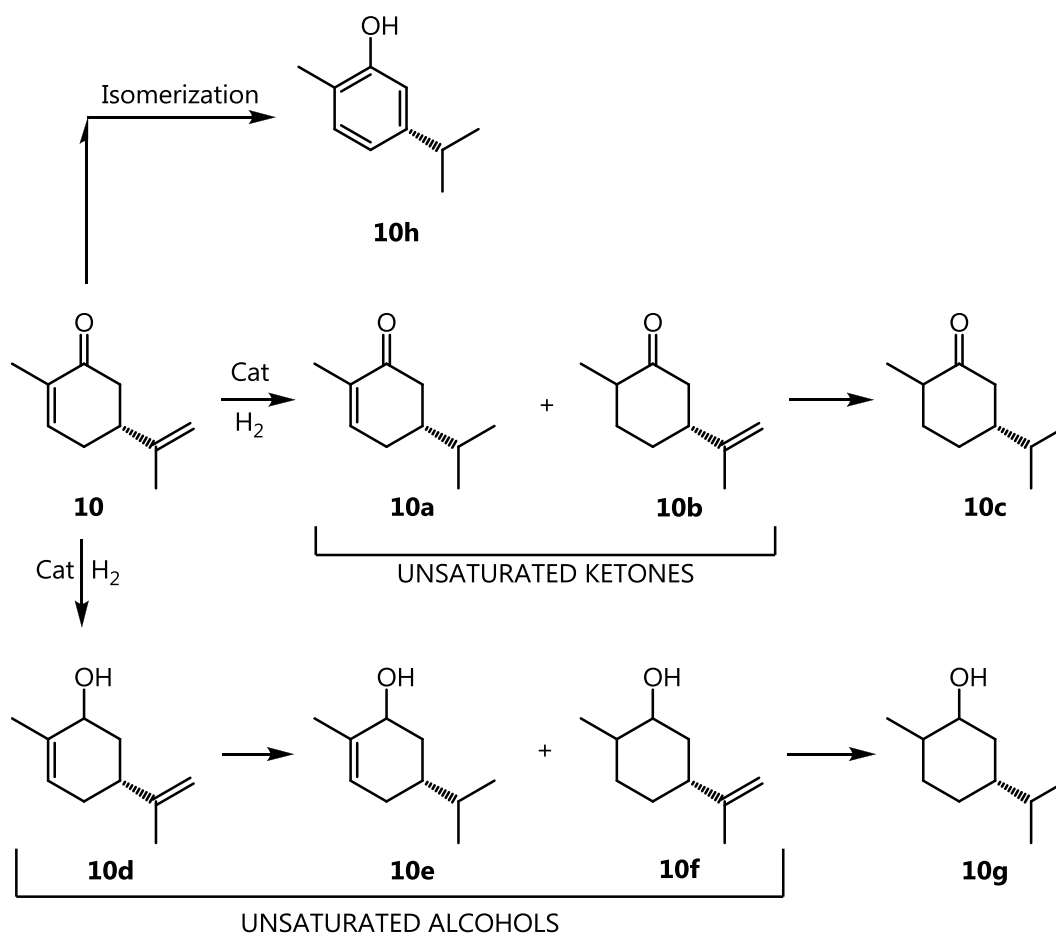
Scheme 4.6. Reaction scheme of the hydrogenation of carvone **10** including all possible products; **10a**: carvotanacetone, **10b**: dihydrocarvone, **10c**: carvomenthone, **10d**: carveol, **10e**: carvotanalcohol, **10f**: dihydrocarveol, **10g**: carvomenthol, and the competitive reaction of isomerisation to give carvacrol **10h.**

Analysis of the results obtained shows that increasing amounts of the unsaturated ketones (carvonacetone and dihydrocarvone) are initially produced from carvone and, as the reaction progresses, these unsaturated ketones are progressively transformed into the saturated ketone carvomenthone which is obtained as the main product at high conversion (45.3% selectivity @ 95.3% conversion). No traces of acetals were detected. Differently, there is a parallel reaction taking place responsible of the presence of carvacrol. Results show that Pd/D(Li) catalyst is selective to the exocyclic –C=C- bond of carvone at the first stage of the reaction, since 62% more carvotanacetone than dihydrocarvone was obtained. However, in a second step the hydrogenation of the endo and exo -

C=C- containing compounds to give carvomenthone seems to be indistinctive as they both disappear at the same rate. Unsaturated alcohols were not detected at any stage and neither was carvomenthol, what indicates that the catalyst is 100% selective to –C=C- bond in the presence of carbonyl groups for the hydrogenation of carvone under the described catalytic conditions. Similar results were reported with a polymer supported palladium catalyst that showed higher selectivity (70% @ 100% conversion)[37] and with Pd/SiO$_2$ which showed lower selectivity (36%) for carvomenthone in favor of carvanacetone[38].
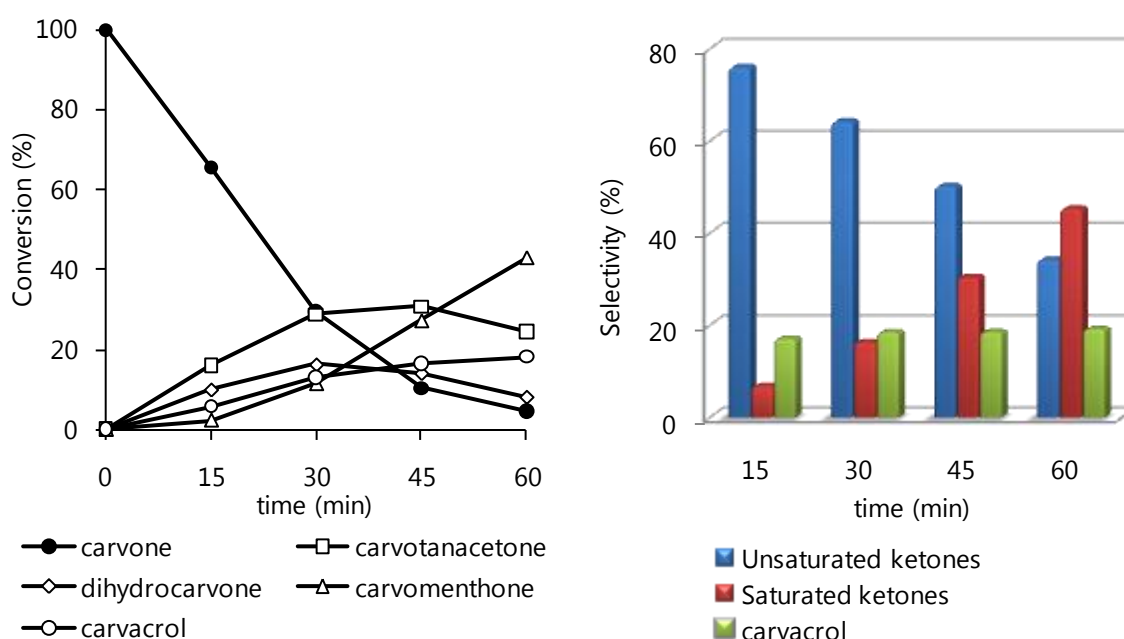

Fig. 4.11. Hydrogenation of carvone **10** with 1.25 wt% Pd/D(Li) *pre* catalyst LiCl post-treatment (50-100 mesh, [Pd(CH$_3$CN)$_4$(BF$_4$)$_2$] precursor). Reaction conditions: methanol, r.t., substrate : Pd = 175 : 1 molar ratio, H$_2$ pressure 1 bar, substrate concentration 0.17 M. (left) Evolution of conversion *vs* time for the different products (dihydrocarvone: isomers mixture). (right) Selectivity data for ketones and the isomerization product.

As previously mentioned, the appearance of carvacrol is detected increasingly since early stages as a result of an isomerization process from carvone, maintaining an average height of 19%. This acid-catalyzed reaction usually performed at high temperature,[39] which mechanism is shown in Scheme 4.7., has been already reported as parallel reaction in the hydrogenation of carvone with

palladium, e.g. M. M. Dell'Anna *et al.* found 30% of carvacrol at 100% conversion when a supported palladium catalyst was used.[37,40] On the other hand, C. Gozzi *et al.* have recently published an example of Dowex® type resin (sulfonic groups, H form) metal-free catalyzing the same process.[41] In this particular case, the presence of carvacrol could be ascribed again to an unavoidable residual acidity of the support (see Chapter 3 / Section 3.3.), even after the washing with LiCl.
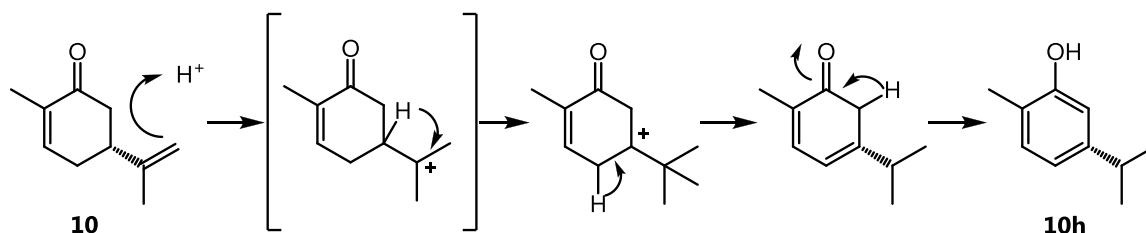

Scheme 4.7. Mechanism of the acid-catalyzed isomerization of carvone **10** to carvacrol **10h**.

4.4.4. HYDROGENATION OF C=O BONDS

Carbonyl compounds can be readily hydrogenated to alcohols under mild conditions (25–60 °C and 1–5 atm). Usually, the precious metal used for catalyzing this reaction is Pt however, Rh and Ru are also utilized.[42] Although Pd catalysts are barely employed, they have found utility in the selective hydrogenation of aromatic carbonyls which are initially reduced to their respective alcohols and under the proper conditions. The aromatic functionality of an aromatic ketone or aldehyde serves to activate the carbonyl bond, thereby allowing for its milder hydrogenation in the presence of commonly used metals or allowing Pd to catalyze the reaction.[43] In fact, when C=O is not activated, as previously seen with isophorne, carvone or benzylidenacetone, Pd rarely hydrogenates in this position.

Pd/D(Li) type catalysts were tested in the hydrogenation of α-substituted aromatic carbonyl compounds (Scheme 4.8.) which results are reported in Table 4.5.
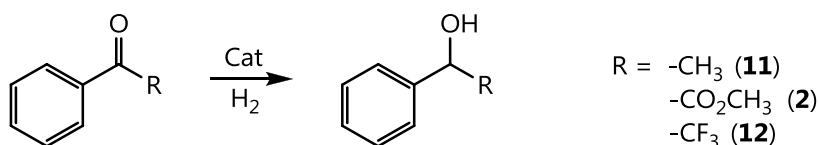
Scheme 4.8. Reaction scheme of the hydrogenation of α-substituted aromatic ketones; acetophenone **11**, methyl benzoylformate **2**, and trifluoroacetophenone **12**.

Table 4.5 Hydrogenation reactions of aromatic ketones by Pd/D(Li) type catalysts.[a]

Entry	Substrate	Selectivity (%)[b]		t (h)	Conv. (%)	TOF (h⁻¹)[c]
11			88.8	0.3	80.3	711
2			100.0	0.3	87.1	723
12			100.0	3.2	62.4	44

[a] React. conditions: methanol, r.t., 1 wt% Pd/D(Li) *in* catalyst (50-100 mesh, $Pd(NO_3)_2$ precursor), substrate concentration 0.17 M, substrate : Pd = 220 : 1 molar ratio, H_2 pressure 0.8 bar, [b] Selectivity to the product @ specified conversion. [c] TOF = mol product / mol Pd x h.

Comparable activities were found for the hydrogenation of acetophenone **11** and methyl benzoylformate **2** with TOF numbers in the range. 700-800 h⁻¹. On the other hand, in the reduction of trifluoroacetophenone **12**, an important decrease in the reaction rate was detected due to the high electrondrawing properties of the CF_3 group.[44] Small amounts of hemiacetal and acetal products were occasionally found in the hydrogenation reaction of **11**.
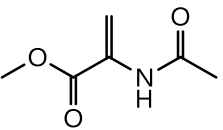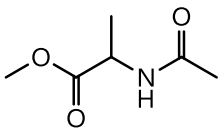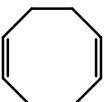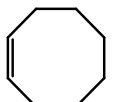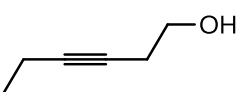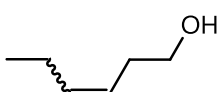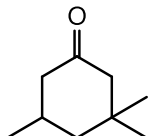
4.5. HYDROGENATION REACTIONS WITH Rh NPs

Rhodium nanoparticles for catalytic applications are mostly used in hydrogenation reactions, and most particularly in olefin and alkyne

hydrogenation.[45] In fact, supported Rh catalysts are the better systems for the total hydrogenation of benzene to cyclohexane.[46]

In order to prove the efficiency of the synthetic procedure devised in the present work to produce effective precious metal supported catalysts, Rh/D(Li) type catalysts were tested in hydrogenation reactions. Table 4.6. summarizes the data obtained for some of the substrates previously studied.

Table 4.6. Hydrogenation reactions by Rh/D(Li) type catalysts.[a]

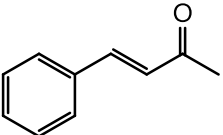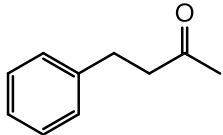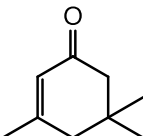| Entry	Substrate		Selectivity (%)[b]	Ratio S/C	t (h)	Conv. (%)	TOF (h^{-1})[c]
1			100.0	300	1.3	95.2	218
4			100.0	250	1.2	92.2	185
5			21.9	250	7.6	97.3	32
7			55.0	100	2.3	94.3	40
8			90.9	250	4.7	97.4	52
9			78.1	100	1.0	92.5	96

[a] React. conditions: methanol, r.t., substrate concentration 0.17 M, 1.40 wt% Rh/D(Li) *in* catalyst (50-100 mesh). [b] Selectivity to the product @ specified conversion. [c] TOF = mol product / mol Pd x h.

In general, polymer supported rhodium nanoparticles showed to be less active in hydrogenations reactions than their homologous with palladium. However, some of the shortcomings seen with Pd NPs such as formation of benzene in the hydrogenation of **4**, or competitive isomerization reaction in the case of **5**, can be

avoided with rhodium, since no trace of these compounds was detected. With regard to selectivity, reactions catalyzed by rhodium were less selective in the partial reduction of multiple double/triple bonds with an important decrease of the mono-hydrogenated product; the mono-ene dropped from 96.7 to 21.9% in the hydrogenation of **5**, while 55.0% of the alkene instead of 98.1% was obtained in the case of **7** On the other hand, chemo-selectivity to double bond was better for Rh NPs that showed a rise in the amount of the saturated ketone obtaining 90.9% in the hydrogenation of **8** compared with the previously reported 83.7% with palladium (see Section 4.3.3.).

The lower activity of supported Rh catalysts could be interpreted as a consequence of the peripherical distribution of the metal within the bead (Chapter 3 / Section 3.7.2.). It is difficult to justify the behaviour of these polymer supported rhodium catalysts in base of their average NPs size, as was previously done for their homologous palladium catalysts (Chapter 3 / Section 3.4.). Some examples found in the literature suggest contradictory conclusions, while in the hydrogenation of alkynes and arenes a negative particle size effect can be found, i.e. an increase in NPs size involved faster reactions;[47,48] the hydrogenation of linear olefins seems to be insensitive to the structure, this is, not dependent of the NPs size.[47] In addition, it is suspicious that in a very recent review on the shape dependent catalytic properties of metal nanoparticles no examples of rhodium were given.[49]

Not many advantages were found for rhodium based catalysts in comparison with their palladium counterparts. For the given reactions in the described conditions, best performances were showed for the palladium catalysts in any case. In addition, the high price of rhodium should be taken into account, which is almost twice the price of the palladium and greatly increase the price of the final catalyst.[50] However, polymer supported rhodium nanoparticles may be an alternative in procedures where side isomerization or dehydrogenation reactions

mean a problem for the overall process.[51] Moreover, rhodium based systems are very useful in fine chemical synthesis when in the hydrogenation of α,β-unsaturated ketones, such as benzylidenacetone **8**, high selectivity is required.[52]

In any case, the above results have proved the feasibility of the synthetic procedure developed for the synthesis of palladium nanoparticles. As it has been shown, the method is general and should also serve for the production of other supported metal nanoparticles.

4.6. OXIDATIONS REACTIONS WITH Au NPs

Currently, the development of new tools to convert biomass into useful chemicals in an economically and environmentally friendly route represents a challenge for the scientific community.[53] For example, furfural, that can be obtained from xyloses (C5 fraction), can be used in soil chemistry and as a building block in the production of Lycra®. Additional transformations of this chemical are highly desired, such as the synthesis of alkyl furoates, which find application as flavour and fragrance components in the fine chemicals industry.

To this purpose, the oxidation of furfural **13** (Scheme 4.9.) was carried out in the presence of the green oxidant molecular oxygen to check the activity of the synthesized polymer supported gold nanoparticles Au/D(Cl). Representative results are reported in Table 4.7.
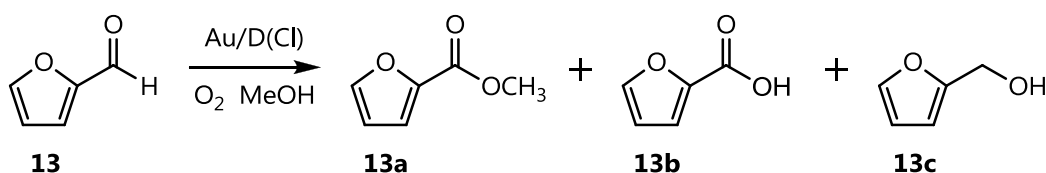
Scheme 4.9. Reaction scheme of the oxidation of furfural **13**.

**Table 4.7.** Oxidation of furfural with Au/D(Cl) type catalysts.[a]

Exp.	Ratio S/C	Conversion (%)	Selectivity (%) 13a	TOF (h^{-1})[b]
1	500	28.3	100.0	8
2	1000	22.6	97.7	13
3	1500	23.5	97.8	21
4	2000	18.8	98.8	22
5	2500	21.4	98.9	31

[a] React. conditions: methanol, 50°C, substrate concentration 0.5 M, 0.7 wt% Au/D(Cl) catalyst, CH_3ONa 8% relative to furfural, Oxygen pressure 8 bar, time 17h, 300rpm. [b] TOF = mol product / mol Pd x h.

The reaction was carried out at very mild conditions (50°C and 8 bar O_2) compared to those reported in literature,[54] affording different molar ratio substrate/Au that ranged from 500 up to 2500. Regardless the ratio, the TOF obtained was regularly low, reaching values under 31 h^{-1}. The low activity of these catalysts could be ascribed to the dimension of the gold nanoparticles that although they showed a mean size of 4.4 nm (Chapter 3 / Section 3.8.2), which is not overly big regarding gold catalysts, more than 50% of the NPs are larger Pinna *et al.* have very recently published a study on the oxidation of furfural that demonstrates the important role that gold cluster size plays in the reaction obtaining, among the different systems, the poorest catalytic behaviour for the bigger nanoparticles of *ca.* 4nm.[55]

Apart from methyl furoate **13a**, the only by-product found, in traces, was the alcohol **13c**. In the presence of base additional reactions could occur, in fact, aldehydes with no α-hydrogen undergo disproportionation in the presence of concentrated hydroxides via the Cannizzaro reaction. This observation has been also noticed by R. M. Krieger *et al.* in the gold-catalyzed oxidation of aldehydes in the presence of non-concentrated hydroxides what suggested Au surface to promote the reaction.[56] The use of sodium alkoxide base in the above experiment would lead to the formation of esters in the Cannizzaro reaction rather than the

acid salts (Scheme 4.10.), increasing in this way the selectivity to the desired product.
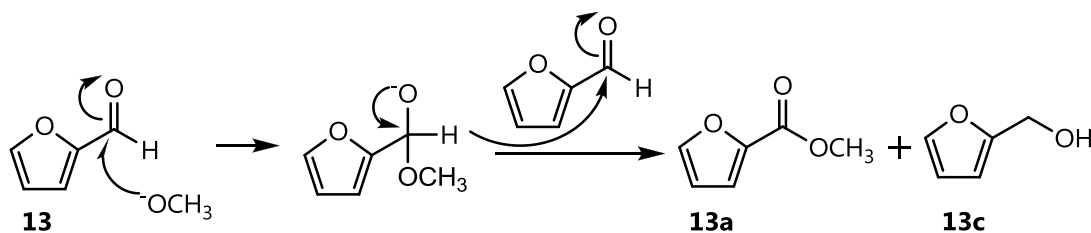
Scheme 4.10. Scheme of the Cannizzaro reaction: base-induced disproportionation of furfural.

4.7. CONCLUSIONS

Catalysts for the sustainable manufacture of fine chemicals on the industrial scale ought to be highly efficient and selective under smooth conditions, easily and effectively reusable. A deep investigation of the performance of Pd-based catalysts demonstrated that the developed systems fulfill the cited requirements.

The best catalytic efficiency was observed in methanol under very mild conditions (room temperature, 0.8 - 1 bar H_2 pressure). Besides being important from an industrial point of view, mild reaction conditions prevent the gradual deterioration of the support, often observed in functionalized polymers.

Selective hydrogenation of hydrocarbons with multiple C=C and/or C≡C bonds to achieve partial hydrogenation products is a highly desired and challenging process, among others, in the pharmaceutical and agrochemical industries. In this sense, supported Pd NPs turned out to be highly selective obtaining 96.7% and 83.2% of the mono-hydrogenated compound in the reduction of 1,5-COD and 1,5,9-CDT respectively. In the particular synthesis of the leaf alcohol *cis*-3-hexyn-1-ol, palladium based heterogeneous catalysts that produced 98.1% alkene, of which 98.1% was cis-isomer, represent a clear alternative to the classic Pd/C not only in terms of selectivity and recycling, but also regarding the recoverability of

the system owing to the fact that polymeric beads can be collected much easier than powders.

The selective hydrogenation of C=C bonds in unsaturated carbonyl compounds plays also an important role in fine chemistry. Pd/D catalysts showed in most cases total chemo-selectivity to C=C bonds, however the overall selectivity was affected by acid-catalyzed side reactions due to a residual acidity in the support, what could be minimized by washing the resin with LiCl prior to use, favouring this way the selectivity.

In general, rhodium based catalysts behaved less efficiently than palladium counterparts; however, they could represent an alternative when competitive side reactions characteristic from Pd as isomerization or disproportionation must be completely avoided. On the other hand, chemo-selectivity to double bond in the presence of other functional groups was also better for Rh NPs in comparison with palladium.

4.8. EXPERIMENTAL

The details about preparation and characterization of the catalysts are reported in the experimental section of Chapter 3. All the chemicals used in hydrogenation and oxidation reactions were reagent grade commercial products and were used as received from Aldrich without further purification. GC and ICP-OES analysis of the recovered solutions after catalysis to determine the content of metal leached were performed on the equipments described in Chapter 2.

Hydrogenation reactions, catalyst recycling

All the hydrogenation reactions were performed in a 100 ml flask using very mild conditions at 1bar of H_2 and room temperature. The experimental procedure shows slight differences depending on the catalytic specie used. ***a) Polymer***

Supported MNPs formed in excess of substrate (Metal/D(Li) in)*:* In a typical experiment, 50 mg of the resin supported metal (n+) specie was added into a flask containing a degassed solution of the substrate 0.17M. A flow of hydrogen gas was bubbled at 1 bar and 15 mL/min at room temperature, using an orbital stirrer at 160 rpm. This was taken as the start time of the reaction. The resin became slowly black (ca. 20 min.). After the desired time, the solution was completely removed under a stream of hydrogen using a gas-tight syringe. A sample of this solution (0.5 μl) was used for GC (product yield), GC-MS (product identification) and ICP-OES analysis (metal leaching), while the remaining aliquot was used for the Maitlis test (catalyst leaching test, see below). A fresh solution of the substrate was then transferred under hydrogen via a gas-tight syringe into the flask containing the recovered supported catalyst. The mixture was stirred at 160 rpm and room temperature under hydrogen flow and, after the desired time, the mixture was treated as described above. The same recycling procedure was used in the subsequent hydrogenation cycles. After use in catalysis, the solid catalyst was washed with methanol (3 x 10 ml) and diethyl ether (3 x 10 ml), dried in a stream of nitrogen overnight and stored under nitrogen for later characterization. Catalyst leaching test: an additional portion of the substrate was added under hydrogen to the clear solution recovered after the first and subsequent cycles, hydrogen was then bubbled through the solution at room temperature for 1h and the mixture analyzed by GC for conversion measurement.

b) Polymer Supported MNPs formed in absence of substrate (Metal/D(Li) pre)*:* In a typical experiment, 50 mg of the resin supported metal (0) specie was added into a flask containing a degassed solution of methanol (12ml) and left it swollen. A portion of the substrate was added under N_2 flow to reach a final concentration of 0.17M. A flow of hydrogen gas was then bubbled at 1 bar and 15 mL/min at room temperature under orbital stirrer at 160 rpm. This was taken as the start time of the reaction. After the desired time, the methanol solution was completely removed under a stream of hydrogen using a gas-tight syringe. From

here on, it proceed as abovementioned.

Oxidation reactions

A typical reaction mixture consisted of 0.8 mL of MeOH, 33.2 μl of furfural (substrate solution 0.5M), 1.7 mg of NaOCH$_3$ and the corresponding amount of 0.7 wt% Au/D(Cl) catalysts leading to molar substrate/metal ratios from 500 to 2500. The reaction mixtures were pressurized to 8 bar O$_2$ and kept at 50ºC while stirring at 300 rpm for 17 h. The oxidations were performed in a high-throughput mode by means of a multi-reactor unit (TOP Industrie, France) containing 10 mini-reactors. GC analyses were performed with the equipments described in Chapter 2.

REFERENCES

1   a) J. Warr, S. Fraser, O. Gouault (Takasago Perfumery Co., Ltd.) Pat. EP 1964542, **2008**; b) J. Y. Choi, B. B. Jeon, H. J. Seo (Amorepacific Corp.) Pat. WO 2007055493, **2007**.

2   http://eur-lex.europa.eu/LexUriServ/LexUriServ.do?uri=OJ:L:2007:136:0003:0280:en:PDF. Retrieved in December **2012**.

3   R. Ballini (Ed), *Eco-Friendly Synthesis of Fine Chemicals*, Royal Society of Chemistry, Cambridge, **2009**.

4   H.-U. Blaser, A. Indolese, A. Schnyder, H. Steiner, M. Studer, *J. Mol. Catal. A: Chem.*, 173, **2001**, 3.

5   a) J.-E. Bäckvall (Ed), *Modern Oxidation Methods*, Wiley VCH, New York, **2004**. b) S. M. Roberts, G. Poignant (Eds) *Catalysts for Fine Chemical Synthesis*, Vol. 1, Wiley-VCH, New York, **2007**.

6   M. Haruta, T. Kobayashi, H. Sano, N. Yamada, *Chem. Lett.,* **1987**, 405.

7   P. Fouilloux, *Heterogeneous Catalysis and Fine Chemicals I*, Elsevier, Amsterdam, **1999**.

8   G. J. Hutchings, *J. Mater. Chem*. 19, **2009**, 1222.

9   a) F. Zaera, *Acc. Chem. Res*. 42, **2009**, 1152; b) L. A. Saudan, *Acc. Chem. Res*. 40, **2007**, 1309.

10   A. Cybulski, M. M. Sharma, R. A. Sheldon, J. A. Moulijn, *Fine Chemicals Manufacture: Technology and Engineering*, Chapter 3, Elsevier Science B.V., Amsterdam, **2001**.

11   a) A. Molnar, A. Sarkany, M. Varga, *J. Mol. Catal. A: Chem*. 173, **2001**, 185; b) C. Godínez, A. L. Cabanes, G. Víllora, *Chem. Eng. Proc*. 34, **1995**, 459.

12   M. Crespo-Quesada, F. Cárdenas-Lizana, A. L. Dessimoz, L. Kiwi-Minsker, ACS Catal. 2, **2012**, 1773.

13   T. Seki, J. D. Grunwaldt, N. van Vegten, A. Baiker, *Adv. Synth. Catal*. 350, **2008**, 691.

14   H. Lindlar, *Helv. Chim. Acta*, 35, **1952**, 446.

15   J. Aumo, J. Lilja, P. Mäki-Arvela, T. Salmi, M. Sundell, H. Vainio, D. Y. Murzin, *Catal. Letters*, 84, **2002**.

16   a) F. Shi, Y. Deng, *J. Catal.,* 211, **2002**, 518; b) F. Shi, Q. Zhang, Y. Ma, Y. He, Y. Deng, *J. Am. Chem. Soc.,* 127, **2005**, 4182.

17   H. Miyamura, R. Matsubara, Y. Miyazaki, S. Kobayashi, *Angew. Chem. Int. Ed.* 46, **2007**, 4151.

18   A. Abad, C. Almela, A. Corma, H. Garcia, *Tetrahedron,* 62, **2006**, 6666.

19   V. L. Bogatyrev, N. P. Sokolova, *Russ. Chem. Bull*. 18, **1969**, 1573.

20   M. Kralik, V. Kratky, M. Hronec, M. Zecca, B. Corain, *Stud. Surf. Sci. Catal.,* 130, **2000**, 2321.

21   Physisorption studies were hampered by the limited accessibility of gas reactants to gel-type resin-embedded metal NPs, see: A. Biffis, H. Landes, K. Jeřábek and B. Corain, *J. Mol. Cat. A: Chemical* 151, **2000**, 283

22   A. Bunjes, I. Eilks, M. Pahlke, B. Ralle, *J. Chem. Educ.*, 74, **1997**, 1323.

23   N. D. Zelinski, P. Pawlow, *Ber. Dtsch. Chem.. Ges*., 57, **1924**, 1066.

24   P. Centomo, M Zecca, M. Kralik, D. Gasparovicova, K. Jerabek, P. Canton, B. Corain, *J. Mol. Catal. A: Chem.*, 300, **2009**, 48.

25   a) X. Ma, T. Jiang, B. Han, J. Zhang, S. Miao, K. Ding, G. An, Y. Xie, Y. Zhou, A. Zhu, *Catal. Commun.,* 9, **2008**, 70; b) O. Dominguez-Quintero, S. Martinez, Y. Enriquez,L. D'Ornelas, H. Krentzien, J. Osuna, *J. Mol. Catal. A: Chem.*, 197, **2003**, 185.

26   a) B. Chen, U. Dingerdissen, J. G. E. Krauter, H.G.J. Lansink Rotgerink, K. Móbus, D.J. Ostgard, P. Panste, T.H. Riermeir, S. Seebald, T. Tacke, H. Trauthwein, *App. Catal. A: Gen.*, 280, **2005**, 17; b) J. G. de Vries, C.J. Elsevier (Eds), *Handbook of homogeneous hydrogenation*, vol 1, Chapter 14, Wiley-VCH, Darmstadt, **2007**.

27   a) A. Mastalir, Z. Király, *J. Catal.*, 220, **2003**, 372; b) N. Marín-Astorga, G. Pecchi, J. L. G. Fierro, P. Reyes,. *Catal. Lett.*, 91, **2003**, 115; b) N. Semagina L. Kiwi-Minsker, , Catal. Lett. 127, **2009**, 334.

28   Maitlis catalyst leaching test, see: J. P. Collman, K. M. Kosydar, M. Bressan, W. Lamanna, T. Garrett, *J. Am. Chem. Soc.*, 106, **1984**, 2569.

29   H. Bönnemann, W. Brijoux, K. Siepen, J. Hormes, R. Franke, J. Pollmann, J. Rothe, *Appl. Organomet. Chem*. 11, **1997**, 783.

30   a) J. C. A. A. Roelofs, P. H. Berben, *Chem. Commun*. **2004**, 970; b) H. Bönnemann, W. Brijoux, A. Schultze Tilling, K. Siepen, *Top. Catal*. 4, **1997**, 217; c) H. Bönnemann, G. A. Braun, *Angew. Chem., Int. Ed. Engl*. 35, **1996**, 1992; d) P. T. Witte (BASF Catalysts LLC) Pat. WO 2009096783, **2009**.

31   K. Weissermel, H. J. Arpe, R. Lindley, *Industrial Organic Chemistry: Important Raw Materials and Intermediates* (4th ed), Wiley–VCH, Weinheim **2002**.

32   a) E. Sulman, V. Matveeva, V. Doluda, L. Nicoshvili, L. Bronstein, P. Valetsky, I. Tsvetkova, *Top. Catal*. 39, **2006**, 187; b) F. Benvenuti, C. Carlini, M. Marchionna, A. M. Raspolli Galletti, G. Sbrana, *J. Mol. Cat. A: Chemical* 145, **1999**, 221.

33   a) M. Fodor, A. Tungler, L. Vida, *Catal Today*, 140, **2009**, 48; b) A. Tungler, Y. Nitta, K. Fodor, G. Farkas, T. Máthé, *J. Mol. Catal. A: Chem*., 149, **1999**, 135; c) É. Sípos, A. Tugler, I Bitter, M. Kubinyi, *J. Mol. Catal. A: Chem*., 186, **2002**, 187.

34   M. G. Hitzler, F. R. Smail, S. K. Ross, M. Poliakoff, *Org. Proc. Res. Dev. 2,* **1998**, 137

35   T. Sato, C. V. Rode, O. Sato, M. Shirai, *Appl Catal B: Environ*., 49, **2004**, 181.

36   M. Lakshmi Kantam, T. Parsharamulu, S. V. Manorama, *J. Mol. Catal. A: Chem.*, 365, **2012**, 115.

37   a) M. M. Dell'Anna, M. Gagliardi, P. Mastrorilli, G.P. Suranna, C. F. Nobile, *J. Mol. Catal. A: Chem.*, 158, **2000**, 515.

38   R. Mélendrez, G. Del Angel, V. Bertin, M. A. Valenzuela, J. Barbier, *J. Mol. Catal. A: Chem.*, 157, **2000**, 143.

39   J. J. Ritter, D. Ginsburg, *J. Am, Chem. Soc*, 72, **1950**, 2381.

40   E. I. Klabunovskii, L. F. Godunova, L. K. Maslova, *Bulletin of the Academy of Sciences of the USSR Division of Chemical Science*, 21, **1972**, 1020.

41   C. Gozzi, A. Convard, M. Husset, *React. Kinet. Catal. Lett.,* 97, **2009**, 301.

42   R.L. Augustine, *Heterogeneous Catalysis for the Synthetic Chemist*, Dekker, New York, **1996**.

43   S. Nishimura, *Handbook of Heterogeneous Catalytic Hydrogenation for Organic Synthesis*, Wiley, New York, **2001**.

44   J. E. True, T. Darrah Thomas, R. W. Winter, G. L. Gard, *Inorg. Chem.,* 42, **2003**, 4437.

45   D. Astruc (Ed), *Nanoparticles and Catalysis*, Wiley-VCH, Weinheim, **2008**.

46   a) J-L. Pellegatta, C. Blandy, V. Collière, R. Choukroun, B. Chaudret, P. Cheng, K. Philippot, , *J. Mol. Catal. A: Chem.,* 178, **2002**, 55; b) Y. Motoyama, M. Takasaki, S. Yoon, I. Mochida, H. Nagashima, *Org. Lett*. 11, **2009**, 5042; c) M. J. Jacinto, P. K. Kiyohara, S. H. Masunaga, R. F. Jardim, L. M. Rossi, , *App. Catal. A: Gen*., 338, **2008**, 52.

47   X-Y. Quek, Y. Guan, E.J.M. Hensen, *Catal. Today*, 183, **2012**, 72.

48   a) K. T. Hindle, S. D. Jackson, D. Stirling, G. Webb, *J. Catal.,* 241, **2006**, 417; b) , H. B. Pan, C. M. Wai, *J. Phys. Chem. C*, 114, **2010**, 11364.

49   K. Zhou, Y. Li, *Angew. Chem., Int. Ed,.* 51, **2012**, 602.

50   http://www.kitco.com/market/. Retrieved Dec **2012**.

51   R.J. Grau, P.D. Zgolicz, C. Gutierrez, H.A. Taher, *J. Mol. Catal. A: Chem*., 148, **1999**, 203.

52   C. Evangelistia, N. Panziera, M. Vitulli, P. Pertici, F. Balzano, G. Uccello-Barretta, P. Salvadori, *Appl. Catal. A: Gen*, 339, **2008**, 84.

53   *Sustainability in the Chemical Industry: Grand Challenges and Research Needs*, National Research Council, The National Academies Press, Washington, **2006**.

54   O. Casanova, S. Iborra, A. Corma, *J. Catal*., 265, **2009**, 109.

55   F. Pinna, A. Olivo, V. Trevisan, F. Menegazzo, M. Signoretto, M. Manzoli, F. Boccuzzi, *Catal. Today*, **2012**, doi:10.1016/j.cattod.2012.01.033

56   R. M. Krieger, P. Jagodzinski, *J. Mol. Struct.,* 876, **2008**, 56.

5

Hydrogenation Reactions in Continuous Mode

5.1. OVERVIEW

In this Chapter continuous flow catalysis and reactors are introduced. The advantages of flow system compared to conventional heterogeneous phase batch setups are shortly explained, with regards to benefits in sustainable fine-chemicals synthesis. Then, the application of polymer supported Pd NPs catalysts to the continuous partial hydrogenation of olefins with multiple double bonds and to the synthesis of cis-3-hexen-1-ol from semi-hydrogenation of 3-hexyn-1ol is performed in continuous flow. A comparison with the state-of-the-art in similar systems is also provided.

5.2. INTRODUCTION

All along this Thesis, it has been pointed out several times that the need of development of sustainable routes for the large scale production of fine chemicals, i.e. cost-effective and environmentally friendly, is one of the major current concerns at the industrial level.[1] During Chapters 3 and 4, it has been shown that highly active and selective catalysts may significantly contribute to solve the problem.[2] Moreover, it has been mentioned that in order to achieve low-impact processes, the immobilization of chemical catalysts onto insoluble support materials offers significant benefits in terms of ease of reuse of the precious catalysts, clean catalyst separation as well as integration in reactor equipments.[3] Due to this, chemical industry has a great preference for solid heterogeneous catalysts.[4] Going a step further, the use of continuous-flow reactors represents a considerable added value in this regard, as they allow reactions to be carried out with higher productivity, much lower energy and space requirements, improved safety, less waste emission compared to the corresponding batch processes. Continuous removal of the reaction products also enhances the catalyst's lifetime and simplifies the purification procedures.[5]
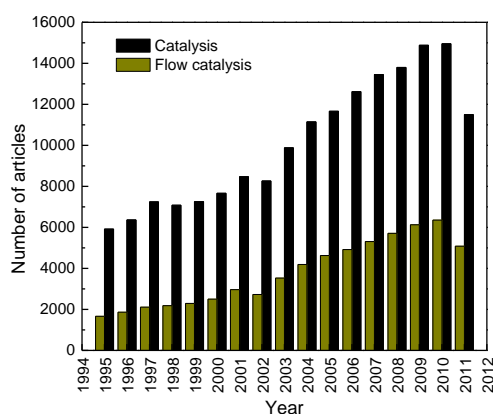

Fig. 5.1. Number of articles published containing the keywords showed in the legend from 1995 to 2011 (data obtained from the database www.sciencedirect.com).

Due to this, there is an increasing interest in the scientific community for developing new continuous flow catalytic systems, as testified by the increasing number of related publications in last years (Fig. 5.1.). Besides the advantages found for continuous flow catalytic reactions, additional benefits can be obtained for heterogeneous hydrogenation reactions as a result of the high specific interfacial area of flow processing in gas–liquid–solid triphasic reactions.[6] Owing to the large interfacial areas and the short path required for molecular diffusion in the very narrow channel space, very efficient gas–liquid–solid interaction, and thus hydrogenation, takes place, which is not attainable in normal batch systems.[7] An additional advantage of hydrogenation mini-reactor systems (Chapter 1 / Section 1.6.) is that the small hold-up reduces the damage potential of explosions and therefore conforms with the twelfth principle of green chemistry (inherently safer chemistry for accident prevention);[8] an important consideration in hydrogenation reactions involving flammable hydrogen gas.

Some similar polymeric based supports than the ones used in this Thesis have been employed for different continuous flow catalytic reactions. As example of continuous organocatalysis, Knoevenagel condensation and acylation reactions were carried out using modified methacrylate-based Amberzyme Oxirane resins, in both cases, microreactor productivity for the flow reactions was more than 3 times greater than the batch reaction owing to the decreased dimensions of the reactor and better mixing.[9] Cross-coupling reactions have been also explored under flow conditions using unsymmetrical salen-type Pd(II) and Ni(II) complexes immobilized onto a polystyrene–divinylbenezene cross-linked Merrifield resin.[10,11] While palladium catalysts were active in the Suzuki and Heck coupling reactions at elevated temperatures,[10] the nickel catalyst was active in the Kumada coupling reaction at room temperature,[11] but in both cases, the use of a mini-flow reactor system gave reasonable conversions and useful quantities of material were produced within minutes rather than overnight for discontinuous systems. Finally,

a wide number of enantioselective reactions have been described for Pericàs and co-workers[12] by using packed-bed micro-reactors filled with functionalized polystyrene resins.

However, the continuous flow selective hydrogenation of alkynes and dienes is dominated by inorganic support based catalysts[6] and very few examples of organic supports have been applied in these reactions.[13] The most similar supports used in continuous flow hydrogenation were some ion-exchangers containing quaternary ammonium groups, in which Ru(II) and Rh(I) complexes containing monosulfonated triphenylphosphine ligands were immobilized.[13b] These catalysts were studied in the hydrogenation of disubstituted alkynes at 50ºC and 30 bar, giving the same selectivity observed in aqueous organic biphasic systems in batch conditions. In addition, the hydrogenation of trans-cinnamaldehyde, acetophenone, and the isomerization of 1-octen-3-ol to octan-3-one using the same catalysts was also demonstrated.

Here, the effectiveness of the polymer containing Pd NPs catalyst developed during this thesis (Chapter 3) was evaluated in a continuous flow mini-reactor. The developed triphasic liquid/gas/solid system for selective hydrogenation reactions allows a fine control of gas and liquid contact times on Pd nanoparticles catalytic sites immobilized onto the polymeric resins.

5.3. CATALYTIC HYDROGENATIONS IN FLOW MODE WITH Pd NPs

The importance of selective partial hydrogenation reactions of hydrocarbons with multiple C=C or C≡C bonds in fine chemical industry has been already pointed out in this Thesis and, to this purpose, an in depth investigation was carried out to evaluate the activity and selectivity of Pd/D(Li) type catalysts in

batch conditions (Chapter 4 / Section 4.3.2.). Prompted by the ease of handling of the developed catalysts, their proved efficiency under mild conditions (1 bar H_2 and r.t.) and their confirmed stability upon recycling, it was decided to step forward and test the system under continuous-flow conditions.

With this aim, a home-made apparatus was used (Chapter 2 / Section 2.6.2.) in which the substrate solution and the H_2 gas flow simultaneously through the catalyst beads packed into a commercial tubular glass mini-reactor (Fig. 5.2.).[15]
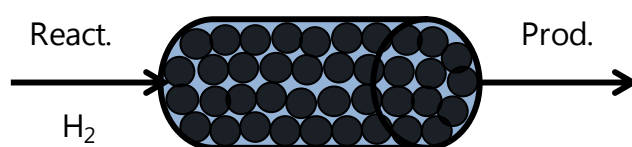

Fig. 5.2. Schematic representation of hydrogenation reaction in continuous flow by using Pd NPs supported on Dowex® resins.

Having established the best catalyst performance for the hydrogenation of cyclooctadiene **5** and 3-hexyn-1-ol **7** in batch, we used these as probe substrates (Scheme 5. 1.) for the evaluation of productivity and selectivity in flow, by monitoring the reaction progress with time under constant (Fig. 5.2.) and variable (Fig. 5.3.) flow rates of solution and H_2 gas.
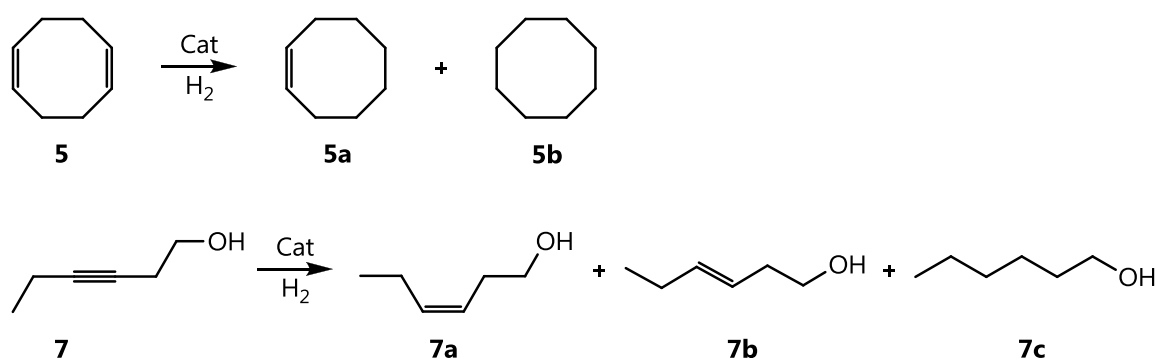
Scheme 5.1. Sketch of the substrates tested in hydrogenation in continuous flow mode.

Before performing catalytic reactions, Pd/D(Li) *in* was packed into the mini-reactor and reduced under a rate flow of 0.4 mL min^{-1} methanol and 0.8 mL min^{-1} molecular hydrogen. The reactions were run under conditions comparable with

those of the batch experiments, resulting in excellent catalyst stability over prolonged reaction periods with no significant activity nor selectivity decay observed for more than 24 hours time on stream, neither Pd leached in solution detected by ICO-OES.
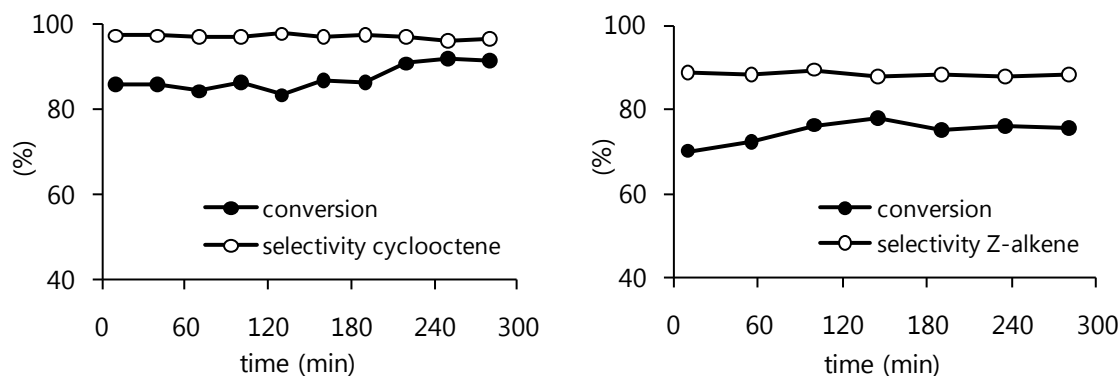

Fig. 5.2. Continuous-flow hydrogenation of **5** (left) and **7** (right) over Pd/D(Li) *pre* catalyst (50-100 mesh, 45 mg, 1.25 wt% Pd, [Pd(CH$_3$CN)$_4$ (BF$_4$)$_2$] precursor). Conversion and selectivity vs. time on stream. React. condit.: 45 mg Pd/D(Li) *pre,* methanol, r.t., substrate concentration 0.2 M, fixed solution flow 0.2 mL min^{-1} and H$_2$ 0.8 mL min^{-1}/ 2.5 bar. Selectivity Z-alkene = **7a**/(**7a**+**7b**)x100, total (*cis*+*trans*) ene selectivity values were similar.

The best compromise between conversion and selectivity for both substrates was obtained for residence times in the range 50-100 s and ca. 2.5 bar H$_2$.[14] Under these conditions, cyclooctene was obtained with ca. 97% selectivity@87% conversion (Fig. 5.2. left), that corresponds to a productivity of 395 h^{-1} (TOF) and 1.30 kg l^{-1} h^{-1} (STY), and to an overall TON of 1700 after 4.7 h.[15] The partial hydrogenation of **5** was previously accomplished using a pore-through-flow Pd@Al$_2$O$_3$ catalytic membrane reactor under 50 °C and 10 bar H$_2$.[16] Similar selectivity/conversions were obtained, however STY was *ca.* one order magnitude lower and also periodic regeneration of the system at 250°C under H$_2$ for 2h was required.

The *cis*-mono-hydrogenation product of **7**, the leaf alcohol 3-hexen-1-ol **7a**, is an important ingredient in the fragrance industry,[17] which is manufactured in ca. 97% selectivity@99% conversion by a batch process using the Lindlar catalyst (Pd

on $CaCO_3$ doped with Pb).[18] The proposed flow system provided **7a** with a 89% selectivity@75% conversion (Fig. 5.2. right), being (*cis+trans*) selectivity *ca.* 80%. This corresponds to a productivity of 352 h^{-1} (TOF) and 1.02 kg l^{-1} h^{-1} (STY), and to an overall TON of 1650 after 4.7 h. Despite the slightly higher selectivity of the industrial process, the system here described represents an alternative with clear benefits in terms of safety, environmental impact and productivity, also avoiding potential contamination by toxic Pb.[19]
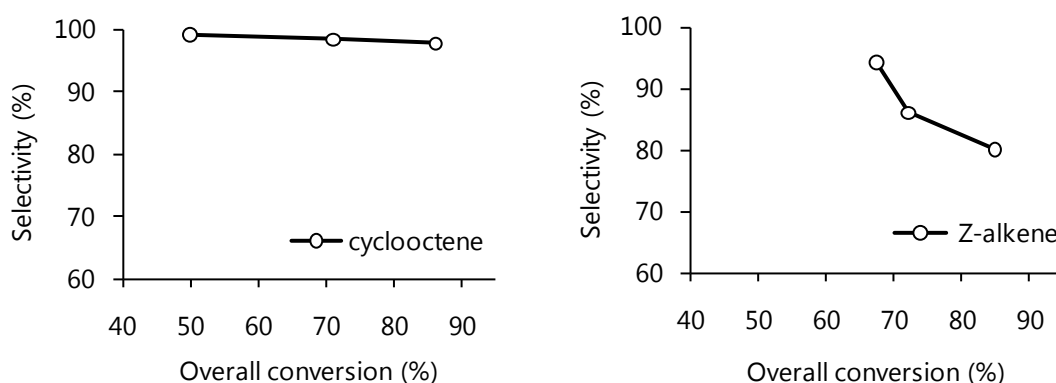

Fig. 5.3. Continuous-flow hydrogenation of **5** (left) and **7** (right) over Pd/D(Li) *pre* catalyst (50-100 mesh, 45 mg, 1.25 wt% Pd, [Pd(CH_3CN)$_4$ (BF_4)$_2$] precursor). Selectivity *vs* conversion diagram React. condit.: 45 mg Pd/D(Li) *pre*, methanol, r.t., fixed H_2:substrate ratio=2.3, variable solution flow [0.1-0.4] mL min^{-1} and H_2 [0.5-1.2] mL min^{-1}. Selectivity = **7a**/(**7a**+**7b**)x100, total (*cis+trans*) ene selectivity values were similar.

To analyze the selectivity of the system at different conversions the yields towards monohydrogenated products were tuned by adjusting the H_2 and the solution flow rates. Irrespective of the substrate, an increase of the solution flow rate (i.e. a decrease of the residence time while keeping a constant H_2:substrate ratio=2.3) invariably led to an increase of selectivity in partial hydrogenation, which could be easily brought to 100 %, although with some conversion decrease.[20] This is illustrated in Fig. 5.3. in which the selectivity/conversion diagram, obtained by varying the flow rate of the solution at fixed H_2/substrate ratio, is reported.

Compared to the corresponding batch reactions (Table 5.1.) the Pd/D(Li) used in continuous flow reactor was *ca.* 50 times more productive in terms of STY and showed a similar selectivity/conversion relationship in the case of **5**, and a worse selectivity performance in the case of **7**. Indeed, the selectivity for **7** was more dependent from conversion than for **5** (see Fig. 5.3.), thus indicating that **5** is a much more sensitive substrate with respect to slight changes in the experimental conditions.

Table 5.1. Comparison Pd/D(Li) type catalysts in batch and flow conditions.

Mode	1,5-COD [5]				3-hexyn-1-ol [7]			
	TOF (h^{-1})	Conv (%)	Select. [5a] (%)	STY $(kg\ l^{-1}\ h^{-1})$	TOF (h^{-1})	Conv (%)	Select. [7a] (%)	STY $(kg\ l^{-1}\ h^{-1})$
[a] Batch	350	98.5	96.7	0.02	322	91.0	98.2	0.02
[b] Flow	395	87.0	97.0	1.23	352	74.9	89.0	1.06

React. Cond.: methanol, r.t., 1.25 wt% Pd/D(Li) type catalysts (50-100mesh, $[(Pd(CH_3CN_4)(BF_4)_2]$ precursor), [a] 50 mg cat., subtrate concentration 0.17 M, molar ratio substrate:Pd = 350, H_2 pressure 1 bar; [b] 45 mg cat., substrate concentration 0.2 M, solution flow 0.2 ml min^{-1}, H_2 flow 0.8 ml min^{-1}, H_2 pressure 2.5 bar.

In order to evaluate the efficiency of the developed system in comparison with other catalysts, three different supported Pd-based catalysts were tested in the continuous hydrogenation of **7** under similar reaction conditions: Pd-MonoSil[21] made of Pd NPs supported onto a macro/mesoporous silica monolith, the commercial Pd/C and Pd/TiO$_2$ monolith[22] made of Pd NPs supported onto a macro/mesoporous titania monolith. The obtained results are shown in Table 5.2.

Pd NPs supported onto ion exchange resins were invariable more effective in terms of activity and selectivity. Similar behaviour was detected for Pd/TiO$_2$ monolith in terms of TOF and STY, nevertheless, polymeric based catalysts provided a higher selectivity at the same conversion in any case.[22] Comparing to the packed bead reactor using a commercial Pd/C catalyst, a great difference was found with regard to the activity, being this catalyst *ca.* 10 times less active. A

possible explanation could be related with mass transfer limitations, unlike the polymeric beads, a powder can pack better inside the reactor and consequently cause higher resistance to the passage of fluid, in fact, H_2 pressure increased up to 9 bars when Pd/C was used. With respect to selectivity, they showed similar values but for Pd/C the conversion was 15% and it has been already seen the strong dependence selectivity has from conversion.

Table 5.2. Comparison with different supported Pd-based catalysts. Continuous flow hydrogenation of 3-hexyn-1-ol **7**.

Catalyst	TOF (h^{-1})	Conv (%)	Select. [7a] (%)	STY (kg l^{-1} h^{-1})
[a] 1.25 wt% Pd/D(Li)	352	74.9	89.0	1.06
[b] 1.30 wt% Pd-MonoSil	81	85.0	78.0	0.27
[c] 5.00 wt% Pd/C	27	15.0	89.0	0.24
[d] 0.24 wt% Pd/TiO$_2$ monolith	350	61.0	87.0	0.93

React. Cond.: methanol, r.t., [a] 45 mg cat., substrate concentration 0.2 M, solution flow 0.2 ml min^{-1}, H_2 pressure 2.5 bar, molar ratio H_2:substrate = 2.4; [b] 150 mg cat., 0.2 M, 0.15 ml min^{-1}, 2.9 bar H_2, molar ratio 2.8; [c] 150 mg cat, 1 M, 0.15 ml min^{-1}, 9 bar H_2, molar ratio 1.2; [d] 140 mg cat., 0.2 M, 0.15 ml min^{-1}, 2.3 bar H_2, molar ratio 2.2.

5.4. CONCLUSIONS

A continuous flow catalytic system was implemented for the selective hydrogenation of hydrocarbons with multiple C=C and C≡C bonds to achieve partial hydrogenation products, very interesting compounds in the synthesis of fine chemicals.[23] Polymer supported Pd NPs catalysts showed very good durability and efficiency under flow conditions with more than 24 h time on stream with neither loss of activity nor selectivity. Catalytic flow processes represent a convenient alternative to batch reaction in terms of productivity, safety, waste emission, purification, space and energy consumption. The catalyst was applied to the flow synthesis of the important leaf alcohol *cis*-3-hexen-1-ol

with significant benefits compared to the industrial process and with better productivities than the homologous discontinuous systems. The results obtained showed a relatively simple approach useful for the production of elaborate molecules, and thus for the long-term production of fine-chemicals.

5.5. EXPERIMENTAL

The details about preparation and characterization of the catalysts are reported in the experimental section of Chapter 3. All the chemicals used in hydrogenation reactions were reagent grade commercial products and were used as received from Aldrich without further purification. GC and ICP-OES analyses of the recovered solutions after catalysis to determine the content of metal leached were performed on the equipments described in Chapter 2

Hydrogenation reactions in continuous flow mode.

Catalytic flow hydrogenations were carried out using a home-made continuous-flow reactor system built at Istituto di Chimica dei Composti Organo Metallici and described in Chapter 2 / Section 2.6.2. At the outlet of the reactor, the product solution was collected for GC analysis and the excess amount of the hydrogen gas released to the atmospheric pressure. Commercially available H_2 (99.995%) was used as received. The catalyst was packed into the mini-reactor as Pd/D(Li) *in* and reduced under flow conditions with H_2 in methanol previously to the catalytic reaction and without further isolation.

In a typical experiment, 45mg of Pd/D(Li) *in* were packed into the commercial tubular glass mini-reactor (3 mm diameter x 25 mm length), then degassed methanol and molecular hydrogen were allowed to flow through the catalytic bed at a constant 0.4 mL min^{-1} and 0.8 mL min^{-1} rate respectively for 1h until the catalyst became black. After that, a degassed solution of substrate in methanol

(0.2 M) was allow to flow through the catalyst beads at a constant 0.2 mL min^{-1} rate, together with a constant H_2 flow of 0.8 mL min^{-1} at RT. This resulted in a H_2 pressure at the reactor inlet of ca. 2.5 bar (corresponding to a H_2:substrate molar ratio of ca. 2.3), while the hydrogen gas was released at atmospheric pressure at the outlet of the reactor. Therefore, the pressure drop generated by the packed bed reactor was ca. 1.5 bar. The attainment of the steady state conditions (ca. 1 h after the activation of the catalyst) was taken as the reaction start time. The product solution was periodically analyzed for conversion by GC, while 12 mL h^{-1} aliquots were continuously sampled for subsequent Pd leaching analysis by ICP-OES.

REFERENCES

1. a) United States Environmental Protection Agency, *Guide to Industrial Assessments for Pollution Prevention and Energy Efficiency*, EPA/625/R-99/003, **2001**; b) Swedish Parliament, *Strategic Challenges - A Further Elaboration of the Swedish Strategy for Sustainable Development*, Government Communication, 2005/06:126, **2006**; c) F. Cavani, G. Centi, S. Perathoner, F. Trifirò (Eds), *Sustainable Industrial Chemistry*, Wiley-VCH, Weinheim, **2009**.

2. a) J. Clark, D. Macquarrie (Eds), Handbook *of Green Chemistry and Technology*, Blackwell Science, Oxford, **2002**; b) R. A. Sheldon, I. Arends, U. Hanefeld, *Green Chemistry and Catalysis*, Wiley-VCH, Weinheim, **2007**.

3. a) D. J. Cole-Hamilton, R. P. Tooze (Eds), *Catalyst Separation, Recovery and Recycling; Chemistry and Process Design*, Springer, Dordrecht, **2006**; b) R. A. Sheldon, H. van Bekkum (Eds), *Fine Chemicals Through Heterogeneous Catalysis*, Wiley-VCH, Weinheim, **2001**.

4. B. Pugin, H. U. Blaser, *Top. Catal.*, 53, **2010**, 953.

5. a) A. Sachse, A. Galarneau, B. Coq, F. Fajula, *New J. Chem.*, 35, **2011**, 259; b) X. Y. Mak, P. Laurino, P. H. Seeberger, *Beilstein J. Org. Chem.*, 5, **2009**, No. 19; c) J. Wegner, S. Ceylan and A Kirschning, *Adv. Synth. Catal.* 354, **2012**, 17; d) M. Irfan, T. N. Glasnov and C. O. Kappe, *ChemSusChem* 4, **2011**, 300; e) J. Wegner, S. Ceylan and A. Kirschning, *Chem. Commun*. 47, **2011**, 4583; f) D. Webb and T. F. Jamison, *Chem. Sci.* 1, **2010**, 675.

6   M. Irfan, T. N. Glasnov, C. O. Kappe, *ChemSusChem*, 4, **2011**, 300.

7   J. Kobayashi, Y. Mori, S. Kobayashi, *Chem. Asian J.*, 1, **2006**, 22.

8   a) P. T. Anastas, J. C. Warner, *Green Chemistry: Theory and Practice*, Oxford University Press, New York, **1998**; b) P. T. Anastas, M. M. Kirchhoff, *Acc. Chem. Res.*, 35, **2002**, 686.

9   A. R. Bogdan, B. P. Mason, K. T. Sylvester, D. T. McQuade, *Angew. Chem. Int. Ed.*, 46, **2007**, 1698.

10   N. T. S. Phan, J. Khan, P. Styring, *Tetrahedron*, 61, **2005**, 12065.

11   a) S. J. Haswell, B. O'Sullivan, P. Styring, *Lab Chip*, 1, **2001**, 164; b) N.T.S. Phan, D.H. Brown, P. Styring, *Green Chem.,* 6, **2004**, 526; c) P. Styring, A. I. R. Parracho, *Beilstein J. Org. Chem.*, **2009**, 5, No. 29.

12   a) M.A. Pericàs, C.I. Herrerías, L. Solà, *Adv. Synth. Catal.*, 350, **2008**, 927; b) D. Popa, R. Marcos, S. Sayalero, A. Vidal-Ferran, M.A. Pericàs, *Adv. Synth. Catal.*, 351, **2009**, 1539; c) J. Rolland, X.C. Cambeiro, C. Rodríguez-Escrich, M.A. Pericàs, *Beilstein J. Org. Chem.*, **2009**, 5, No. 56; d) E. Alza, C. Rodríguez-Escrich, S. Sayalero, A. Bastero, M.A. Pericàs, *Chem. Eur. J.*, 15, **2009**, 10167.

13   a) K. Mennecke, R. Cecilia, T. N. Glasnov, S. Gruhl, C. Vogt, A. Feldhoff, M. A. L. Vargas, C. O. Kappe, U. Kunz, A. Kirschning, *Adv. Synth. Catal.*, 350, **2008**, 717; b) H. H. Horváth, G. Papp, C. Csajági, F. Joó, *Catal. Commun.*, 3, **2007**, 442.

14   H$_2$ gas was released at atmospheric pressure at the outlet of the reactor. Therefore, the pressure drop generated was ca. 1.5bar.

15   Turnover frequency (TOF = mol product / mol Pd x h) and space-to-time yield (STY = kg product / litre reactor volume x h) calculated on overall conversion. See: M. Boudart, *Chem. Rev*. 95, **1995**, 661.

16   a) A. Schmidt, A. Wolf, R. Warsitz, R. Dittmeyer, D. Urbanczyk, I. Voigt, G. Fischer andR. Schomäcker, *AIChE J.* 54, **2008**, 258; b) J. Caro et al. *Ind. Eng. Chem. Res.* 46, **2007**, 2286.

17   a) J. Warr, S. Fraser and O. Gouault (Takasago Perfumery Co., Ltd.) Pat. *EP 1964542*, 2008 b) J. Y. Choi, B. B. Jeon and H. J. Seo (Amorepacific Corp.) Pat. *WO 2007055493*, 2007.

18   a) H. Bönnemann, W. Brijoux, K. Siepen, J. Hormes, R. Franke, J. Pollmann and J. Rothe, *Appl. Organomet. Chem.* 11, **1997**, 783; b). H. Lindlar, *Helv. Chim. Acta* 35, **1952**, 447.

19   European Agency for the Evaluation of Medicinal Products, *Note for guidance on specification limits for residues of metal catalysts*, CPMP/SWP/QWP/4446/00, June **2002**.

20 As expected, an increase in the H_2 flow rate caused a conversion increase and a small selectivity drop, due to the change in the H_2:substrate molar ratio.

21 A. Sachse, N. Linares, P. Barbaro, F. Fajulaa, A. Galarneau, *Dalton Trans.,* **2012**, doi: 10.1039/c2dt31690k.

22   N. Linares, S. Hartmann, A. Galarneau, P. Barbaro, *ACS Catal.*, 2, **2012**, 2194

23 See, e.g.: a) S. Nishimura, *Handbook of Heterogeneous Catalytic Hydrogenation for Organic Synthesis*, John Wiley and Sons, New York, **2001**; b) A. Molnar, A. Sarkany, M. Varga, *J. Mol. Catal. A: Chem.* 173, **2001**, 185; c) C. Godínez, A. L. Cabanes, G. Víllora, *Chem. Eng. Proc.*, 34, **1995**, 459.

6

Polymer Supported Colloidal Palladium Nanoparticles: Synthesis, Characterization and Hydrogenation Tests.

6.1. OVERVIEW

This Chapter initiates with a brief introduction to the topic of colloidal nanoparticles focusing on palladium nanocatalysts and supported colloids on organic materials and giving practical examples of the state of art. The study carried out is then described, which encompasses the synthesis and characterization of supported palladium catalysts starting from colloidal nanoparticles. The performance of the catalysts in terms of activity and selectivity was evaluated in the semi-hydrogenation of substituted acetylenes, an important reaction in fine chemistry to obtain *cis*-olefins, by using the previously studied 3-hexyn-1-ol as model substrate. Finally, comparison with palladium colloids immobilized on different supports was also carried out

6.2. INTRODUCTION

The term "colloid" refers to the suspension of a phase (solid or liquid) into a second phase, which neither settled not deposited spontaneously. This definition includes a large group of materials divided in polymer suspensions in solution, emulsions constituted by amphiphilic molecules in aqueous or organic mixture and dispersions of inorganic particles. For long time, the properties of inorganic colloids, and more precisely metal nanoparticles, have awoken great interest within the scientific community.[1] The small size of the colloidal particles, usually in the nanometer scale, is responsible for their unique properties allowing a wide range of applications, among others, in the catalytic field.[2] However, this nanometric scale makes metal nanoparticles unstable since they tend to agglomerate to reduce their surface tension; therefore the stabilization of metallic colloids is a crucial aspect to be considered.[3]

Different synthetic methods have been described for the preparation of metallic nanoparticles, including physical and chemical approaches. In the first group, the mechanic subdivision of bulk metals yields dispersions with a very wide size distribution, usually not reproducible, while with chemical methods an easier control of the nanoparticles size can be achieved.[4] In this sense, there are several chemical methods for the synthesis of colloidal suspensions leading to different size distributions: i) chemical reduction of transition metal salts,[5] ii) thermal,[6] photochemical,[7] or sonochemical[8] decomposition, iii) ligand reduction and displacement from organometallics,[9] iv) metal vapour synthesis,[10] and v) electrochemical reduction.[11] However, whatever the method used, the presence of stabilizing ligands is required in order to prevent agglomeration, in this sense, linear polymers or surfactants such as tetraalkylammonium salts are usually employed.

Among the chemical methods abovementioned, the most extensively used is the reduction of transition metals salts in solution. To obtain the colloidal materials by this generally simple procedure, there is a broad range of reducing agents that can be used including gases such as molecular hydrogen and carbon monoxide, hydrides, salts like sodium borohydride or sodium citrate or even oxidable alcohols that can act as both, solvent and reducing agent. Hirai and co-workers[12] have extensively used aqueous alcohols as reducing agents in the synthesis of colloidal transition metals such as Rh, Pt, Pd, Os, or Ir. All these colloidal suspensions were stabilized by organic polymers or oligomers such as polyvinylic alcohol (PVA), polyvinylpyrrolidinone (PVP), polyvinylic ether (PVE), or cyclodextrine. On the other hand, Tan *et al.*[13] reported aqueous colloidal solutions of Au, Ag, Ir, Pt, Pd, Rh or Ru stabilized by PVA and prepared by hydrogen reduction of the corresponding chloride salts. Differently, Turkevitch *et al* [14] synthesized colloidal suspensions of gold by using sodium citrate that acted as both reducing agent and ionic stabilizer. When borohydrides ($NaBH_4$ or KBH_4) are used, usually surfactants (anionic or cationic) and water-soluble polymers are the stabilizers utilized. As an example, Nakao and co-workers[15] described the preparation of Ru, Rh, Pd, Pt, Ag, or Au nanoparticles stabilized by quaternary ammonium, sulfates, or poly(ethylene glycol).

The catalytic application of colloidal suspensions presents several drawbacks with regard to separation from the reaction mixture and recycling. The immobilization of suspensions on solid insoluble supports may be a clear alternative for an easy recycling by simple filtration. However, the presence of surfactants or salts that can also be adsorbed on the surface may adversely affect the catalytic activity. Usually, the immobilization of metal colloids takes place by either adsorption or chemical bond to the support. In the first method, the most often used solid supports are activated carbon, silica, alumina, or other oxides such as TiO_2 and MgO. The main advantage of this process is that generally,

regardless the support, the size of the colloidal nanoparticles does not change during the immobilization, differently from the most traditional prepared catalysts where the nanoparticles size is highly affected by the support. In this sense, Reetz *et al.*[16] reported Pd colloids on alumina disks where alteration neither of structure nor of particle size was detected by TEM. Bönnemann *et al.*[17] prepared a supported Pt-Pd colloid stabilized by quaternary ammonium salts by stirring the colloidal suspension in the presence of activated carbon. On the other hand, polymeric supports have been also used to heterogenized colloidal metals. Toshima *et al.*[18] reported polymer-protected platinum and rhodium clusters immobilized on cross-linked polymers. Nakao and co-workers[19] immobilized aqueous suspensions of Rh, Pd, Pt, Ag, or Au colloids stabilized by a wide range of surfactants on ion-exchange resins.

No many further examples of colloidal nanocatalysts supported onto ion exchange resins can be found in the literature. However, as has been described and demonstrated for traditional supported metal nanoparticles in this Thesis, these materials show inherent advantages in their application as catalytic supports. For this reason, immobilization of palladium colloids onto ion exchange resins and testing of the resulting catalyst were carried out.

6.3. SYNTHESIS OF COLLOIDAL SUPPORTED PALLADIUM CATALYSTS

The preparation of the catalysts starts with the synthesis of colloidal palladium suspensions and the subsequent immobilization of the stabilized nanocatalysts onto Dowex® resins. The resins used were gel type (2% divinylbenzene as cross-linker), either strong cation-exchange (containing sulfonic groups, DOWEX® 50WX2) or strong anion-exchange (trimethylbenzyl ammonium groups, DOWEX® 1X2), and with bead dimensions ranging from 150 to 300 μm. Strong cation-

exchange resins were used in their protonated form as manufactured, or converted into the parent lithium salt.[20] A sketch of the ion-exchange resins is reported in Chapter 3 / Scheme 3.2.

The highly stable solution of Pd colloids, from here on referred to as c-Pd, was prepared through a commercialized route called NanoSelect.[21] In this procedure, (hexadecyl)(2-hydroxyethyl)dimethylammonium (HHDMA) dihydrogenphosphate, a cationic ammonium surfactant (depicted in Scheme. 6.1), is used as both a stabilizing and a reducing agent in water.
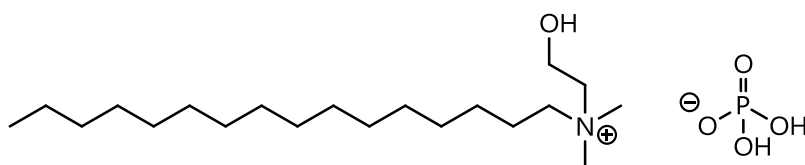
Scheme 6.1. Commercial ammonium surfactant [HHDMA] [H_2PO_4].

The alcohol function acts as an electron donor for the reduction of noble metal salts, with no additional reducing agent required, thus leading to the straightforward growth of Pd NPs. During the reduction of Pd(II) (in the form of Na_2PdCl_4) to Pd^0, the surfactant adsorbs onto the surface of the preformed NPs, which stabilizes the colloidal particles in water. Bönnemann *et al.*[22] described a similar system for the reduction of metal salts with tetraalkylammonium hydrotriorganoborates [NR_4][BEt_3H] in THF. In the reported process, both the stabilizing agent (the NR_4^+ group) and the reducing group were also coupled in the same reagent.

The resultant c-Pd, obtained as acidic aqueous solution of pH 3, were analyzed by Dynamic Light Scattering (DLS) to verify the mean diameter of the colloids was within the acceptable range of 40 – 50 nm; it must be taken into account that the colloids consist of a nanoparticle metal core surrounded by a shell of stabilizing agent, therefore, the actual size of the MNP is lower, as was proved by TEM (see Section 6.4.). After that, the nanocatalysts were deposited onto polymeric resins

differently functionalized (Table 6.1.) by mixing c-Pd with the heterogeneous support to achieve a theoretical loading of 0.5 wt% Pd.

Table 6.1. Pd deposition on functionalized ion exchange resins.

Resin	Functional group	Pd deposition
Dowex® 50WX2	$-SO_3^-H^+$	yes
Dowex® 50WX2	$-SO_3^-Li^+$	no
Dowex® 1 X 2	$-CH_2NMe_3^+Cl^-$	no

The colloids were supported onto the resin by ion exchange mechanism (see Section 6.4.). In the case of the anionic resin, no exchange was possible and therefore, the attachment of the stabilized nanoparticles to the polymer did not happen. For the cationic resin, differences were found between the protonated and the lithiated form. While the colloids were immobilized onto the resin when the protonated form was used, in the case of the lithiated form not only the immobilization did not take place, but also the precipitation of palladium was detected. The presence of lithium somehow destabilized the colloid forcing the precipitation of palladium.

Following the evidences, the cation exchange resin in the protonated form was utilized to prepare a set of catalysts, referred to as c-Pd/D(H) and summarized in Table 6.2., by changing the pH and the dilution ratio of the colloidal suspension. The metal content, analyzed by ICP-OES, indicated that the concentration of palladium affected the metal uptake, since solutions less concentrated led to higher metal uptake. No distinction was found with regard to the pH. P. T. Witte *et al*. have previously reported the immobilization of these colloids onto different supports, among them, activated carbon, titanium silicate, or different functionalized organic polymer fibers with the latest behaving in a very similar way to that above described.[21,23]

Table 6.2. Polymer supported c-Pd catalysts prepared.

Catalyst label	pH	Dilution ratio	% H$_2$O (LOI) [a]	wt% Pd (dry catalyst) [b]	wt% Pd (wet catalyst) [c]	M uptake [d] (%)
c-Pd/D(H) 1	3	-	22.6	0.16	0.12	24.8
c-Pd/D(H) 2	3	1	19.7	0.21	0.17	33.8
c-Pd/D(H) 3	3	3	21.1	0.24	0.19	37.8
c-Pd/D(H) 4	7	1	8.9	0.19	0.17	34.6
c-Pd/D(H) 5	10	3	9.0	0.20	0.18	36.4

[a] Loss on ignition: Treatment at 105ºC for 1 h. [b] Pd content measured by ICP-OES in the dry sample. [c] Pd content calculated taken into account the amount of water present in the support [d] Percentage of metal in the catalyst regarding the theoretical amount (0.50 wt%).

6.4. CHARACTERIZATION OF COLLOIDAL SUPPORTED PALLADIUM CATALYSTS

The polymer supported Pd colloids were characterized in the solid state by a combination of microscopic and scattering techniques employing the equipments described in Chapter 2. Palladium loading was obtained from ICP-OES (Table 6.2.)

STEM imaging showed the presence of palladium nanoparticles supported onto the resins. Representative pictures are shown in Fig. 6.1 and Fig 6.2. From STEM characterization, it can be seen that the size of supported Pd NPs was scarcely affected by the acid-base conditions or the dilution ratio of the immobilization process. For basic conditions (Fig. 6.1.) metal nanoparticles of 17.1 nm mean diameter were found, with a size distribution a bit more spread than for Pd NPs supported under acid conditions (Fig 6.2.). The latest showed a mean size of 15.7 nm with 60% of the particles within the range (14-16 nm).
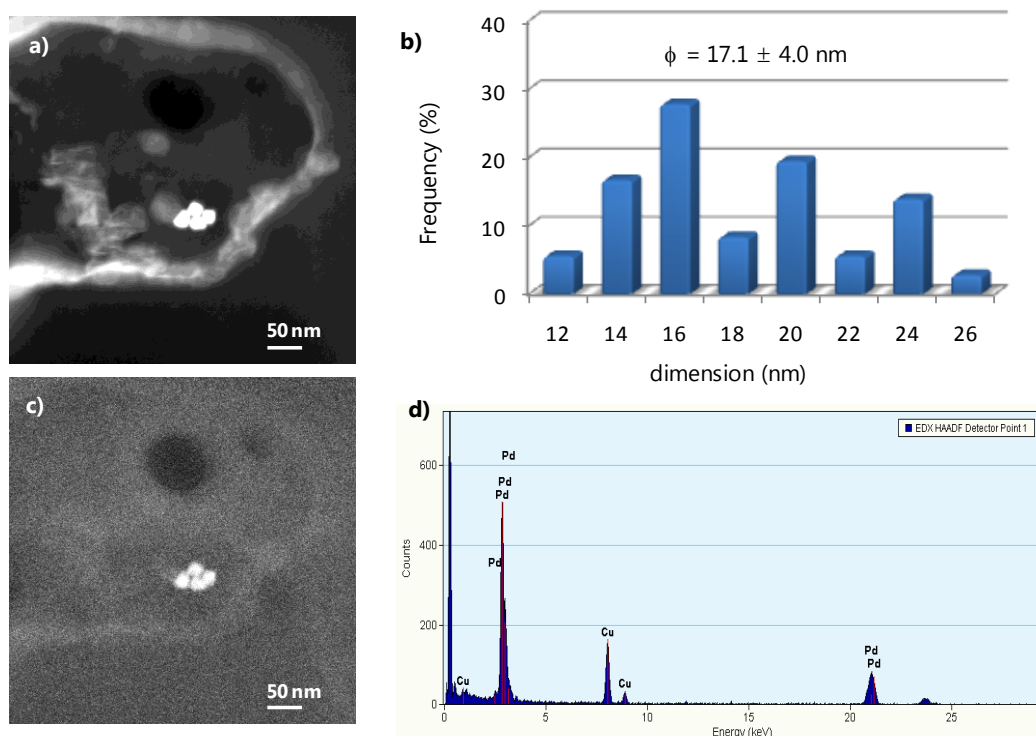
Fig. 6.1. STEM analysis of sample c-Pd/D(H) 5 (pH 10): a) High-Angle Annular Dark-Field image, b) nanoparticle size distribution determined from TEM, c) secondary electrons image of the same area and d) EDXS microanalysis.
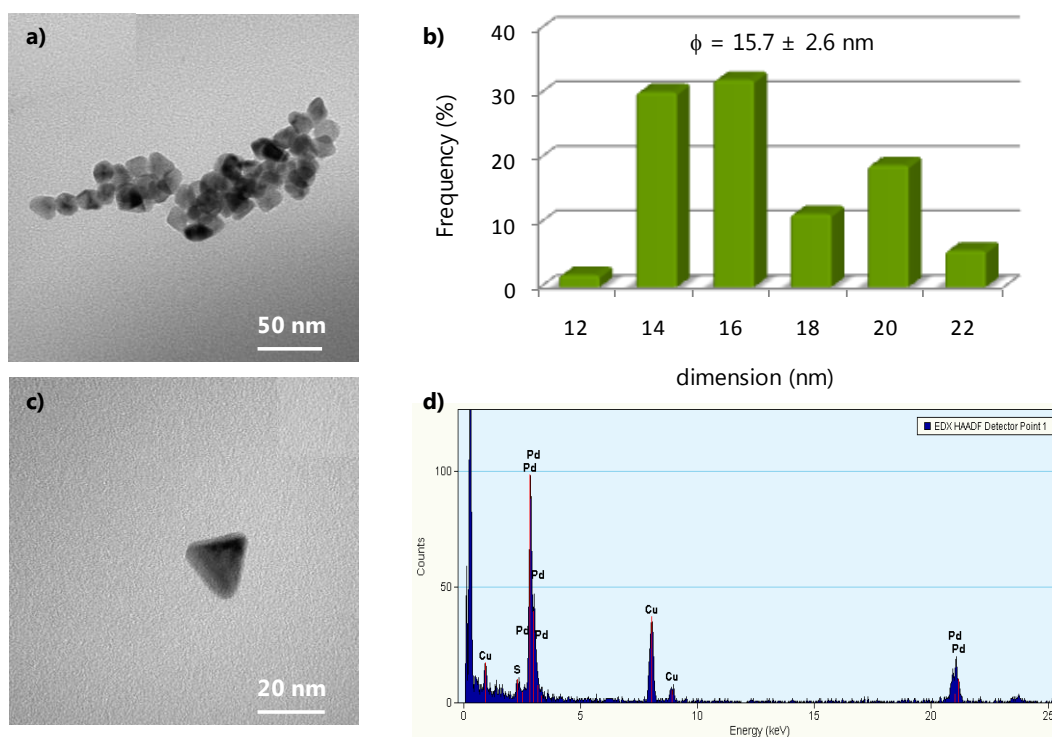

Fig. 6.2. STEM analysis of c-Pd/D(H) 1 (pH 3): a-c) TEM images at different magnifications b) nanoparticles size distribution from TEM analysis and d) Elemental analysis by EDXS.

148

Regardless the acid-base conditions, TEM images showed aggregates of nanoparticles (small and big clusters), but also single nanoparticles were detected. According to the shape, most of Pd nanoparticles presented polyhedron geometries, usually octahedral and tetrahedral, prevailing over spheres. The adoption of polyhedral shapes has been already described for colloidal palladium nanoparticles of similar dimensions.[24]

Some hypothesis has been done concerning the interaction system between nanoparticles, stabilizer and support. P. T. Witte *et al.* proposed a flexible mechanism in which a double layer of stabilizer, with polar groups directed inwards towards the metal and outwards towards the solution, surrounds the nanoparticle making these colloids soluble in water, and at the same time allowing the attachment to the support. A graphic representation is shown in Scheme. 6.2.
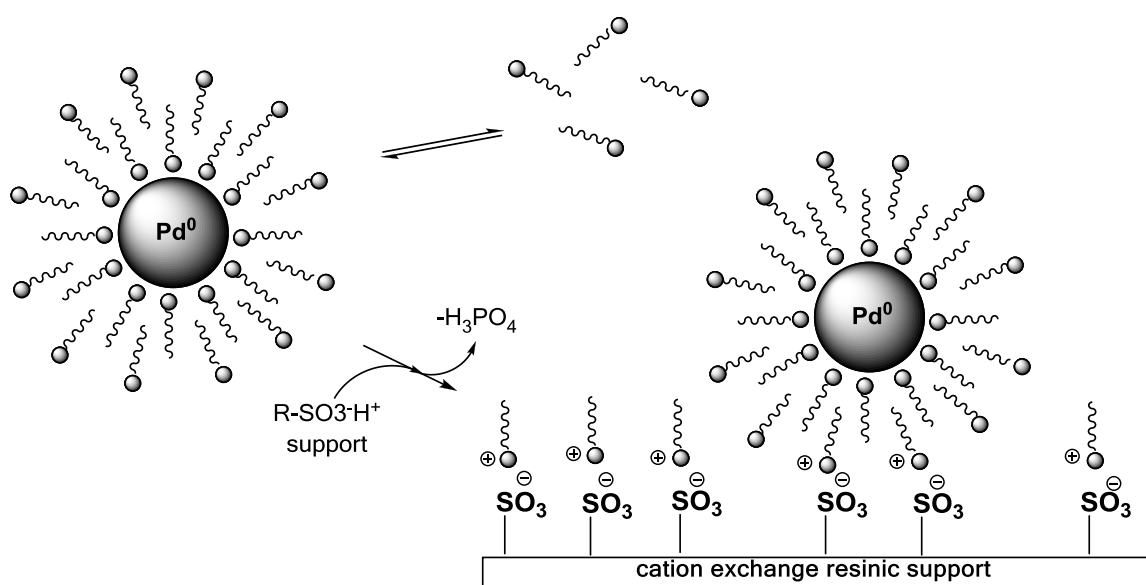
Scheme 6.2. Proposed mechanism of stabilization of colloidal nanoparticles by means of a double layer of HHDMA and deposition on cation exchange resin support. Adapted from reference [23]

Nakao *et al.* reported a comparable system where an aqueous solution of stabilized colloids was supported onto ion exchange resins and they presumed similarly that free surfactant molecules contained in the sols first attach to the resin surface to give it a hydrophobic character to some extent.[15,19]

It seems to be clear that the interaction of the colloids with the support was through the polar head groups of the stabilizer. The best interaction took place when negatively charged surface was easily available, as happened with the polymer functionalized with sulfonic groups (H form), on the contrary, the positively charged surface by quaternary ammonium groups generated an electrostatic repulsion that did not allow the attachment (see Section 6.3.).

6.5. HYDROGENATION OF 3-HEXYN-1-OL

It was already mentioned in Chapter 4 the importance that partial hydrogenation of alkynes to obtain mono-enes has in fine chemicals industry and, to this purpose, the hydrogenation of 3-hexyn-1-ol has been extensively studied in this Thesis either in batch or flow conditions (Chapters 4 and 5).

The synthesized polymer supported Pd colloids were tested in the hydrogenation of the substituted acetylene (Scheme 6.3) in order to evaluate the activity of these catalysts and the selectivity to the *cis*-olefin.
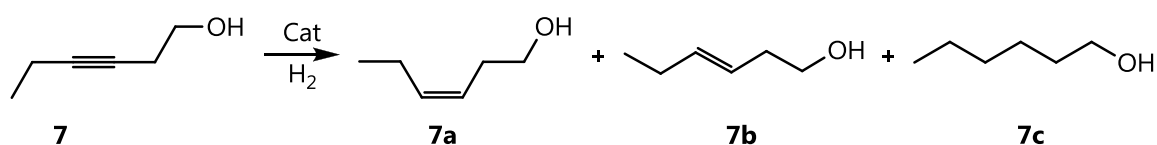
Scheme 6.3. Reaction scheme of the hydrogenation of 3-hexyn-1-ol **7**.

In order to get a first evaluation of the activity of the catalysts, hydrogenation of 3-hexyn-1ol to the saturated alcohol was carried out (see Fig. 6.3.) The catalytic reaction was performed under mild conditions (3 bar of H_2 and 30ºC) and the

progress of the hydrogenation was followed by measuring the volume of H_2 uptake. Full hydrogenation to hexanol **7c** was achieved after absorption of 2.0 L H_2, while the consumption of 1 L H_2 led to the mono-hydrogenated product.
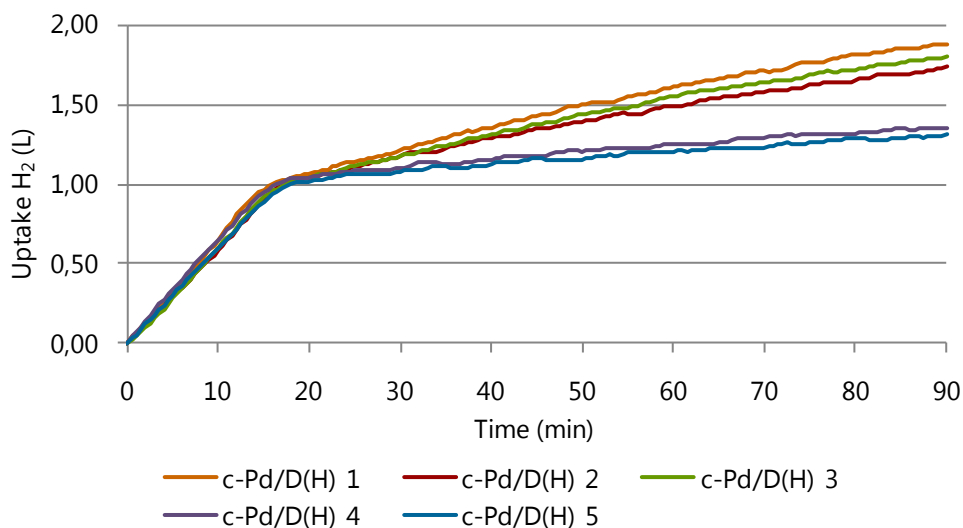

Fig 6.3. H_2 uptake curves for hydrogenation of 3-hexyn-1-ol by c-Pd/D(H) type catalysts. React. Conditions: 96%EtOH, 30°C, substrate concentration 0.38M, substrate : Pd = 3900:1 molar ratio, H_2 pressure 3 bar, 1500rpm, time 90 min.

As shown in Fig. 6.3., no notable differences were found in the first stage of the reaction with all the catalysts being very fast in the semi-hydrogenation reaction (< 20 min), unlike the overhydrogenation process, a slower reaction, that shown the catalysts immobilized under acid conditions to be faster than those at pH 7 and 10. The results evidenced in any case the selectivity of these catalysts to the olefin since a significant decrease in the H_2 uptake could be noticed after 1 L consumption.

The hydrogenation was performed repeatedly under identical catalytic conditions and stopped immediately before 1 L H_2 uptake to evaluate the selectivity at nearly full conversion. The results, reported in Fig. 6.4. and Table 6.3., proved the developed catalysts to be highly selective to the *cis*-isomer **7a**.
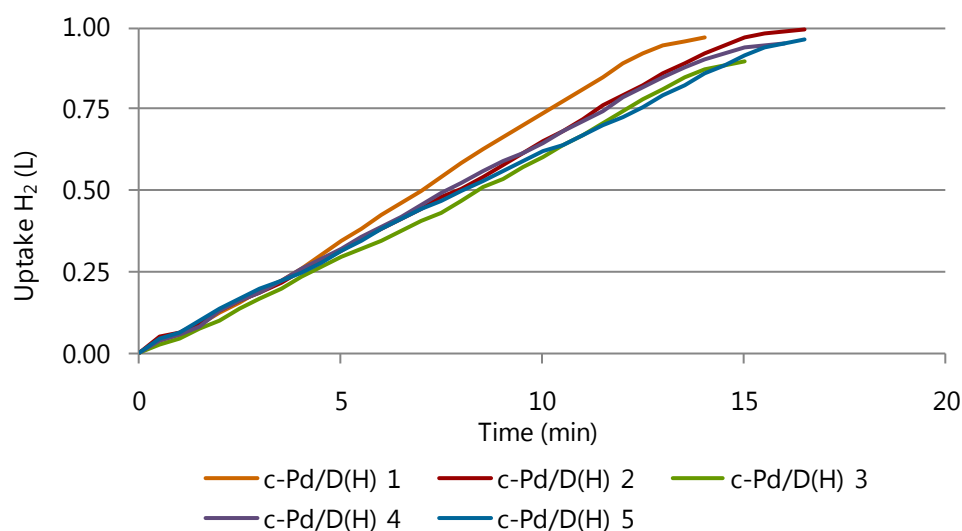
Fig 6.4. H$_2$ uptake curves for hydrogenation of 3-hexyn-1-ol by c-Pd/D(H) type catalysts. React. Conditions: 96%EtOH, 30°C, substrate concentration 0.38M, substrate : Pd = 3900:1 molar ratio, H$_2$ pressure 3 bar, 1500rpm.

Table 6.3. Hydrogenation of 3-hexyn-1-ol **7** with c-Pd/D(H) type catalysts.[a]

Catalyst	time (min)	Conv. (%)	Select. Alkene (%)	Select. Z-Alkene (%)[b]	TOF (h^{-1})[c]
c-Pd/D(H) 1	0.24	99.8	96.5	92.2	16118
c-Pd/D(H) 2	0.28	100.0	95.9	91.4	14195
c-Pd/D(H) 3	0.25	97.0	97.6	94.2	15151
c-Pd/D(H) 4	0.27	99.1	96.9	94.1	14510
c-Pd/D(H) 5	0.28	97.2	97.6	94.8	13801

[a] React. Conditions: 96%EtOH, 30°C, substrate concentration 0.38M, substrate : Pd = 3900:1 molar ratio, H$_2$ pressure 3 bar, 1500rpm. [b] Selectivity = **7a**/(**7a**+**7b**)x100. [c] TOF (on overall conversion) = mol product / mol Pd x h

Analyzing the results reported in Table 6.3, small differences with regard to selective partial hydrogenation were noticed. In general, with conversions over 97%, the olefin 3-hexen-1-ol (**7a** + **7b**) was obtained with more than 96% selectivity while the leaf alcohol **7a** was within the range 91.4% – 94.8%. Concerning the activity of these catalysts (Fig. 6.4.), c-Pd/D(H) 1 synthesized

without changing either pH or concentration of the original colloids, resulted to be the most active with a TOF of 16118 h^{-1}.

In order to evaluate the efficiency of the developed system in comparison with palladium colloids supported on different supports, the same reaction was performed under equal catalytic conditions with supported colloidal Pd NPs of similar dimensions, *ca.* 15 nm, immobilized on titanium silicate and activated carbon (see Table 6.4.).

Table 6.4. Comparison different supports in the hydrogenation of 3-hexyn-1-ol **7**.[a]

Catalyst	time (min)	Conv. (%)	Select. Alkene (%)	Select. Z-Alkene (%)[d]	TOF (h^{-1})[e]
[b] 0.12% c-Pd (15nm)/D(H) 1	0.24	99.8	96.5	92.2	16118
[c] 0.5% c-Pd (15nm) / C	0.31	94.6	95.5	94.9	13441
[c] 0.5% c-Pd (15nm) / TiS	0.28	96.4	96.5	95.5	12776

[a] React. Conditions: 30°C, substrate concentration 0.38M, substrate : Pd = 3900:1 molar ratio, H$_2$ pressure 3 bar, 1500rpm. [b] methanol. [c] ethanol. [d] Selectivity = **7a**/(**7a**+**7b**)x100. [e] TOF (on overall conversion) = mol product / mol Pd x h

In spite of being also very active, in no case, c-Pd supported either on C or TiS showed higher activities than the new proposed c-Pd supported onto ion exchange resins. The higher activity of supported colloids in comparison with conventional supported metal NPs is related to the fact that they combine the advantages of heterogeneous catalysts in a near-homogeneous format.[25] This behaviour was revealed during the present study as colloidal supported catalysts turned out to be *ca.* 20 times more active than the conventional catalysts previously described (Chapter 4 / Section 4.4.2.). Regarding the selectivity to the *cis*-olefin **7a**, colloids supported onto ion exchange resins were slightly less selective than those supported on C and TiS (notice the selectivity data were recovered at slightly higher conversion). Comparing these nanocatalysts with the conventional polymer supported Pd NPs, the latest were invariably more selective

to the leaf alcohol with values around 98%. Nevertheless, the different conditions used for both supported c-Pd NPs and Pd NPs in the hydrogenation of **7** must be taking into account, since meticulous comparison is not possible.

6.6. CONCLUSIONS

A new catalytic system was developed by combining Pd colloids and their immobilization onto ion exchange resins. The supported nanocatalysts were prepared through the reduction-deposition method NanoSelect,[21] and tested in the semi-hydrogenation of 3-hexyn-1-ol showing very good activities (TOF= 16118 h^{-1}) and selectivities to the cis-olefin (92.2%). Comparing with supported colloids on C or TiS, the efficiency of the developed catalysts was higher in terms of activity and very similar in terms of selectivity representing a suitable lead-free alternative to the Lindlar catalyst, the most used for the partial hydrogenation of substituted acetylenes.

6.7. EXPERIMENTAL

DOWEX® 50WX2 - 100 (H$^+$ form, 2% cross-linked, gel-type, 50-100 mesh [150-300 μm] bead size, 4.8 meq/g exchange capacity) strong cation-exchange resin and DOWEX® 1X2 - 100 (Cl$^-$ form, 2% cross-linked, gel-type, 50-100 mesh [150-300 μm] bead size, 3.5 meq/g exchange capacity) strong anion-exchange resin were obtained from Aldrich. The palladium precursor Na_2PdCl_4 (aqueous solution) was obtained from BASF Rome. The cationic ammonium surfactant (hexa-decyl) (2-hydroxyethyl) dimethylammonium (HHDMA) dihydrogenphosphate was obtained from Sigma Aldrich.

The synthesized catalysts were characterized by using different techniques explained in detail in Chapter 2. STEM (Scanning Transmision Electron Microscopy) was used to evaluate the dimension and size distribution of the clusters. EDS (Energy Dispersive X-ray Spectrometer) helped to observe the distribution of metal within the bead as well as to analyse qualitatively the composition. Reactions under a controlled pressure of hydrogen were performed using a 250 mL stainless steel Premex autoclave. The catalytic solutions were analyzed by GC, products were identified by comparison with the commercially available compounds obtained from Sigma Aldrich. The metal content in the resin-supported catalysts was determined by ICP-OES (Inductively Coupled Plasma – Optical Emission Spectrometry). This technique was also applied for the quantification of leached metal content in the heterogeneous catalysis solutions recovered after reaction.

Preparation of colloidal suspensions of Pd

A solution of 15g HHDMA in 1 L water was heated at 60°C. Then, a solution of 0.75g Pd (as Na_2PdCl_4) in 10 ml water was added. Upon mixing HHDMA and the palladium salt the colour change from yellow to red. The mixture was heated at 80°C and stirred at this temperature for 2 h. After all, the dimension of the colloids was analyzed by Dynamic light scattering (DLS)

Immobilization of the colloids onto the polymeric resins

The commercial resins were washed prior to use as reported in the experimental section in Chapter 3.

Colloids immobilized under acid conditions (pH = 3): 5g of dry cation-exchange resin (*R-SO₃⁻H⁺*) were added into a becker containing the c-Pd, the mixture was stirred for 1h at room temperature. The resin obtained was transferred into a glass filter and washed sequentially with deionised water (3 x 50 ml), methanol (3 x 50 ml) and diethyl ether (3 x 50 ml) before being dried in a

stream of nitrogen overnight. The polymer supported colloidal palladium, c-Pd/D(H), was obtained as black beads

Colloids immobilized under neutral and base conditions (pH = 7, pH = 10): The c-Pd was added into a becker, then NaOH 10% was added till the desired pH. 5g of dry cation-exchange resin ($R\text{-}SO_3^-H^+$) were added to the solution causing a decrease of the pH that was readjusted by adding again NaOH 10%. The mixture was stirred for 1h at room temperature and from here on it preceded as abovementioned.

Hydrogenation reaction of 3-hexyn-1-ol

All the hydrogenation reactions were performed in a 250 ml stainless steel autoclave and using mild conditions at 3 bar of H_2 and 30ºC. In a typical experiment, the autoclave was charged with 50 mg of catalyst (dry weight) and 100g 4.5 wt% 3-hexyn-1-ol in 96% ethanol, then the mixture was heated to 30˚C. Without stirring the autoclave was flushed with hydrogen and pressurized with 3 bar of H_2. The reaction was started by starting the stirring (1500rpm). After the desired time, the solution was completely removed and a sample of this solution (0.5 μl) was used for GC (product yield and product identification).

REFERENCES

1   E. Roduner (Ed.), *Nanoscopic Materials Size-Dependent Phenomena*, RSC Publishing, Cambridge, **2006**, pp. 239–262.

2   a) J. M. Thomas, *Pure Appl. Chem, 60.* **1988**, 1517; b) W. Ostwald, *Colloid-Z. 1*, **1907**, 291.

3   R. G. Finke, *Metal Nanoparticles: Synthesis, Characterization and Applications,* Chapter 2; D. L. Feldheim, C. A. Foss Jr., (Eds), Marcel Dekker, New York, **2002**.

4   A. Roucoux, J. Schulz, H. Patin, *Chem. Rev.*, 102, **2002**, 3757.

5   T. Teranishi, M. Miyake, *Chem. Mater.*, 10, **1998**, 594.

6   K. Esumi, T. Tano, K. Meguro, *Langmuir, 5,* **1989**, 268.

7   M. Michaelis, A. Henglein, *J. Phys. Chem.*, 96, **1992**, 4719.

8   N. A. Dhas, H. Cohen, A. Gedanken, *J. Phys. Chem. B*, 101, **1997**, 6834.

9   J. S. Bradley, E. W. Hill, S. Behal, C. Klein, B. Chaudret, A. Duteil, *Chem. Mater*. 4, **1992**, 1234.

10 (a) H. Hahn, R. S. Averback, *J. Appl. Phys.*, 67, **1990**, 1113. (b) Y. Li, J. Liu, Y. Wang, Z. L. Wang, *Chem. Mater.*, 13, **2001**, 1008.

11 M. T. Reetz, W. Helbig, *J. Am. Chem. Soc.* 116, **1994**, 7401.

12 a) H. Hirai, Y. Nakao, N. Toshima, *J. Macromol. Sci., Chem. A,* 12*,* **1978**, 1117; b) H. Hirai, Y. Nakao, N. Toshima, *J. Macromol. Sci., Chem. A,* 13*,* **1979**, 727; c) A. Borsla, A. M. Wilhelm, H. Delmas, *Catal. Today, 66,* **2001**, 389; d) H. Hirai, *J. Macromol. Sci., Chem. A, 13,* **1979**, 633; e) H. Hirai, *Makromol. Chem., Suppl.* 14*,* **1985**, 55; f) H. Hirai, Y. Nakao, N. Toshima, *Chem. Lett.* **1978**, 545; g) N. Toshima, M. Kuriyama, Y. Yamada, H. Hirai, *Chem. Lett.,* **1981**, 793; h) M. Komiyama, H. Hirai, *Bull. Chem. Soc. Jpn.* 56, **1983**, 2833.

13 C. K. Tan, V. Newberry, T. R. Webb, C. A. McAuliffe, *J. Chem. Soc., Dalton Trans.,* **1987**, 1299

14 J. Turkevitch, P. C. Stevenson, J. Hillier, *Discuss. Faraday Soc*. 11, **1951**, 55.

15 Y. Nakao, K. Kaeriyama, *J. Colloid Interface Sci.,* 110, **1986**, 82.

16 M. T. Reetz, S. A. Quaiser, R. Breinbauer, B. Tesche, *Angew. Chem., Int. Ed.,* 34, **1995**, 2728.

17 H. Bönnemann, W. Brijoux, R. Brinkmann, A. Schulze Tilling, T. Schilling, B. Tesche, K. Seevogel, R. Franke, J. Hormes, G. Köhl, J. Pollmann, J. Rothe, W. Vogel, *Inorg. Chim. Acta,* 270 **1998**, 95.

18 N. Toshima, M. Ohtaki, T. Teranishi, *React. Polym.*, 15, **1991**, 135.

19 Y. Nakao, K. Kaeriyama, *J. Colloid Interface Sci.,* 131, **1989**, 186.

20 P. Barbaro, C. Bianchini, G. Giambastiani, W. Oberhauser, L. Morassi Bonzi, F. Rossi, V. Dal Santo, *Dalton Trans.*, **2004**, 1783.

21 a) P. T. Witte, M. de Groen, R. M. de Rooij, P. Bakermans, H. G. Donkervoort, P. H. Berben, J. W. Geus, *Stud. Surf. Sci. Catal.*, 175, **2010**, 135; b) P. T. Witte (BASF NL), Patent WO2009096783

22 H. Bönnemann, W. Brijoux, R. Brinkmann, E. Dinjus, T. Joussen, B. Korall, *Angew. Chem., Int. Ed.* 30, **1991**, 1312.

23 P. T. Witte, S. Boland, F. Kirby, R. van Maanen, B. F. Bleeker, D. A. Matthijs de Winter, J.A. Post, J.W. Geus, P. H. Berben, *ChemCatChem*, **2012**, DOI: 10.1002/cctc.201200460

24 J. A. Baeza , L. Calvo, M. A. Gilarranz , A. F. Mohedano, J. A. Casas, J. J. Rodriguez, *J. Catal.*, 293 **2012**, 85.

25 K. Gude, R. Narayanan, *J. Phys. Chem. C*, 115, **2011**, 12716.

7

Overall Conclusions

In the research work presented in this Thesis, a new method for the synthesis of precious metal catalysts supported onto insoluble polymers has been described. The strategy consists in the direct growth of metal nanoparticles within ion exchange resins under the conditions of catalytic hydrogenation. Featured by simplicity and versatility, the method proved to be applicable to different resins and metals allowing the preparation of both hydrogenation (Pd and Rh) and oxidation (Au) catalysts.

An in depth investigation was carried out with palladium based catalysts to optimize the synthetic procedure, showing that an appropriate selection of starting materials (cation exchange resin, lithiated form, simple metal cations) allows for the preparation of polymer supported Pd or Rh hydrogenation catalysts with no need nor benefits of pre-reduction steps. Similarly, the best hydrogenation conditions for an optimal performance of these systems resulted to be methanol solvent, room temperature and atmospheric pressures. The proposed approach fulfils many of the requirements for the catalysts used in the fine chemicals industry:

- it uses cheap and commercially available materials (ion-exchange resins),

- the heterogeneous catalyst is generated in one-pot,

- the procedure uses H_2 as green reducing reagent and

- the catalyst does not require any particular care of handling nor storage.

Selective hydrogenation reactions are important processes in fine chemicals industry. To this regard, the Pd NPs based catalysts prepared during this work, showed to be highly selective in the partial hydrogenation of hydrocarbons with multiple C=C bonds, a highly desired and challenging reaction, providing nearly 100% selectivity to the monoalkene product in the hydrogenation of 1,5-cyclooctadiene. The catalysts showed total chemo-selectivity to C=C bonds in the

selective hydrogenation of unsaturated carbonyl compounds in most cases, with the overall selectivity being affected only by acid-catalyzed side reactions due to a residual acidity in the support, that could be minimized by washing the resin with LiCl prior to use.

The special case of 3-hexyn-1-ol substrate was extensively studied during this Thesis, since the semi-hydrogenation product, the leaf alcohol *cis*-3-hexyn-1ol, is an important chemical in the fragrance industry. The hydrogenation was performed both under batch and flow conditions demonstrating the excellent stability, activity and selectivity of the supported Pd catalysts. In a similar approach, colloidal Pd NPs were immobilized onto ion exchange resins and tested in the hydrogenation reaction. A summary with the results obtained during this work for the different catalysts prepared is as follows:

- In batch with Pd/D(Li): 98% *cis*-isomer @ 91% conversion (1bar H_2, rt)

- In flow with Pd/D(Li): 89% *cis*-isomer @ 75% conversion (2.5bar H_2, rt)

- In batch with c-Pd/D(H): 92% *cis*-isomer @ 99.8% conversion (3bar H_2, 30ºC)

In addition, it was proved that these catalysts represent a convenient alternative to the conventional Pd/C catalyst not only in terms of selectivity and reuse, but also regarding the recoverability of the system owing to the fact that polymeric beads can be collected much easier than powders. On the other hand, they represent a suitable lead-free alternative to the Lindlar catalyst, the most used industrial catalyst for the partial hydrogenation of substituted acetylenes.

Notably, the synthetic approach described, while satisfying most Principles of Greener Nanomaterial Production, affords a solid catalyst whose metal leach accomplish to the specification limits for residues of metal catalysts according to EMEA.

Annexes

Annex 1. Scientific results: Publications and communications

The research work presented along this Thesis has given as a result the following scientific contributions in different peer reviewed journals and international conferences. Moreover, part of the work here presented has taken place during stages in other international research centers which are also specified next.

Peer Reviewed ISI Publications:

1. P. Barbaro, F. Liguori, N. Linares, **C. Moreno-Marrodan**, Bifunctional metal / acid catalysts for selective chemical processes*, Eur. J. Inorg. Chem.*, **2012**, 3807–3823. Impact Factor: 3.049.

2. C. Moreno-Marrodan, D. Berti, F. Liguori, P. Barbaro, In-situ generation of resin-supported Pd nanoparticles under mild catalytic conditions: a green route to highly efficient, reusable hydrogenation catalysts. *Catal. Sci. Technol.*, **2012**, 2**,** 2279-2290. Impact Factor: not available (Launched 2011)

3. C. Moreno-Marrodan, P. Barbaro, M. Catalano, A. Taurino, Green production of polymer-supported Pd NPs: application to the environmentally benign catalyzed synthesis of cis-3-hexen-1-ol under flow conditions. Dalton Trans., 2012, 41, 12666-12669. Impact Factor: 3.838.

Conference Communications:

Oral Communications

   1. C. Moreno-Marrodan, *NANO-HOST Final Review Meeting*, 2012, Florence, Italy.

   2. C. Moreno-Marrodan, *NANO-HOST 3rd Yearly Meeting*, 2011. St. Andrews Scotland (UK)

   3. C. Moreno-Marrodan, *NANO-HOST Mid Term Review Meeting*, 2010, Montpellier, France

Poster Communications

   1. C. Moreno-Marrodan, N. Linares, P. Barbaro, "Resin-supported metal nanoparticles for hydrogenation reactions; recyclability, selectivity and application to continuous flow systems", *International Conference "Catalysis in Organic Synthesis"*, 2012, Moscow, Russia. **Best Poster Presentation Award**.

   2. C. Moreno-Marrodan, P. Barbaro, F. Liguori, N. Linares, "Immobilization of metal nanoparticles onto ion exchange resins for production of fine chemicals", *International Symposium on Relations between Homogeneous and Heterogeneous Catalysis*, 2011, Berlin, Germany.

   3. C. Moreno-Marrodan, P. Barbaro, F. Liguori, W. Oberhauser, A. Galarneau, "Preparation of Pd NPs onto solid supports for hydrogenation reactions and production of fine chemicals", *International Conference on Organometallic Chemistry*, 2010, Taipei, Taiwan.

4. C. Moreno-Marrodan, P. Barbaro, F. Liguori, W. Oberhauser, A. Galarneau, "Pd NPs onto solid supports for hydrogenation & production of fine chemicals", *Marie Curie Actions International Conference*, 2010, Turin, Italy.

International stages:

1. BASF The Chemical Company, De Meern, (The Nederlands).

March 2012. Duration: 3 weeks.

Activity: Preparation and characterization of supported colloids.

2. Katholieke Universiteit Leuven, Leuven (Belgium).

Aug –Sept. 2011. Duration: 8 weeks.

Activity: Catalytic oxidation by supported gold nanoparticles.

Annex 2. List of Figures

Chapter 1. Introduction

Fig. 1.1. Difference between Sustainability and Green Chemistry.

Fig. 1.2. Segmentation within the chemical industry.

Fig. 1.3. Catalysis behind sustainable energy and chemicals.

Fig. 1.4. Steps involved in a chemical reaction catalyzed by supported MNPs.

Fig. 1.5. Evolution of the *dispersion* as a function of *n* for cubic clusters up to n=100 (N=10^6). The structure of the first four clusters is displayed.

Fig. 1.6. Schematic representation of the micro- and nanoscale morphology of gel-type **(a)** and macroreticular **(b)** resins.

Chapter 2. Description of Experimental Techniques Used

Fig. 2.1. Signals generated when a high-energy beam of electrons interacts with a thin specimen.

Fig. 2.2. Scheme of X-Ray diffraction from a cubic crystal lattice.

Fig. 2.3. Schematic representation of a SAXS set up.

Fig. 2.4. Stainless steel autoclave constructed at ICCOM-CNR (left) and non-metallic Büchi Miniclave® (right).

Chapter 3. Polymer Supported Metal Nanoparticles. Synthesis and Characterization

Fig. 3.1. Scheme of the synthetic procedure for the preparation of supported palladium nanoparticles onto cation-exchange resins (top) and anion-exchange resins (bottom).

Fig.3.2. a) Dowex® 50WX2: R-SO$_3^-$ H$^+$ (H$^+$, 200-400 mesh); b) R-SO$_3^-$Li$^+$/Pd^{2+} (200-400 mesh, 1 wt% Pd); c) R-SO$_3^-$Li$^+$/Pd^{2+} (50-100 mesh, 1 wt% Pd); d) R-SO$_3^-$Li$^+$/Pd^0 (50-100 mesh, 1 wt% Pd).

Fig. 3.3. ESEM image (secondary electrons). (left) DOWEX® 50WX2 after lithiation D(Li); and (right) after subsequent metallation D/Pd(Li) *pre*, (Li$^+$, 50-100 mesh, Pd(NO$_3$)$_2$, 1 wt% Pd, H$_2$ reduction, before use in catalysis).

Fig. 3.4. (left) ESEM image (1 torr, 25 KeV, 800 magnifications) and EDS maps of an equatorial section of D/Pd(Li) *pre* catalyst bead (Li$^+$, 50-100 mesh, Pd(NO$_3$)$_2$, 1 wt% Pd, H$_2$ reduction). Top left: secondary electrons image; top right: carbon map (C Kα1); bottom left: sulphur map (S Kα1); bottom right: palladium map (Pd Lα1). (Right) EDS microanalysis; X-ray *counts* are plotted as a function of their energy, the present elements are identified.

Fig 3.5. TEM images of supported Pd NPs obtained from Pd(NO$_3$)$_2$ and H$_2$ reduction (Table 3.3): (left) Pd/D(Li) *in*, (center) Pd/D(Li) *pre* before use in catalysis, (right) Pd/D(Li) *pre* recovered after catalysis.

Fig. 3.6. Size distribution from TEM analysis of resin-embedded Pd NPs, before and after use in catalysis (1 wt% Pd/D(Li), 50-100 mesh, Pd(NO$_3$)$_2$, H$_2$ reduction).

Fig 3.7. (left) TEM image of 1.25 wt% Pd/D(Li) *in* catalyst (50-100 mesh, [Pd(CH$_3$CN)$_4$(BF$_4$)$_2$] precursor,) recovered after catalysis, (center) Size distribution from TEM analysis, (right) XRD diffractogram form the same catalysts.

Fig. 3.8. XRD diffractograms for supported Pd NPs samples indicated in Table 3.4.

Fig 3.9. SAXS differential spectra of Pd/D(Li) *pre* resin (Li$^+$, 50-100 mesh, Pd(NO$_3$)$_2$, 1 wt% Pd, H$_2$ reduction) before (○) and after (Δ) use in catalysis, obtained by subtraction of the scattering intensity due to the metal-free matrix. Solid lines represent the best-fit data.

Fig. 3.10. Hydrogenation reaction of 1 using 1.25 wt% Pd/D catalysts (50-100 mesh, [Pd(CH$_3$CN)$_4$(BF$_4$)$_2$] precursor). Reaction conditions: methanol, r.t., substrate : Pd = 250 : 1 molar ratio, H$_2$ pressure 1 bar, substrate concentration 0.17 M.

Fig. 3.11. Hydrogenation of **2**; recycle of 1 wt% Pd/D catalyst (50-100 mesh, Pd(NO$_3$)$_2$ precursor). Reaction conditions: methanol, rt, H$_2$ pressure 0.8 bar, substrate : Pd = 220:1 molar ratio, substrate concentration 0.17M, duration of each cycle 20min. Selectivity to **2a** > 99.5%. No Pd detected in solution by ICP-OES. (left) comparison between Pd NPs formed *in situ* Pd/D(Li) *in* (●) and *prior* to use Pd/D(Li) *pre* (▲), catalysts obtained by 2bar H$_2$ reduction; (right) comparison between protonated form Pd/D(H) *in* (♦) and lithiated form Pd/D(Li) *in* (●).

Fig. 3.12. Hydrogenation of **2**: reuse of 1 wt% Pd/D(Li) *in* catalysts (Pd(NO$_3$)$_2$ precursor) using Dowex® with different bead size. Reaction conditions: methanol, H$_2$ pressure 0.8 bar, r.t, substrate : Pd = 220 : 1 molar ratio, substrate concentration 0.17 M, orbital stirring 150 rpm. (●) 50-100 mesh, (o) 200-400 mesh. TOF (h^{-1}) at 90% conversion. Selectivity to **2a** > 99.5 %.

Fig 3.13. Hydrogenation of **2** by cation and anion-exchange resins-supported Pd^0 catalysts. Reaction conditions: methanol, H$_2$ pressure 0.8 bar, r.t., substrate : Pd = 220 : 1 molar ratio, substrate concentration 0.17 M. 1 wt% Pd/D catalysts (50-100 mesh, NaBH$_4$ reduction). (●) lithium sulfonate exchanger (o) trimethylbenzyl ammonium chloride exchanger.

Fig. 3.16. Scheme of the synthetic procedure for the preparation of supported rhodium nanoparticles onto cation-exchange resins.

Fig. 3.17. ESEM image (1 torr, 25 KeV, 800 magnifications) of an equatorial section of 1.4 wt% Rh/D(Li) catalyst (50-100 mesh). Top left: back scattered image; top right: secondary electrons image; bottom left: sulphur map (S Kα1); bottom right: rhodium map (Rh Lα1).

Fig. 3.18. (left) TEM image of 1.4 wt% Rh/D(Li) catalyst, (center) Size distribution from TEM analysis, (right) XRD diffractogram form the same catalysts.

Fig. 3.19. Hydrogenation of **1** with 1.4 wt% Rh/D(Li) catalyst (50-100 mesh). Reaction conditions: methanol, rt, H$_2$ pressure 1 bar, substrate : Pd = 250:1 molar

ratio, substrate concentration 0.17M. No Rh detected in solution by ICP-OES. (●) catalyst formed *in situ* Rh/D(Li) *in*, (○) catalyst formed *prior* to use Rh/D(Li) *pre.*

Fig. 3.20. Scheme of the synthetic procedure for the preparation of supported gold nanoparticles onto anion-exchange resins.

Fig. 3.21. (left) TEM image of 0.7 wt% Au/D(Cl) *pre* (right) Size distribution from TEM analysis,

Chapter 4. Catalytic Reactions in Batch Mode

Fig. 4.1 Solvent effect in the hydrogenation of **2**; catalyst recycle. Reaction conditions: H_2 pressure 0.8 bar, r.t., substrate : Pd = 220 : 1 molar ratio, substrate concentration 0.17 M, 1 wt% Pd/D(Li) *pre* catalyst (50-100 mesh, $Pd(NO_3)_2$ precursor, obtained by 2 bar H_2 reduction), conversions > 93.5%. (●) solvent CH_3OH, duration of each cycle 45min. (○) solvent $CH_3OH:H_2O$ 3:1, duration of each cycle 60 min.

Fig. 4.2. Catalytic hydrogenations of **2** under 1 - 8 bar H_2 pressure. Reaction conditions: methanol, 1 wt% Pd/D(Li) *in* catalyst (50-100 mesh, $Pd(NO_3)_2$ precursor), r.t., substrate : Pd = 250 : 1 molar ratio, time 15 min, substrate concentration 0.1 M.

Fig. 4.3. Hydrogenation of cyclohexene **4** with 1.25 wt% Pd/D(Li) catalyst (50-100 mesh, $[Pd(CH_3CN)_4(BF_4)_2]$ precursor). React. conditions: methanol, 1bar H_2, r.t., substrate concentration 0.17 M, substrate : Pd = 350 : 1 molar ratio.

Fig. 4.4. Hydrogenation of 1,5-COD **5** with 1.25 wt% Pd/D(Li) catalyst (50-100 mesh, $[Pd(CH_3CN)_4(BF_4)_2]$ precursor). React. conditions: methanol, 1bar H_2, r.t., substrate concentration 0.17 M, substrate : Pd = 350 : 1 molar ratio.

Fig. 4.5. Hydrogenation of 1,5-COD **5** (left) and 1,5,9-CDT **6** (right) with 1.25 wt% Pd/D(Li) *pre* catalyst (50-100 mesh, $[Pd(CH_3CN)_4(BF_4)_2]$ precursor). React.

conditions: methanol, 1bar H_2, r.t., substrate concentration 0.17 M. substrate : Pd = 350 : 1 molar ratio.

Fig. 4.6. Recycle of Pd/D(Li) *in* catalyst in the hydrogenation of **7**. left) TOFs (on overall conversion indicated in right figure) and Selectivity = **7a**/(**7a**+**7b**)x100; right) Conversion upon recycling. Reaction conditions: methanol, 1.25 wt% Pd/D(Li) *in* catalyst (50-100 mesh, [Pd(CH$_3$CN)$_4$(BF$_4$)$_2$] precursor), substrate concentration 0.19M, r.t., 1 bar H_2, substrate : Pd = 390 : 1 molar ratio, time 26 min.

Fig. 4.7. Recycle of Pd/D(Li) *in* catalyst in the hydrogenation of **7**. Conversion upon recycling. Reaction conditions: methanol, 1.25 wt% Pd/D(Li) *in* catalyst (50-100 mesh, [Pd(CH$_3$CN)$_4$(BF$_4$)$_2$] precursor), substrate concentration 0.17M, r.t., 1 bar H_2, substrate : Pd = 350 : 1 molar ratio.

Fig. 4.8. Hydrogenation of 3-hexyn-1-ol **7** with (•) 1.25 wt% Pd/D(Li) *in* (50-100 mesh, [Pd(CH$_3$CN)$_4$(BF$_4$)$_2$] precursor), substrate concentration 0.17M, substrate : Pd = 350 : 1 molar ratio, and (o) 5 wt% Pd/C, substrate concentration 0.5M, substrate : Pd = 250 : 1 molar ratio. Reaction conditions: methanol, r.t., H_2 pressure 1 bar. Selectivity = **7a**/(**7a**+**7b**)x100.

Fig. 4.9. Recycle of 1 wt% Pd/D(Li) *in* catalyst (50-100 mesh, (Pd(NO$_3$)$_2$ precursor). in the hydrogenation of **8**: TOFs (on overall conversion) and selectivities. Reaction conditions: methanol, r.t., H_2 pressure 0.8 bar, substrate : Pd = 220 : 1 molar ratio, time 15 min. Selectivity = **8a**/(**8a**+**8b**+**8c**+**8d**)x100.

Fig. 4.10. Hydrogenation of isophorone **9** with 1.25 wt% Pd/D(Li) catalyst (50-100 mesh, [Pd(CH$_3$CN)$_4$(BF$_4$)$_2$] precursor). Reaction conditions: methanol, r.t., substrate : Pd = 175 : 1 molar ratio, H_2 pressure 1 bar, substrate concentration 0.17 M. (left) Pd/D(Li) *in* catalyst (right) Pd/D(Li) *pre* catalyst LiCl post-treatment.

Fig. 4.11. Hydrogenation of carvone **10** with 1.25 wt% Pd/D(Li) *pre* catalyst LiCl post-treatment (50-100 mesh, [Pd(CH$_3$CN)$_4$(BF$_4$)$_2$] precursor). Reaction conditions: methanol, r.t., substrate : Pd = 175 : 1 molar ratio, H_2 pressure 1 bar, substrate

concentration 0.17 M. (left) Evolution of conversion *vs* time for the different products (dihydrocarvone: isomers mixture). (right) Selectivity data for ketones and the isomerization product.

Chapter 5. Hydrogenation Reactions in Continuous Mode

Fig. 5.1. Number of articles published containing the keywords showed in the legend from 1995 to 2011 (data obtained from the database www.sciencedirect.com).

Fig. 5.2. Schematic representation of hydrogenation reaction in continuous flow by using Pd NPs supported on Dowex® resins.

Fig. 5.2. Continuous-flow hydrogenation of **5** (left) and **7** (right) over Pd/D(Li) *pre* catalyst (50-100 mesh, 45 mg, 1.25 wt% Pd, [Pd(CH$_3$CN)$_4$ (BF$_4$)$_2$] precursor). Conversion and selectivity vs. time on stream. React. condit.: 45 mg Pd/D(Li) *pre,* methanol, r.t., substrate concentration 0.2 M, fixed solution flow 0.2 mL min^{-1} and H$_2$ 0.8 mL min^{-1}/ 2.5 bar. Selectivity Z-alkene = **7a**/(**7a**+**7b**)x100, total (*cis+trans*) ene selectivity values were similar.

Fig. 5.3. Continuous-flow hydrogenation of **5** (left) and **7** (right) over Pd/D(Li) *pre* catalyst (50-100 mesh, 45 mg, 1.25 wt% Pd, [Pd(CH$_3$CN)$_4$ (BF$_4$)$_2$] precursor). Selectivity *vs* conversion diagram React. condit.: 45 mg Pd/D(Li) *pre,* methanol, r.t., fixed H$_2$:substrate ratio=2.3, variable solution flow [0.1-0.4] mL min^{-1} and H$_2$ [0.5-1.2] mL min^{-1}. Selectivity = **7a**/(**7a**+**7b**)x100, total (*cis+trans*) ene selectivity values were similar.

Chapter 6. Polymer Supported Colloidal Palladium Nanoparticles: Synthesis, Characterization and Hydrogenation Tests

Fig. 6.1. STEM analysis of sample c-Pd/D(H) 5 (pH 10): a) High-Angle Annular Dark-Field image, b) nanoparticle size distribution determined from TEM, c) secondary electrons image of the same area and d) EDXS microanalysis.

Fig. 6.2. STEM analysis of c-Pd/D(H) 1 (pH 3): a-c) TEM images at different magnifications b) nanoparticles size distribution from TEM analysis and d) Elemental analysis by EDXS.

Fig 6.3. H_2 uptake curves for hydrogenation of 3-hexyn-1-ol by c-Pd/D(H) type catalysts. React. Conditions: 96%EtOH, 30°C, substrate concentration 0.38M, substrate : Pd = 3900:1 molar ratio, H_2 pressure 3 bar, 1500rpm, time 90 min.

Fig 6.4. H_2 uptake curves for hydrogenation of 3-hexyn-1-ol by c-Pd/D(H) type catalysts. React. Conditions: 96%EtOH, 30°C, substrate concentration 0.38M, substrate : Pd = 3900:1 molar ratio, H_2 pressure 3 bar, 1500rpm.

Annex 3. List of Tables

Chapter 5. Hydrogenation Reactions in Continuous Mode

Chapter 6. Polymer Supported Colloidal Palladium Nanoparticles: Synthesis, Characterization and Hydrogenation Tests

Annex 4. List of Schemes

Chapter 1. Introduction

Scheme 1.1. Preparation methods for supported catalysts.

Scheme 1.2. Examples of ion exchange resins with different functionalization, a strongly acidic sulphonated polystyrene cation exchange resin (left) and a strongly basic quaternary ammonion anion exchange resin.

Chapter 2. Description of Experimental Techniques Used

Scheme 2.1. Schematic view (top) and image of the core (bottom) of the continuous-flow, high-pressure reactor system used.

Chapter 3. Polymer Supported Metal Nanoparticles. Synthesis and Characterization

Scheme 3.1. Schematic representation of the one-pot synthesis of MIBK.

Scheme 3.2. Sketch of the resin used.

Chapter 4. Catalytic Reactions in Batch Mode

Scheme 4.1. Sketch of the probe substrates tested for optimization of the reaction conditions.

Scheme 4.2. Sketch of the substrates tested in hydrogenation reactions of hydrocarbons with multiple C=C or C≡C bonds.

Scheme 4.3. Reaction scheme of the hydrogenation of benzylidenacetone **8**.

Scheme 4.4. Reaction scheme of the hydrogenation of isophorone **9** including all possible products; **9a**: dihydorisophorone, **9b:** homomenthol, **9c**: : isophorol and the parallel reaction of acetilization to give **9d**.

Chapter 5. Hydrogenation Reactions in Continuous Mode

Chapter 6. Polymer Supported Colloidal Palladium Nanoparticles: Synthesis, Characterization and Hydrogenation Tests

Annex 5. Frequently Used Abbreviations

Au/D(Cl) *pre* Au NPs supported onto anion exchange resins reduced with NaBH$_4$ and isolated

CFP Cross-linked Functional Polymers.

c-Pd/D(H) colloidal Pd NPs supported onto cation exchange resins (protonated form)

DLS Dynamic Light Scattering.

EDS Energy Dispersive X-ray Spectroscopy.

ESEM Environmental Scanning Electron Microscopy.

GC Gas Chromatography.

GC/MS Gas Chromatography / Mass Spectrometry.

ICP-OES Inductively Coupled Plasma - Optical Emission Spectroscopy.

MNPs Metal Nanoparticles.

NMR Nuclear Magnetic Resonance.

NPs Nanoparticles.

Pd/D(Cl) *pre* Pd NPs supported onto anion exchange resins reduced with NaBH$_4$ and isolated

Pd/D(H) *in* Pd NPs supported onto cation exchange resins (protonated form) and reduced *in situ* under catalytic conditions

Pd/D(H) *pre* Pd NPs supported onto cation exchange resins (protonated form) isolated

Pd/D(Li) *in* Pd NPs supported onto cation exchange resins (lithiated form) and reduced *in situ* under catalytic conditions

Pd/D(Li) *pre* Pd NPs supported onto cation exchange resins (lithiated form) isolated

Rh/D(Li) *in* Rh NPs supported onto cation exchange resins (lithiated form) and reduced *in situ* under catalytic conditions

Rh/D(Li) *pre*   Rh NPs supported onto cation exchange resins (lithiated form) isolated

SAXS   Small Angle X-ray Scattering.

STEM   Scanning Transmission Electron Microscopy.

STY   Space to Time Yield parameter.

TEM   Transmission Electron Microscopy.

TOF   Turnover Frequency parameter.

TON   Turnover Number.

wt%   Percentage by Weight.

XRD   X-ray powder Diffraction.

Acknowledgements

Wow! Satisfaction, this is the feeling right now, for all the work done and for all the people I have had the pleasure to share with this experience, both at work and outside.

First of all, I would like to thank Pierluigi Barbaro, my supervisor, for giving me this huge opportunity of working with him, within a great European Project that gave me the possibility of growing in my professional and personal life. I would like to thank Serena, for all the help and support, before even I came here and that last until today. Francesca, of course, she introduced me to the practical work and we started together the foundations of this Thesis, and Werner also for his assistance with the XRD. Noemi, I really have no words, thank you so much for everything, for making work easier and funnier, for all the laughs, the help, the jokes, for *Lágrimas Negras, Tonight Tonight...*, it was awesome to share this trip with you ☺

As part of NanoHost, I had the chance to spend some time in partner laboratories abroad. I would like to thank Dirk de Vos for letting me work in his group in Katholieke Universiteit Leuven and Paulo Forte for helping me in and outside the lab. Peter T. Witte from BASF, thank you for showing me how research works in the industrial world, and also Fiona Kirby, thank you for making my stay so nice in Utrecht and for so many kilometers cycled together!

I would like to thank all the guys from ICCOM, Lapo thank you for making things more interesting, always thinking further ;) Carlo, thank you for fixing everything! and of course for the cover of this work... I would like to thank Antonella, Vincenzo and Valentina for making easier being far from home. And finally, I would like to thank my family, my friends, Toni and specially my mum, for being always there, for supporting me in everything.

The development of greener and more economical routes for chemicals production is one of the major current concerns at industrial level. This is particularly true in the fine chemicals sector, where the large amount of waste produced contribute to the characteristic high *E*-factor (Kg waste/Kg product). Catalysis may be the key to solve the problem provided that active and selective catalysts are elaborated. These are the distinctive features of homogeneous phase catalysts, which indeed dominate the sector. However, they show severe drawbacks in terms of recovery and reuse of the precious catalysts. The immobilization of chemical catalysts onto solid insoluble supports offers significant benefits to this regard.

The present Thesis reports a simple one-pot strategy for the synthesis of solid-supported metal catalysts based on ion-exchange resins, and *in-situ* formed metal nanoparticles under mild catalytic hydrogenation conditions (room temperature, 1 bar H_2). The so-formed heterogeneous palladium system was carefully characterized and tested in hydrogenations processes for the synthesis of high added value chemicals. The catalyst showed high activity and selectivity and could be readily reused several times with neither detectable metal leaching in solution nor significant efficiency decay under batch conditions. Application to the synthesis of the leaf alcohol *cis*-3-hexen-1-ol was explored both under batch and continuous mode showing significant advantages compared to established industrial process.